

**DEVELOPMENT OF A LOW COST INSULATION
SYSTEM USING BOTTOM ASH FOR CFRP-
CONCRETE COMPOSITES**

Kahandawa Arachchige Dona Yamali Tharika Kahandawa Arachchi

198040T

Degree of Master of Science

Department of Civil Engineering

University of Moratuwa

Sri Lanka

July 2020

**DEVELOPMENT OF A LOW COST INSULATION
SYSTEM USING BOTTOM ASH FOR CFRP-
CONCRETE COMPOSITES**

Kahandawa Arachchige Dona Yamali Tharika Kahandawa Arachchi

198040T

Thesis submitted in partial fulfillment of the requirements for the degree Master of
Science in Civil Engineering

Department of Civil Engineering

University of Moratuwa

Sri Lanka

July 2020

DECLARATION

I declare that this is my own work and this thesis does not incorporate without acknowledgement any material previously submitted for a Degree or Diploma in any other university or institute of higher learning and to the best of my knowledge and belief it does not contain any material previously published or written by another person except where the acknowledgement is made in the text.

Also, I hereby grant to University of Moratuwa the non-exclusive right to reproduce and distribute the thesis, in whole or in part in print, electronic or other medium. I retain the right to use this content in whole or part in future works (such as articles or books).

Signature:

Date:

The above candidate has carried out research for the Masters under my supervision.

Name of the supervisor: Dr. (Mrs.) J.C.P.H. Gamage

Signature of the supervisor:

Date:

Name of the supervisor: Dr. G.I.P. De Silva

Signature of the supervisor:

Date:

ABSTRACT

The civil engineering industry is moving towards more greener and sustainable means of construction materials today. Improving the thermal comfort in buildings while conserving the natural resources is essential to maintain the ecological balance whilst improving health, wellbeing and productivity of humans. On the other hand, concrete structures have been the main construction element for the past five decades. Retrofitting these concrete structures using fiber reinforced polymer (FRP) has been a popular trend in the recent years. An insulation material has been developed using bottom ash which is a byproduct of the coal power generation process. The developed plaster could be used for either thermal comfort in buildings or as a cementitious insulation material for CFRP/Concrete composites. The research was conducted in four phases. Properties of bottom ash and properties of developed material were investigated in the first two phases. Modification of developed insulation material and application of CFRP/Concrete composites were investigated in the latter two phases. A N-type plaster was developed by replacing fine aggregates in conventional cement sand plaster by bottom ash. 60% of the sand was replaced by bottom ash. A thickness of 20 mm of the developed plaster can decrease the heat transfer 45% than conventional plaster. Furthermore, the developed plaster is 8% more cost effective than conventional plaster.

ACKNOWLEDGEMENT

This research addresses one of the main concerns of the civil engineering industry when it comes for Fiber Reinforced Polymer Composites. The knowledge I gained through my undergraduate work and post graduate studies has been a great influence in completing this project up to the standards.

There are many individuals to whom I owe this success to. Foremost, I would like to acknowledge my research supervisors, **Dr. (Mrs.) J.C.P.H. Gamage**, Senior Lecturer, Department of Civil Engineering, University of Moratuwa and **Dr. G.I.P. De Silva**, Senior Lecturer, Department of Materials Science and Engineering, University of Moratuwa. Without their guidance none of this would be possible.

Next, I would like to thank **Dr.(Mrs.) H.L.D.M.A. Judith**, Chairman, Research and Development Division, Road Development Authority, Chairperson of my Research Assessment Panel and **Prof. A.A.D.J. Perera**, Senior Professor, Department of Civil Engineering, University of Moratuwa, research coordinator (Nominee) for evaluating and guiding throughout the research progress presentations.

I would like to appreciate the National Research Council, Sri Lanka and Airow Solutions (Pvt.) Ltd. for the financial support of the project (Grant No. PPP18-01). Specially, **Mrs. Naduni Wanniarachchi**, Scientific Officer, National Research Council and **Mr. Vajira Attanayake**, General Manager, Airow Solutions (pvt.) Ltd. for their support.

Moreover, I would like to express my gratitude to **Mr. D.M.N.L. Dissanayaka** of Structural Testing Laboratory and **Mr. H.T.R.M. Thanthirige** of Building Materials Laboratory, University of Moratuwa for their support throughout the experimental program.

At last but not least, I would like to thank my parents and family for believing me and supporting throughout these years.

K.A.D.Y.T.K. Arachchi
Department of Civil Engineering,
University of Moratuwa.
2020.07.10

LIST OF PUBLICATIONS

International Conferences

1. **K.A.D.Y.T. Kahandawa Arachchi**, J.C.P.H. Gamage and G.I.P. De Silva, “Thermal insulation systems for CFRP/Concrete Composites: A Review”, in *International Conference on Structural and Construction Management*, 2019 - Published
2. **K.A.D.Y.T. Kahandawa Arachchi**, J.C.P.H. Gamage and E.R.K. Chandrathilake, “Bond Performance of Carbon Fiber Reinforced Polymer (CFRP) strengthened Reinforced Curved Beams”, in *International Conference on Civil Engineering and Applications*, 2019 – Published
3. **K.A.D.Y.T. Kahandawa Arachchi**, J.C.P.H. Gamage and G.I.P. De Silva, “Modification of a Bottom Ash Based Insulation Material using Saw Dust, EPS and Aggregate Chips”, in *International Conference on Structural and Construction Management*, 2020 - Submitted

International Journals

1. A. Selvaratnam, **K.A.D.Y.T. Kahandawa Arachchi**, S. Kajian and J.C.P.H. Gamage, “Behavior of Carbon Fiber Reinforced Polymer strengthened out-of-plane Curved Reinforced Concrete beams” – In Preparation
2. **Kahandawa Arachchi K.A.D.Y.T.**, Selvaratnam A., Gamage J.C.P.H. and De Silva G.I.P, “Development of an Innovative Insulated Plaster using Bottom Ash to Enhance Thermal Comfort in Buildings” – In Preparation
3. **K.A.D.Y.T. Kahandawa Arachchi**, A. Selvaratnam, J.C.P.H. Gamage, V. Attanayaka, “Development and Application of a Bottom Ash based Cementitious Insulation material on CFRP/Concrete Composites” – In preparation
4. Selvaratnam A., **Kahandawa Arachchi K.A.D.Y.T.**, Gamage J.C.P.H, “Experimental and Numerical analysis of an Innovative Wall Plaster Developed using Recycled EPS to Enhance the Thermal Comfort in Buildings” – In preparation

TABLE OF CONTENTS

DECLARATION	i
ABSTRACT.....	ii
ACKNOWLEDGEMENT	iii
LIST OF PUBLICATIONS	iv
International Conferences	iv
International Journals.....	iv
LIST OF FIGURES	viii
LIST OF TABLES	x
1 Introduction.....	1
1.1 Research Background.....	1
1.2 Objectives.....	2
1.3 Methodology	2
1.4 Research Significance	2
1.5 Arrangement of the thesis	3
2 Literature Review.....	5
2.1 Introduction	5
2.2 Cementitious insulation materials	7
2.2.1 Available systems	7
2.2.2 Thermal properties of cementitious insulation systems.....	8
2.2.3 Sustainable materials for insulated motor developments.....	9
2.3 Bottom ash.....	10
2.3.1 Properties of Bottom-ash (BA)	10
2.3.2 Bottom ash as a partial replacement for fine aggregates	12
2.3.3 Increasing thermal resistivity using BA.....	13
2.4 Insulation materials for CFRP/Concrete composites	14
2.5 Summary	16
2.6 Further research needs.....	16
3 Physical and Chemical structure of Bottom ash – Phase 1	17
3.1 Introduction	17
3.2 Experimental program.....	18
3.3 Results and Discussion.....	18
3.3.1 SEM imaging	18

3.3.2	XRD analysis	20
3.3.3	Chemical analysis	22
3.3.4	Particle size distribution.....	23
3.4	Summary	24
4	Physical and meCHANical properties of the developed Plaster – Phase 2	25
4.1	Introduction	25
4.2	Experimental program.....	26
4.2.1	Materials	26
4.2.2	Sample Preparation	27
4.3	Results and Discussion.....	29
4.3.1	Thermal conductivity	29
4.3.2	Compressive Strength	32
4.4	Experimental program.....	34
4.4.1	Materials	34
4.5	Sample preparation.....	34
4.6	Results and Discussion.....	35
4.7	Summary	40
5	Heat Transfer Analysis	41
5.1	Introduction	41
5.2	Procedure.....	41
5.3	Calculation	43
5.4	Summary	44
6	Modification of developed plaster – Phase 3	45
6.1	Introduction	45
6.2	Experimental program.....	46
6.2.1	Materials	46
6.2.2	Sample preparation	47
6.2.3	Results and Discussion	48
6.3	Summary	51
7	Application of Developed Plaster on CFRP/Concrete Composites – Phase 4... 52	
7.1	Introduction	52
7.2	Experimental program.....	53

7.2.1	Materials	53
7.2.2	Sample preparation	54
7.3	Results and Discussion	55
7.4	Experimental program	58
7.4.1	Sample preparation	58
7.5	Results and Discussion	61
7.6	Summary	63
8	Cost Analysis	64
9	Conclusions and Recommendations	66
9.1	Conclusions	66
9.2	Recommendations	67
	REFERENCES	68
	Annexes.....	xi
	Annex 1 – Thermal conductivity testing cooling curves	xi
	Annex 2 – Furnace test results	xv
	Annex 3 – Datasheet	xx
	Annex 4 - Publications	xxiv

LIST OF FIGURES

Figure 1-1 Overview of the test series	4
Figure 2-1 - Overview of literature review	6
Figure 2-2 - Thermocouple Locations	7
Figure 2-3 - How pore spaces increase thermal performance (Udawatte et al).....	8
Figure 2-4 - Thermal conductivity testing methods (Asadi et al).....	9
Figure 2-5 - Morphology of bottom ash (Cherif et al.)	11
Figure 3-1 - Overview of phase 1	17
Figure 3-2 - Bottom ash physical appearance.....	18
Figure 3-3 - Morphology a) Literature (Cherif et al) b) Current Study	19
Figure 3-4 - XRD Imaging - Literature (Mal'Chik et al) [62].....	20
Figure 3-5 - RD imaging - Current Study	21
Figure 3-6 - Sieve analysis.....	23
Figure 4-1 - Overview - Phase 2	25
Figure 4-2 - Iterative process	26
Figure 4-3 - Materials – a) Cement b) Sand c) Bottom ash	27
Figure 4-4 - Thermal conductivity samples - a) Molds b) Casting c) Curing.....	28
Figure 4-5 - Lee's disc apparatus	28
Figure 4-6 - a) Compressive strength test cubes b) Compressive strength testing	29
Figure 4-7 Thermal conductivity variation	31
Figure 4-8 - Variation of compressive strength	32
Figure 4-9 - Materials measured for BA60.....	34
Figure 4-10 - Compressive strength and workability variation	36
Figure 4-11 – a) Plaster without admixture b) Plaster with admixture.....	37
Figure 4-12 - Variation of density with amount of Superplasticizer	39
Figure 5-1 - Schematic Diagram for heat transfer	41
Figure 5-2 - Lee's Disc apparatus a) test setup b) Computer program.....	41
Figure 5-3 - Cooling curve for BA0	42
Figure 6-1- Overview of phase 3	45
Figure 6-2 – a) Polystyrene (EPS) b) Saw dust	46
Figure 6-3 - Aggregate chips passing through $\mu 00$ mm sieve	47

Figure 6-4 Compressive strength cubes a) EPS and saw dust b) Aggregate chips 40% and 50%	48
Figure 6-5 -Variation of a) Compressive Strength b) Flow c) Thermal Conductivity	49
Figure 6-6 Flow table test a) EPS b) Saw dust c) Aggregate chips 40% d) Aggregate chips 50%	50
Figure 7-1 - Overview of phase 4	52
Figure 7-2 - Ingredients of BA60 a) bottom ash b) cement c) river sand d) admixture	53
Figure 7-3 - a) Coarse aggregates b) CFRP fabric c) Adhesive - base d) Adhesive - Hardener.....	54
Figure 7-4 - a) Sand blasted blocks b) Application of CFRP and thermo-couples....	54
Figure 7-5 - Schematic diagram for arrangement of thermo couples	55
Figure 7-6 - a) Application of insulation layer b) Testing in Furnace	55
Figure 7-7 - Temperature variation	57
Figure 7-8- a) Sand blasted blocks b) Application of CFRP and thermo couples	58
Figure 7-9 - Schematic diagram.....	59
Figure 7-10 - a) Application of insulation layer b) Halogen lamps for elevating temperature	59
Figure 7-11 - a) Universal testing machine (UTM) b) Pullout failure.....	60
Figure 7-12 - Shear lap test results and variation of average pullout strength with temperature	62
Figure 8-1 - Cost comparison	65
Figure 0-1 - Schematic diagram of an insulation system	Error! Bookmark not defined.
Figure 0-2 - How pore spaces improve thermal performance (Udawattha et al)	Error! Bookmark not defined.

LIST OF TABLES

Table 2-1 - Insulation Thickness (Ranasinghe et al).....	7
Table 2-2 – Chemical Composition of BA (Hendawitharana et al).....	11
Table 2-3- Thermal Properties of Insulation Materials (Dong et al)	16
Table 3-1 - Chemical Composition.....	22
Table 4-1 - Mix proportions.....	27
Table 4-2 - Control sample thermal conductivity literature review.....	29
Table 4-3 - Thermal Conductivity results	30
Table 4-4- Compressive strength results.....	32
Table 4-5 - Modified mix proportions	35
Table 4-6 - Results for compressive strength and workability of BA60 with different w/c ratios	35
Table 4-7- Average test results	37
Table 5-1 - Lee's disc method results.....	44
Table 6-1 - Mix proportions.....	46
Table 6-2 - Mix proportions for Aggregate chips	47
Table 6-3 - Results for mechanical and physical properties of modified mixes.....	48
Table 7-1 -Material properties of FRP and adhesive	53
Table 7-2 - Thermal analysis test results - Summary	56
Table 7-3 - Results for single lap shear test.....	61
Table 8-1 - Cost analysis.....	64

1 INTRODUCTION

1.1 Research Background

Concrete is so far the most widely used construction material in the civil engineering industry. Reaching towards the second decade of the millennium, there are concrete structures that are older than 100 years and counting. Retrofitting these structures, strengthening concrete structures or enhancing the performance of concrete structures have been the one of the main focuses of Fiber Reinforced Polymer (FRP) materials in the recent past. Their applicability on bridges, buildings and many other civil engineering structures has made them popular all throughout the industry. External application or embedment near the surface of FRP could enhance the structural performance of the structures up to 200% of its original capacity [1].

The use of Carbon Fiber Reinforced Polymer (CFRP) in international and local construction industry has faced many challenges over the years. The performance of CFRP composites at elevated temperatures has always been one of the major concerns. However, the performance of CFRP/Concrete composites under fire has been widely investigated with degradation of mechanical properties of composites in the event of a fire. Application of different insulation materials, introducing more viable epoxy adhesive, as well as new application methodologies is being investigated widely.

On the other hand, the existing insulation methods for CFRP/Concrete composites are not cost effective. And as many other industries, the FRP composite industry is looking towards developing an economical and sustainable solution for the existing problems.

The use of sustainable and easily accessible materials as thermal and fire insulation materials is a wide research area. When locally available alternative insulation materials that could be incorporated in plasters was investigated, Polystyrene (EPS), Bottom ash and Rice husk ash were identified as possible solutions for the problem at hand. Although the thermal resistivity of bottom ash has been already identified, its application of FRP composites is yet to be specified. Hence, this research is focused

on understanding the material and thermo – mechanical properties of bottom ash as a possible insulation system for CFRP composites.

1.2 Objectives

The main objective of this research is to develop an insulation material using bottom ash which is cost effective and sustainable than the available materials in the market for CFRP/Concrete composites or masonry structures.

1.3 Methodology

The research methodology was widely divided into four phases as given in Figure 1-1 (page 3). A comprehensive literature review was conducted as the first part of the research and then physical and chemical composition of bottom ash was investigated. Then the process of developing a mortar has been carried out by investigating mechanical and physical properties of the developed plaster step wise. Attempts have been made to further develop the plaster by incorporating other materials apart from bottom ash. Next, the developed plaster has been applied on CFRP composites and thermo-mechanical properties of the composite have been investigated.

1.4 Research Significance

FRP composites themselves were identified to be more susceptible to failure at elevated temperatures. Although several attempts have been made over the years to rectify the fire performance of FRP composites, the current solutions deem less cost-effective and sustainable.

On the other hand bottom ash, which is an industrial waste when from the coal power generation process, has not been commercially utilized yet. Currently, most of the bottom ash generated during the process occupy open dump sites which depreciate the and value itself.

Thereby, this research aims on finding solutions for both said issue by incorporating them together. No insulation material for FRP composites has been commercialized using bottom ash as per authors knowledge to date.

1.5 Arrangement of the thesis

In this thesis, the research project has been presented in nine chapters. The **first chapter** stipulates an introduction to the research, the overall objectives and the methodology followed.

The **second chapter** presents the literature review conducted throughout the research project.

Third, Fourth, Fifth and Sixth chapters cover the phases 1-3, of the development of insulation plaster as given in Figure 1-1.

The **Seventh chapter** provides the application of the developed insulating material on CFRP/Concrete composites and the bond performance of the developed insulation plaster.

The **Eighth chapter** provides a cost analysis and finally, the **Ninth chapter** concludes the results and findings of the research project.

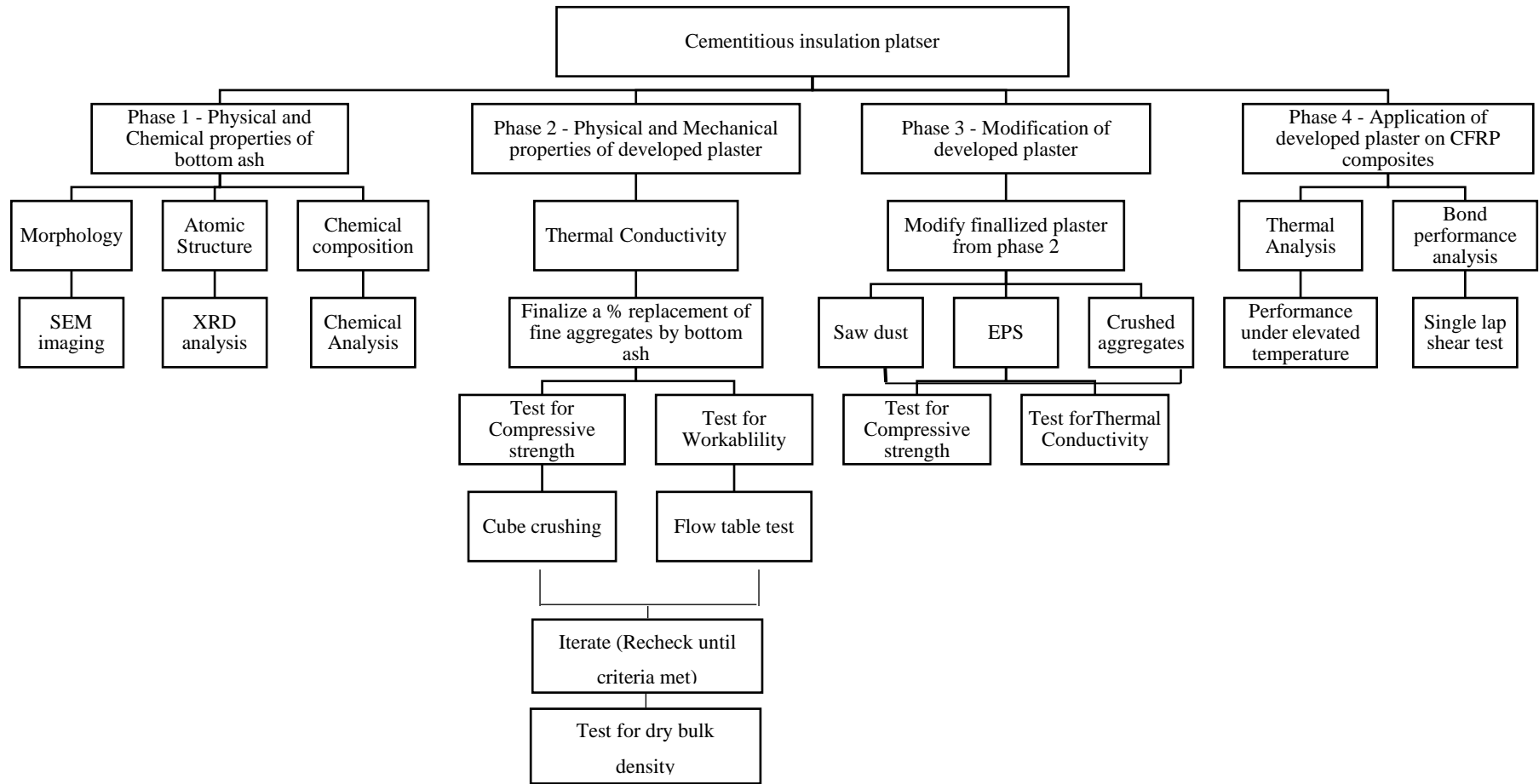


Figure 1-1 Overview of the test series

2 LITERATURE REVIEW

2.1 Introduction

From late 90's the use of Fiber Reinforced Polymer (FRP) has doubled in the global context with a larger portion of the industry focusing on Carbon Fiber Reinforced Polymer (CFRP) [2], [3]. Its superior qualities have replaced conventional materials [3]–[5]. Applications of CFRP/Concrete composites are investigated widely [6]–[8]. The applications of FRP would simply cover a wide range from military applications to sports applications [9]. However, the fire performance of its civil engineering applications with respect to the fire ratings of the buildings when strengthened with FRP raises a serious dilemma [10]–[13]. FRP strengthening is used in many structural components in civil engineering like columns [14], beams [15], [16], curved elements [7], [8], slabs [17].

The degradation of mechanical properties of structural materials as concrete, steel and Fiber Reinforced Polymers (FRP) in elevated temperatures is inevitable [13], [18]–[21]. When it comes to EBR (externally bonded reinforced) application systems, the CFRP-concrete interface is a precarious area accountable for upholding the efficiency at elevated temperatures [22]. The performance criteria for fire endurance of structural elements is commonly defined upon reliability, load carrying capacity and insulation; throughout the required time duration of subjecting to a standard fire [23]. This is commonly evaluated through furnace tests wherein the structural members are isolated and exposed to perpetual service load levels [11].

In accordance with AS1530.4 [24], the fire resistance could be outlined as the capability of a structural element to withstand fire through a specified interval of time with the entailed structural competence, reliability, thermal insulation or other anticipated performance stated, throughout a fire test [13]. Carbon fibers are more or less unaffected by temperatures in excess of 1000°C and said to have excellent thermal stability [13], [25]. However, the epoxy adhesive is much more susceptible to higher temperatures. Therefore, it can be noted that the thermal endurance of CFRP strengthened concrete member depends on the resin matrix [25]. According to the experiment conducted by Gamage et.al [26], the CFRP sheet failed in peeling off when

the temperature was high (epoxy temperature > 60°C). At low temperatures (epoxy temperature < 50°C), the adhesive failed along with concrete rupture. These results were in harmony with the results of Wu et al [27]; bond strength reduced substantially with temperature. When the temperature was increasing up to 50 °C, a mixture of bond failure and concrete rupture occurred until peeling-off adhesive failure occurred at temperatures above 60 °C [11].

In general, at elevated temperatures, mechanical/bond strength of the polymer matrices implemented in FRP materials in concrete elements for strengthening tend to depreciate and these properties are dominated by their glass transition temperature (T_g) [22], [23]. Experimental determination of glass transition temperature (T_g) can be obtained through dynamic mechanical analyses (DMA) or differential scanning calorimetry (DSC) which makes T_g the “critical temperature” in design procedures [11]. Typically from 50°C to 120 °C, the T_g of the adhesive fluctuates and is usually reliant on the resin type, the polymeric matrix of the ingredients etc. [22]. According to Cree et al [14], T_g ranges from 60 °C to 82 °C in commercially available polymers and the bond between FRP and the concrete surfaces can be preserved at temperatures below the T_g of the polymer [14]. By definition, glass transitioning happens when composites original state of being hard and brittle changes to more viscous or rubbery with the increase in temperature [11]. Figure 2-1 gives an overview of the literature review conducted.

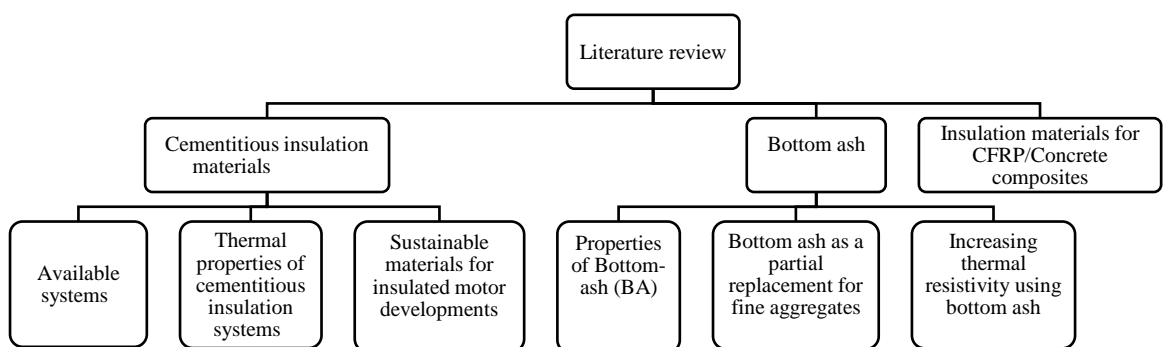


Figure 2-1 - Overview of literature review

2.2 Cementitious insulation materials

2.2.1 Available systems

The research of Kodur and Baingo [17] suggested that the commonly used fire protection methods or coatings could also be applicable for the FRP composites. In their research vermiculite has been used as passive fire protection aimed at CFRP strengthened concrete members. Ideally, this is a mixture of vermiculite and cement [17]. However, as per Ranasinghe et al. [25] the required thickness to maintain adequate fire endurance is large and requires additional support for installation like mechanical reinforcement. This makes Vermitex - DX inconvenient in practical applications as well as influences the aesthetic appearance of the structure [25].

Gamage et al. [28] used two concrete blocks, with the size of 130 x 130 x 300 in mm, with 55 MPa concrete strength and strengthened with CFRP plates. Then vermiculite was applied as an insulation material. Thermocouples were applied at the locations stated in Figure 2-2. The conclusion was in agreement with the fact that the adhesive layer is vulnerable at elevated temperatures. When epoxy reaches 70 °C-81 °C, the composite tends to lose its ability to force transfer [28].

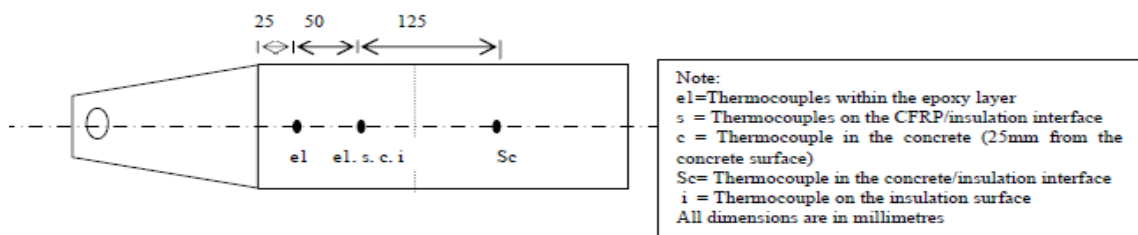


Figure 2-2 - Thermocouple Locations

According to Ranasinghe et al. [25] and Gamage et al. [13], the thermal conductivity of Vermitex is 0.114 Nmm/s/mm/°C according to manufactures' datasheet. They further states that according to manufacturers, the thickness of the insulation layer varies as per Table 2-1.

Table 2-1 - Insulation Thickness (Ranasinghe et al)

FRL (Hours)	Manufacturers' recommended insulation thickness (mm)
1	45
2	60
3	75

However, according to a parametric study, Ranasinghe et al. [25] suggests that, if the thermal conductivity of the insulation layer was reduced to $0.08 \text{ Nmm/s/mm}^\circ\text{C}$, FRL would be 2 hours for the same 50 mm thickness insulation.

2.2.2 Thermal properties of cementitious insulation systems

The thermal conductivity of conventional concrete or mortar is mainly attributed to the aggregate volume fraction, moisture content, admixture type and the age of concrete [29]. In case of materials used for insulation porosity and micro structure played a substantial role [18], [30], [31]. Thereby, the material to be developed needed to be of porous nature with adequate morphological features as well.

According to Udawatte et al. [30] the pore spaces between the particles would enhance the amount of heat that could be withheld through the material and hence increase the resistivity towards thermal propagation (Figure 2-3).

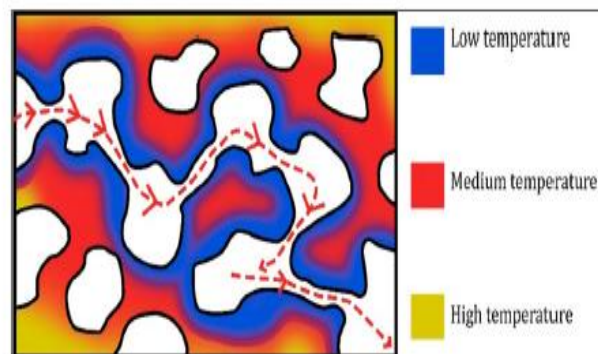


Figure 2-3 - How pore spaces increase thermal performance (Udawatte et al)

The main thermo-physical properties of concrete are believed to be thermal conductivity, specific heat and thermal diffusivity. Transfer of heat through conduction in concrete contributes towards its thermal conductivity [32]. The conditions of transferring heat through materials are mainly steady state and transient state [33]. If the heat transfer is independent of time it is called the steady state. The transient method suggests variation of temperature with time [34]. As per testing the thermal conductivity of a material Asadi et al [34] have used four different recognized

techniques to evaluate the thermal conductivity of cementitious materials (Figure 2-4).

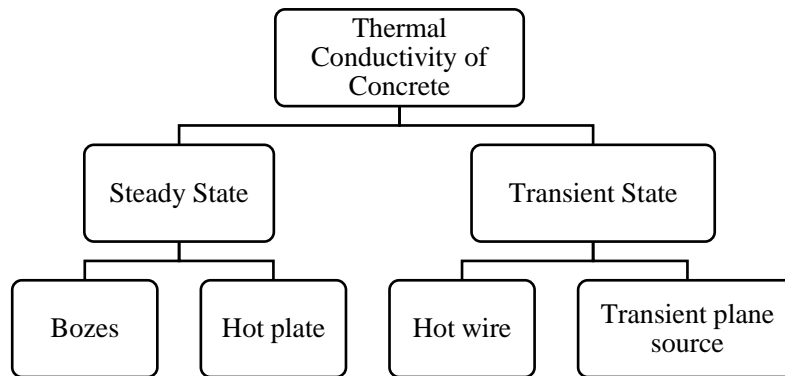


Figure 2-4 - Thermal conductivity testing methods (Asadi et al)

Main factors that affect thermal conductivity according to Kim et al. [29], are as follows for both mortar and concrete.

- Humidity
- Age
- Temperature
- Water-cement (w/c) ratio
- Fine aggregate fraction
- Type of admixture
- Total aggregate volume fraction

2.2.3 Sustainable materials for insulated motor developments

There are several areas investigated with respect to thermal insulation materials in the industry at present. Fly ash [35], [36], Bottom ash [37], [38], EPS (Expanded polystyrene)[39], rice husk ash [40], [41], [42] are some of the common areas that are under research for thermal insulation systems. Incorporating bottom ash in mortars have been investigated and already proven as a viable solution for disposal of the waste product [43], [44]. However, using these materials for the purpose of insulating FRP systems has not been investigated according to author's knowledge. Of these materials, bottom ash deemed an easily accessible waste material in Sri Lanka which is not currently been used for any industrial purposes. And the physical and micro structural properties suggested for bottom ash seem appropriate for the purposes of the study. Hence, it was decided to focus the study on bottom ash, if it is possible to use it as an insulation material for FRP/Concrete composites.

2.3 Bottom ash

Worldwide, one of the major environmental problems which encounter the conception of waste products which keep on increasing owed to the lingering requirement for resources used by humans. There rises the necessity to administer and recycle industrial, residential and other wastes alongside with the usage of non-renewable resources consciously and competently. In a coal power plant, once the combustion of coal within the furnace is done, in the electrostatic precipitators, the finer particles of non-combustible ash are extracted. Fly ash is collected at the electrostatic precipitators and bottom ash(BA) from the bottommost of the furnace [37].

In detail, according to Mandal et al [45], the pulverized coal is burnt in dry bottom boilers. The larger amount of unburned ash which is detained in the flue gas is called the fly ash. The residual of the ash is accumulated in water-filled hoppers at the bottom are called bottom ash, a porous, dark grey, granular, sand size material [45]. The pressing complications of using the bottom ash for fashioning geo-polymer products or as a replacement for cement are attributable to the relatively coarse nature, presence of high carbon content and heavy metal content [45]. Therefore, BA is generally exploited as a partial replacement for fine aggregates of normal concrete and lightweight concrete. However, due to the porous nature of the particles and high water absorption, it will not improve the compressive strength of mortar or concrete with increased amount of bottom ash [46].

2.3.1 Properties of Bottom-ash (BA)

As a material, BA is slightly grey or black as per the color, has a quite angular nature, with a porous surface structure [47].

2.3.1.1 Physical Properties

The surface texture of bottom ash is mainly porous and the particles usually have quite angular nature. When it comes to size, it includes a size range of fine stone to the sand. They are generally coarser in size than fly ash coal. According to the guidelines for coal ash on average sized coal as sand, with 50 to 90 % passing size 4.75mm (No. 4), to 10 to 60 % passing 0.42mm (No 40), and 0 to 10 % passing 0.075mm sieve size (No. 200) [48].

Spherical particles, rounded particles and sometimes intermittently shaped grains were exhibited in the electron micrograph scan of the ash (Figure 2-5). The specific gravity was 2.0 when measured by the pycnometer method. Low specific gravity value implies that void particles are present in substantial quantities in the ash [49] .

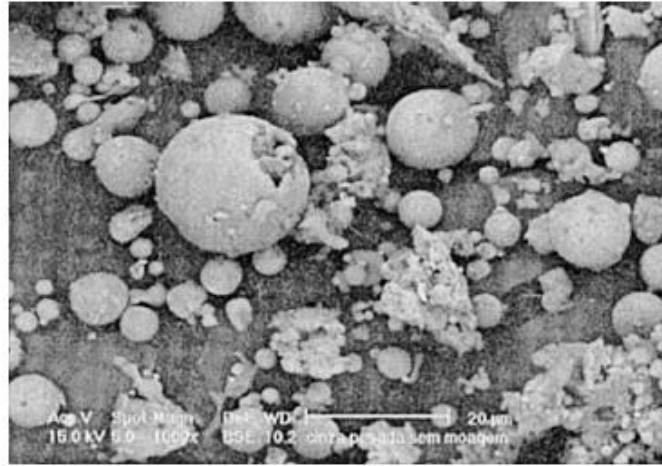


Figure 2-5 - Morphology of bottom ash (Cherief et al.)

2.3.1.2 Chemical properties

This material mainly comprises of silica, alumina and iron. However, calcium, magnesium and sulfate are also there in small numbers. In some cases the pH and also the salt content of the bottom ash tend to be low [47].

Norochcholai Thermal Power Plant is the only coal power plant in Sri Lanka. When the Bottom Ash from there was studied (Table 2-2) , it was found that the harmful elements; As, Pb, Cr, Cd, Cu, Ni are within the internationally specified toxicity limits [50].

Table 2-2 – Chemical Composition of BA (Hendawitharana et al)

Oxides (wt. %)								
SiO ₂	Al ₂ O ₃	Fe ₂ O ₃	MgO	CaO	K ₂ O	TiO ₂	S	LOI
56.0	26.7	5.8	0.6	0.8	2.6	1.3	0.1	4.6

Cherief et al [49] suggested that the reaction of bottom ash with calcium hydroxide is almost non-existence at early ages. Furthermore, they suggested that if grinded sufficiently the pozzolanic activity can be enhanced in bottom ash [49].

According to the chemical composition of BA of Brazil as per Cherief et al.[49], the Calcium content is much lower as of one percent and the combination of SiO₂ + Al₂O₃

+Fe₂O₃ has attained 88.5%, which implies that this ash can be categorized in to Type F ash in the ASTM standards [51]. Due to the presence of carbon, the loss on ignition (LOI) has occurred in this bottom ash[49].

2.3.1.2 *Mechanical properties*

The maximum dry density of BA is usually about 10% - 25% lesser than typical of the granular material nature. In other cases, the optimum moisture content could exceed that of the natural granular material.[47]

2.3.1.3 *Sustainability*

Apart from being a non- hazardous material, BA contributes towards reducing the amount of carbon dioxide. This is a much prudent choice in sustainable developments in order to minimize the carbon dioxide emission and in the sense of recycling the waste materials. [47]

As per a study conducted by SIRIM [47], the following points have been concluded:

- The waste sample was of physical hazards like volatility, ignitability and flammability.
- The major constituents do not include any toxic chemicals.
- The ash sample was environmental friendly and is free from any infectious microorganisms (SIRIM).

The construction industry can benefit at large from the utilization of bottom ash in building materials. With a world more focused on green and sustainable designs, sustainability of the final product can act as a key advantage in this application. Bottom ash also strikes as a cost economical material when compared to other alternatives.

2.3.2 Bottom ash as a partial replacement for fine aggregates

If bottom ash to be incorporated in a cementations mortar some of the conventional materials used in mortar is obviously need to be replaced. The two main constituents of cement mortar are cement and sand. However, due to the high carbon content and the granulose nature of bottom ash [45] it is hardly a replacement for cement. Thereby, bottom ash is often considered as a partial replacement for fine aggregates [44], [52]–[56].

In a study by Yang et al [54] it has been observed that, the compressive strength would decline when the % of bottom ash increases and a low w/c ratio or mineral admixtures like fly ash will not have a counter effect.

Aggarwal et al [44] incorporated bottom ash in concrete as a partial replacement for fine aggregates and concluded that it decreases the workability when the % of bottom ash increases in the mortar attributing to the high water demand. Compressive strength, density and the splitting tensile strength would also decrease with the increase in the % of BA.

As a matter of fact, Ramadoss and Sundararajan [43] agrees with the high demand of BA for water and recommends bottom ash in cement mortars. In each of these cases, the w/c ratio was between 0.5-0.6 which indicated the scarcity of water. However, Piyarathna et al. [57] has experimented with bottom ash as a replacement for river sand with a water cement ratio of 1.4. Their results show an increase of compressive strength when the % of bottom ash is increased contrary to the other literature. The w/c ratio has been maintained at 1.4 for the control sample and the % of BA replacing sand has been increased. This suggests that there could be an optimum w/c ratio which would give an increase in compressive strength.

2.3.3 Increasing thermal resistivity using BA

In the experiments carried out by Wongkeo et al [46] BA was used as a partial replacement for cement. Cement was replaced by BA at 10%, to 20% and 30% to weight and a thermogravimetry analysis was carried out. The results they obtained are showed in Figure 2-6. It can be observed that the thermal conductivity of the system has increased with the percentage of BA. This implies that when the percentage of BA increases thermal resistivity increases. Hence, bottom ash may be used as a thermal insulation material, and it might be a viable option due to low thermal conductivity and approach in sustainability,

In the experiments conducted by Torkittikul et al. [37] noticeable thermal insulation qualities were exhibited in BA blended mortar and concrete. It was observed that the thermal resistivity increases when the % of BA increases. More specifically, the thermal conductivity of mortar declines from 1.666 to 0.523 W/m K and that of concrete declines from 2.052 to 1.089 W/m K (Figure 2-7) [37].

When the content of BA was increased, the permeable pore space also increased. However, the negative effect on compressive strength was nonexistence [37].

A study by Cheng [58] confirmed that mortars with BA was observed to have a higher total porosity and capillary porosity which would help in increasing the thermal resistivity of the mortar.

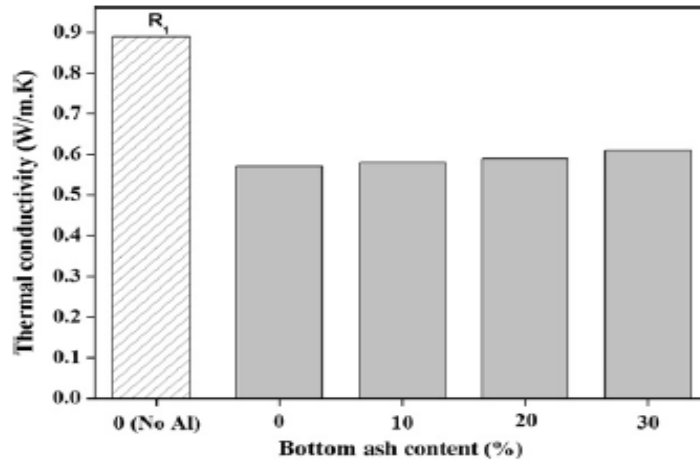


Figure 2-6 - Experimental results of Wongkeo et al.[45]

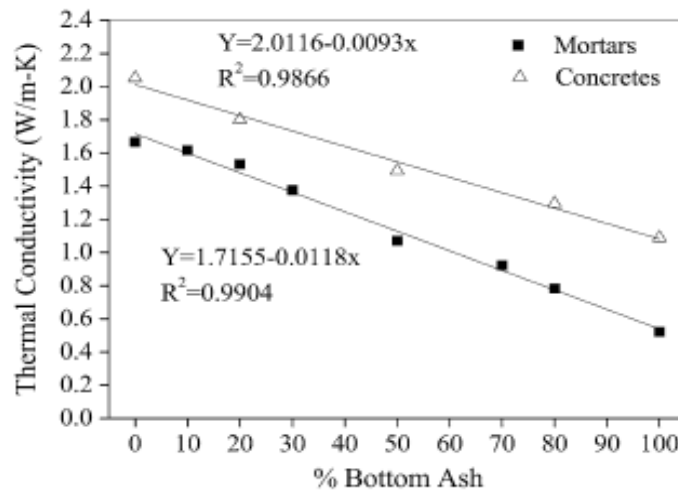


Figure 2-7 - Results of Torkittikul et al.[37]

2.4 Insulation materials for CFRP/Concrete composites

In the experiments carried out by Cree et al. [14], the surface of the FRP wrapped columns was spray-applied using an insulation system that they have developed called Sikacretes-213F, which was dispersed using a shotcrete rig to cover the surface of the column. The Sikacrete-213F was initially developed to be used as fire-resistant tunnel lining insulation and it was developed as a cement- based, dry mix fire protection

mortar for wet sprayed application. It comprises of hydrocarbon fire resisting phyllosilicate aggregates. The vermiculite in it serves as a filler material. Around temperatures between 700 °C and 1000 °C, the vermiculite filler expands, as the bound water evaporates until twenty times its initial size. This provides the protection scheme its exceptional heat insulation characteristics [14]. However, they concluded that, four hour fire endurance ratings could be achieved according to ASTM E119 [59] through Sikacrete-213F for FRP wrapped columns. However, the results from the fire endurance test concluded that the insulation system failed in maintaining the temperature of the epoxy layer below T_g [14].

Williams et al. [60] developed two reinforced concrete T-beams and reinforced them with CFRP sheets in flexure. Their performance under fire was investigated. Vermiculite/gypsum fire resistant cementitious insulation was used as a further protection mechanism. In both beams, the insulation was applied on side faces and the bottom face. Support conditions were made “axially restrained” and 48% of the predicted strength was applied as the loading. Both beams had a fire endurance period of 240 min. However, the beam 1 reached T_g within 16 – 36 min and beam 2 reached T_g between 55-57 min. Hence, the results indicated fire resistance period of 240 min is doubtful.

Six CFRP-strengthened RC beams were tested by Blontrock et al[61]. They were exposed to fire as per ISO 834 [62] and 38% of the flexural capacity was applied as the load. Combinations of gypsum board and rock wool were used to protect these beams from fire. The influences of the total thickness, location, method of bonding and length of insulation on fire performance were studied. In all cases, when the strengthening material reached approximately 66 - 81 °C, debonding of the CFRP took place. The temperature was in the range of the reported T_g of the epoxy adhesive used. Once the epoxy failed, the composite action was lost differing between 10 min and 60 min of fire exposure with the applied fire protection scheme.

Four CFRP – strengthened reinforced concrete beams were tested by Dong et al [10], where two of them were protected using a fireproof coating (SJ-2) [10] with different thicknesses. A calcium silicate board [10]was used to insulated the third beam, and it was glued with a high temperature adhesive. An ultrathin fireproof coating (SB60-2) [10], was layered via roller application on the fourth beam (Table 2-3).

Table 2-3- Thermal Properties of Insulation Materials (Dong et al)

Insulation Material	Property		
	$\lambda/W \cdot K^{-1} \cdot m^{-1}$	$c/J \cdot kg^{-1} \cdot K^{-1}$	$\rho/kg \cdot m^{-3}$
Thick Coating (SJ-2)	0.12	500	1000
Calcium Silicate Board	0.061	740	250
Ultrathin Coating (SB60-2)	0.06	800	600

They concluded that the adequate fire endurance of 2 hours on the whole span can be gained for concrete beams strengthened with CFRP and insulated with thick coating (SJ-2) [10]. U-shaped insulation was also deemed as an effective method. Furthermore, specimens 1, 3 and 4 were able to withstand the load throughout the test procedure although the glass transition temperature T_g was reached within 60 minutes. It was concluded from the results that the main objective of the insulation materials at early stage was to hinder the failure of the adhesive. For the later stage it was to downgrade the performance degradation of concrete, and internal reinforced bars [10].

2.5 Summary

Through the initial literature review it was learnt that, in case of CFRP- Concrete composites, the behavior at elevated temperature is mainly affected by the glass transitioning temperature of the adhesive binding the CFRP to the concrete. The insulation material should have a low thermal gradient such that it prevents adhesive from reaching T_g . Among the locally available materials which can be used as cementitious insulation materials, bottom ash seems to be a viable option considering the sustainability and cost efficiency.

2.6 Further research needs

In order to develop an insulation system using bottom ash for CFRP-Concrete composites, first the micro structure of bottom ash from Norochcholai power plant should be investigated. It was identified that further research on thermal conductivity, compressive strength and workability of materials will be required in order to develop an insulation material. Then, it would require to research on their applicability on CFRP composites.

3 PHYSICAL AND CHEMICAL STRUCTURE OF BOTTOM ASH – PHASE 1

3.1 Introduction

The methodology proposed in Chapter 1 – Figure 1-1 suggests that the initial approach of this research is to develop a cementitious thermal insulation mortar which is later to be applied on CFRP composites. The first part of developing a mortar is to get familiarized with a possible improvement material for conventional mortar. With the knowledge gathered from literature review, bottom ash was selected for partial replacement of fine aggregates. Figure 3-1 gives an overview for the test program for phase 1.

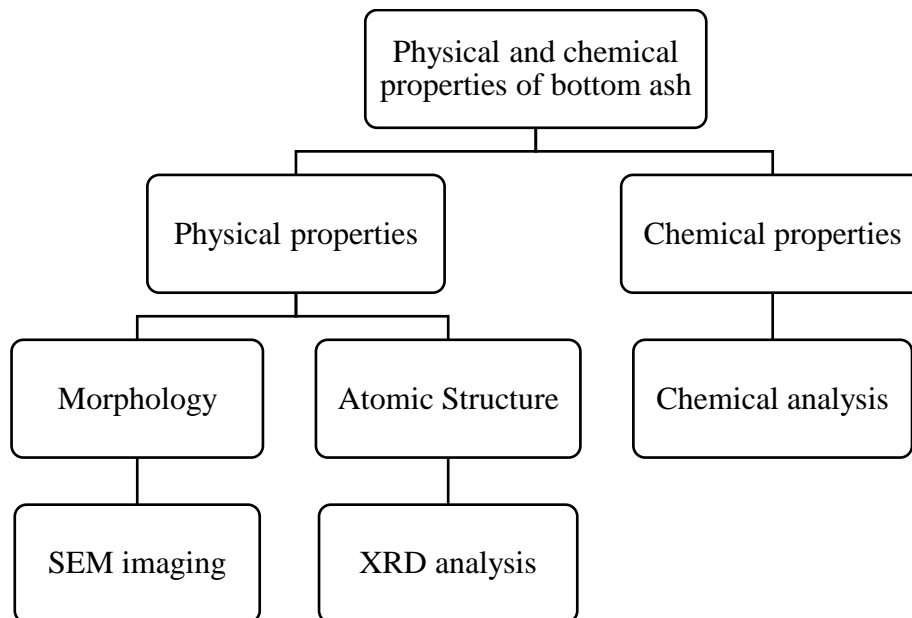


Figure 3-1 - Overview of phase 1

As the literature suggested, physical, chemical and mechanical characteristics of bottom ash can be highly depended on the microstructure of bottom ash [45], [49]. Therefore, it was investigated prior to the commencement of the development of the insulation material. This chapter elaborates on the finding on physical and chemical properties of bottom ash extracted from Norochcholai Lakvijaya Coal Power Plant of Sri Lanka.

3.2 Experimental program

As mentioned before, Norochcholai coal power plant is the only power plant in the country in operation. Therefore, BA from their power generation process was used for the experiment (Figure 3-2)



Figure 3-2 - Bottom ash physical appearance

The particle variation was observed using the Scanning Electron Microscope (SEM) “Zeiss EVO 18 research” for understanding the physical nature of BA. Next, a chemical analysis was carried out for the purpose of identifying the chemical composition of the material. Furthermore, an X-Ray Diffraction (XRD) imaging was carried out using a “BRUKER ECO D8 advance diffractometer” and the results for 2-theta values between 0 -100 was observed.

3.3 Results and Discussion

3.3.1 SEM imaging

Figure 3-3-(a) provides morphology of Brazilian bottom ash. And Figure 3-3-(b) is from Norochcholai power plant. Scanning electron microscopy (SEM) depends upon a finely focused beam that is scattered across the sample. As it can be observed, the particle sizes and distribution seem to differ with the sample. This suggests that the topography of the particles might differ with the samples obtained from different sources. The lack of dense inner structure and considering the shape of BA particles would collaborate in lowering the thermal conductivity. However, the specific gravity of 2.0 suggested that the material is consisting hollow particles in significant proportions. In case of a porous material, its thermal conductivity relies upon the geometrical distribution of the void phases (i.e. pore structure) and volume fraction of its solid constituents [31].

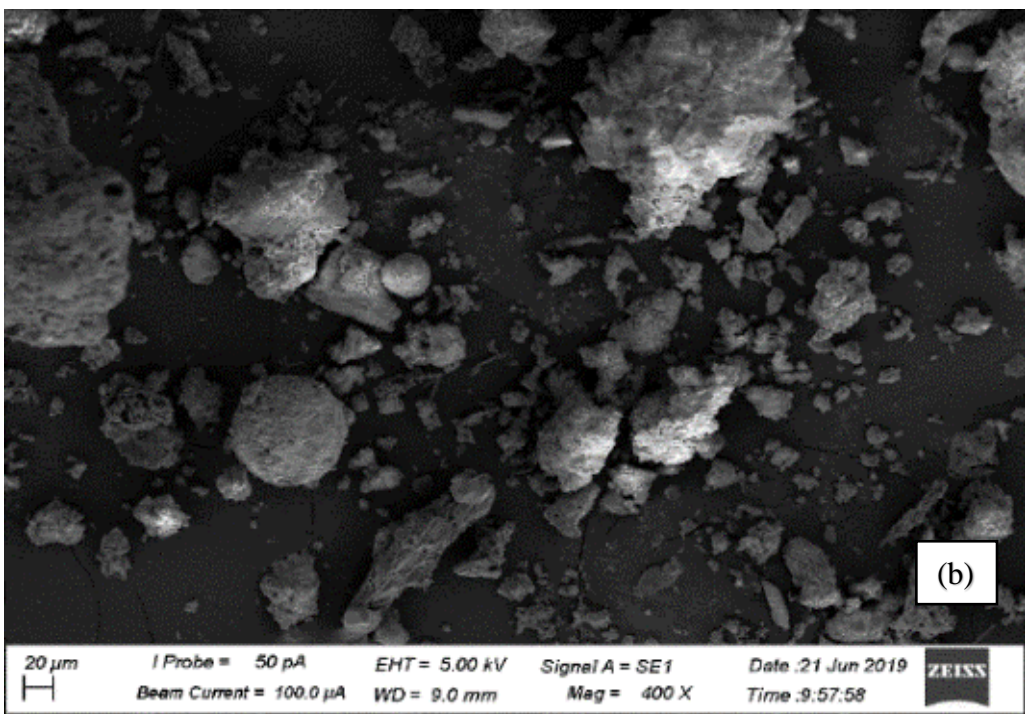
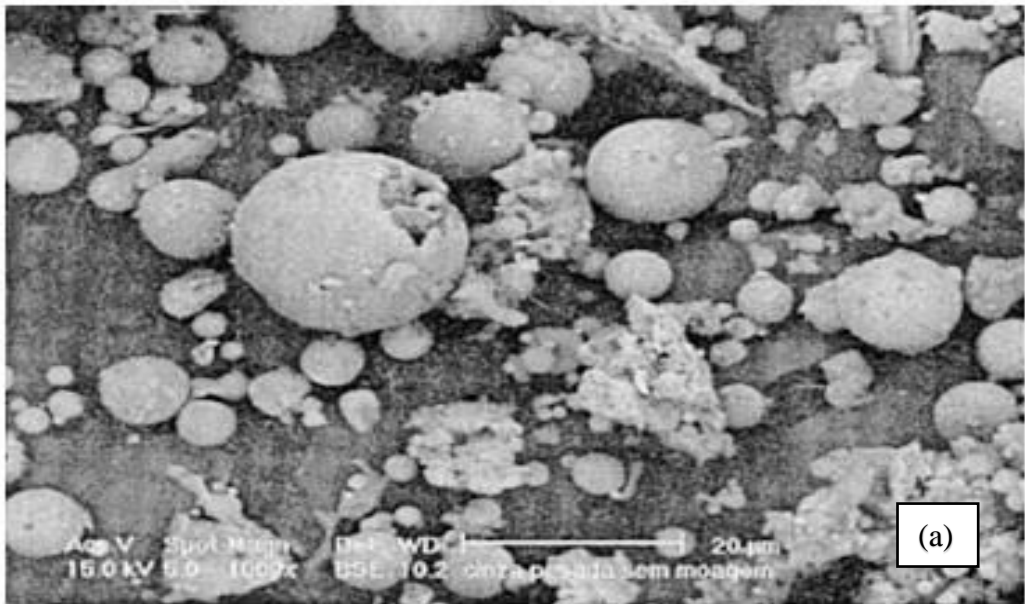


Figure 3-3 - Morphology a) Literature (Cheriat et al) b) Current Study

3.3.2 XRD analysis

Figure 3-4 gives the XRD imaging for a samples of BA from Russia [63] and Figure 3-5 gives the XRD imaging for samples of BA from Sri Lanka (Current Study).

Quartz (SiO_2), Mullite ($3\text{Al}_2\text{O}_3 \cdot 2\text{SiO}_2$) and Aluminum oxide (Al_2O_3) crystalline phases were dominantly appeared in XRD spectra of Norochcholai sample whereas Quartz (SiO_2) and Calcite (CaCO_3) were identified in sample from Russia. These results show that Norochcholai bottom ash has shown significant variation with sample from Russia. However, it was revealed that the XRD results of Norochcholai BA sample are closer to the generally accepted XRD results of BA [29, 30] in terms of crystalline phases, diffraction peak positions (2θ) and their intensities. Moreover, literature [35] suggest that the fused structure BA amongst Mullite pose lessened conductance than the quartz silica structure of river sand.

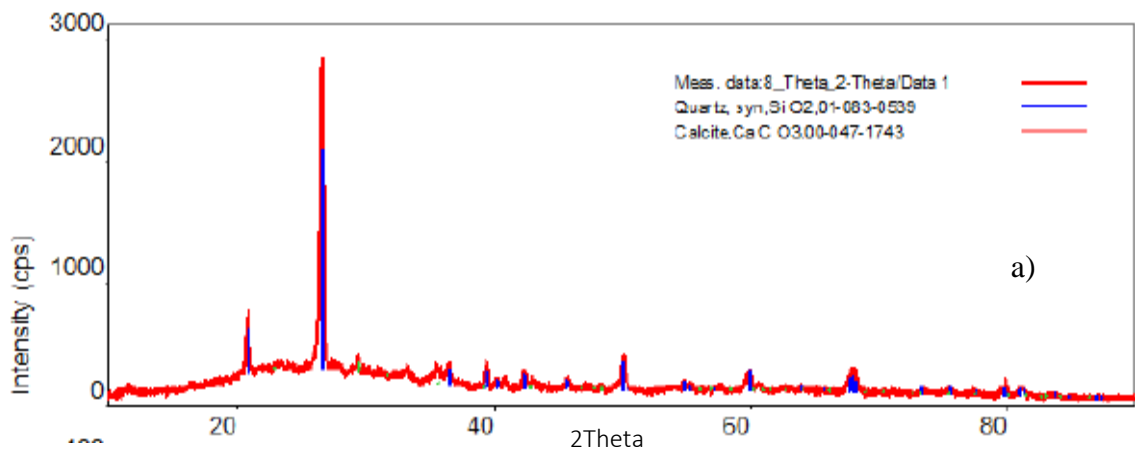
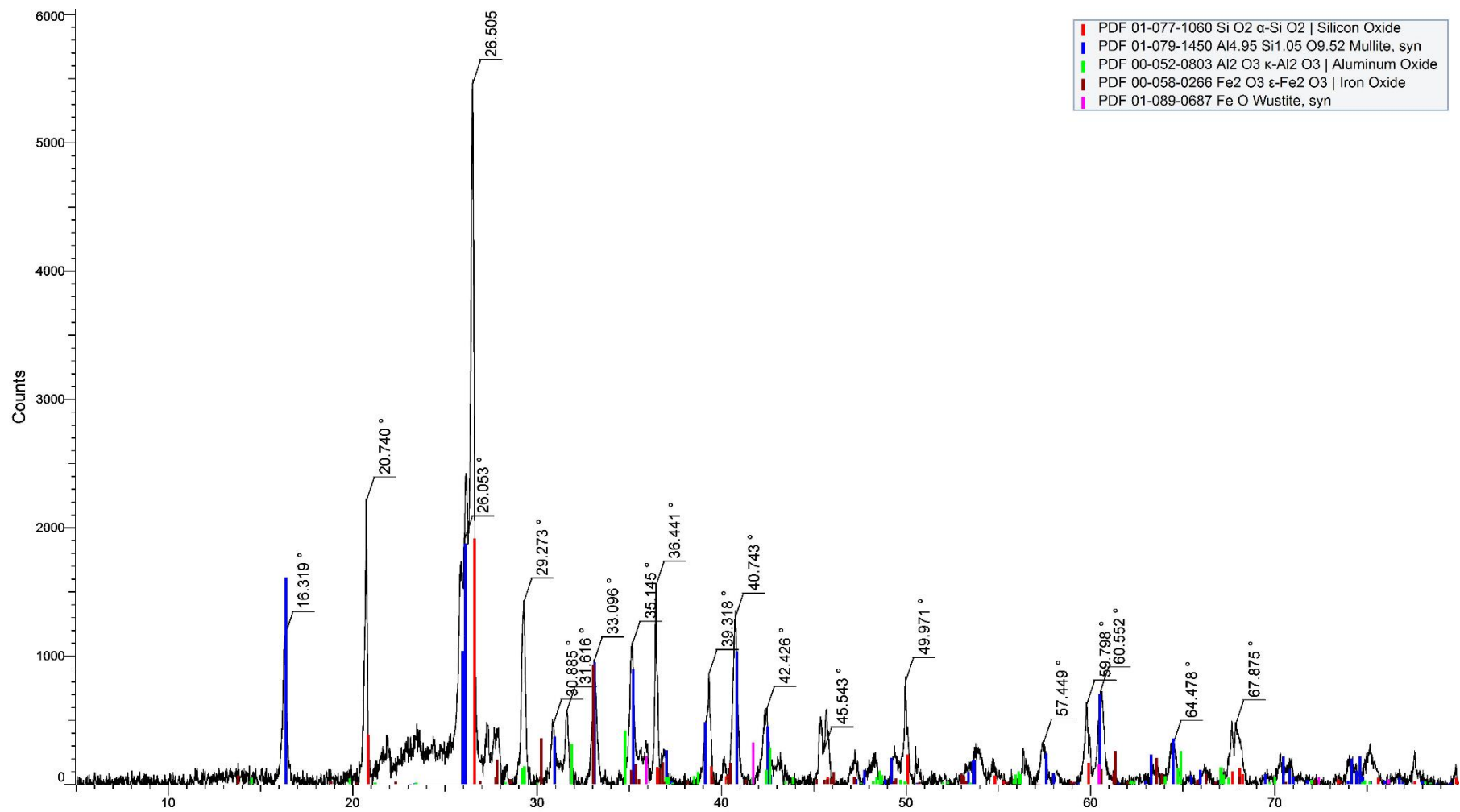


Figure 3-4 - XRD Imaging - Literature (Mal'Chik et al) [63]



2Theta (Coupled TwoTheta/Theta) WL=1.54060

Figure 3-5 - RD imaging - Current Study

3.3.3 Chemical analysis

When the chemical composition of BA is considered, literature suggests that major component of the material is consisting of silica, alumina and iron [47], [49], [50]. However, the byproduct of a combustion process tend to differ from each other due to various environmental factors. For example, the coal for the Norochcholai power plant are imported from Indonesian ores. The process of coalification itself suggests that the composition of coal could vary with the dead vegetation that involves in the process. The coal from the literature would be from different ores, hence having different chemical compositions. Note that the differences will not be drastically different (Table 3-1). However, the composition must be taken in to account. Furthermore, the toxicity limits of BA from Norochcholai also are within the allowable limits considering the elements like As, Pb, Ni, Cd etc.

Table 3-1 - Chemical Composition

Oxide	Brazil [49]	Russia [63]	Sri Lanka (Current Study)
	Percentage %	Percentage %	Percentage %
SiO₂	56.0	55.7	48.23
Al₂O₃	26.7	21.83	19.39
Fe₂O₃	5.8	7.44	3.61
MgO	0.6	1.95	1.33
CaO	0.8	6.8	7.74
Na₂O	0.2		0.95
FeO	-	6.69	-
K₂O	2.6	3.53	0.62
TiO₂	1.3	1.11	1.18
S	0.1	-	-
P₂O₅	-		1.16
SO₃	-	0.72	-

The chemical composition of sand comprises from more than 90% of SiO₂. However, the results in Table 3-1 shows that the % of Silica (SiO₂) in bottom ash is around 50% and around 25% is Alumina (Al₂O₃). The research of McQuarrle [64] shows that the thermal resistivity of Al₂O₃ increases at elevated temperatures. Thereby, as the decrease of SiO₂ in bottom ash than sand is mainly fulfilled by Al₂O₃, it could be assumed that the insulation properties of the material would increase if bottom ash was to be introduced.

3.3.4 Particle size distribution

Figure 3-6 shows the particle size distribution of bottom ash with river sand. A sieve analysis was carried out as per BS1377:Part 2:1990 [65]. The variation suggests that the particles are fairly less graded as river sand. Consider the sieve size 2.36 mm. even though more than 80% of river sand particles pass through the sieve only 50% of bottom ash samples pass through indicating higher particle sizes when compared to river sand. More graded the particles are, more they could be compacted and more voids will be filled on its own. On the other hand, the lesser graded bottom ash would have more voids when compacted which would later accommodate heat passing through the material to be entrained. Hence, acting as a better insulation.

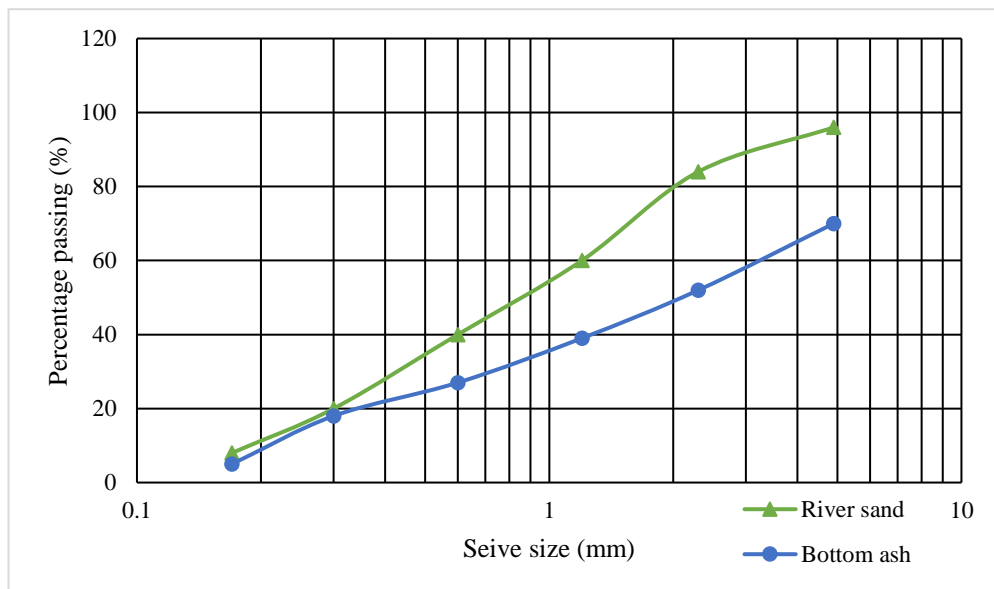


Figure 3-6 - Sieve analysis

3.4 Summary

The objective of this chapter was to understand and investigate the physical and chemical properties of BA. As literature suggested, the morphology and chemical properties of BA can affect the mechanical and thermal characteristics of any mixture made using it. It was concluded that BA retrieved from Norochcholai power plant seem to be more or less in agreement with results from literature sources. However, the changes in chemical composition suggest that there can be slight differences of how BA would work. However, not drastically.

4 PHYSICAL AND MECHANICAL PROPERTIES OF THE DEVELOPED PLASTER – PHASE 2

4.1 Introduction

Phase 2 of the research expects to the innovate an insulation plaster using BA. Considering the general industry practices for plaster, 1:3 cement : sand ratio was selected. Then, sand was replaced with bottom ash in percentages to weight and several samples were developed. The overview of the test series for phase 2 is given in Figure 4-1.

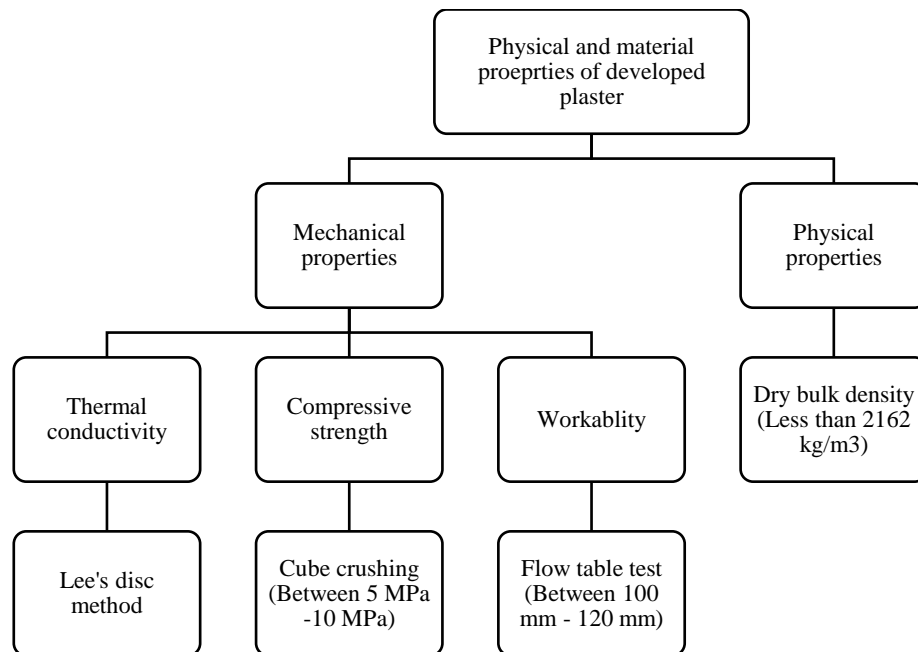


Figure 4-1 - Overview - Phase 2

The mix proportions, where sand was replaced with BA were first tested for their thermal conductivity. Literature suggests that both thermal conductivity and compressive strength of mortars should decrease when a porous material is introduced. Hence, several samples with good thermal performances were isolated and compressive strength was tested. Then, attempts were made to bring the plaster in accordance with the guidelines for N type mortars [66] which could be applied on superstructure of buildings. Figure 4-2 gives the iterative process followed for the development of insulation plaster.

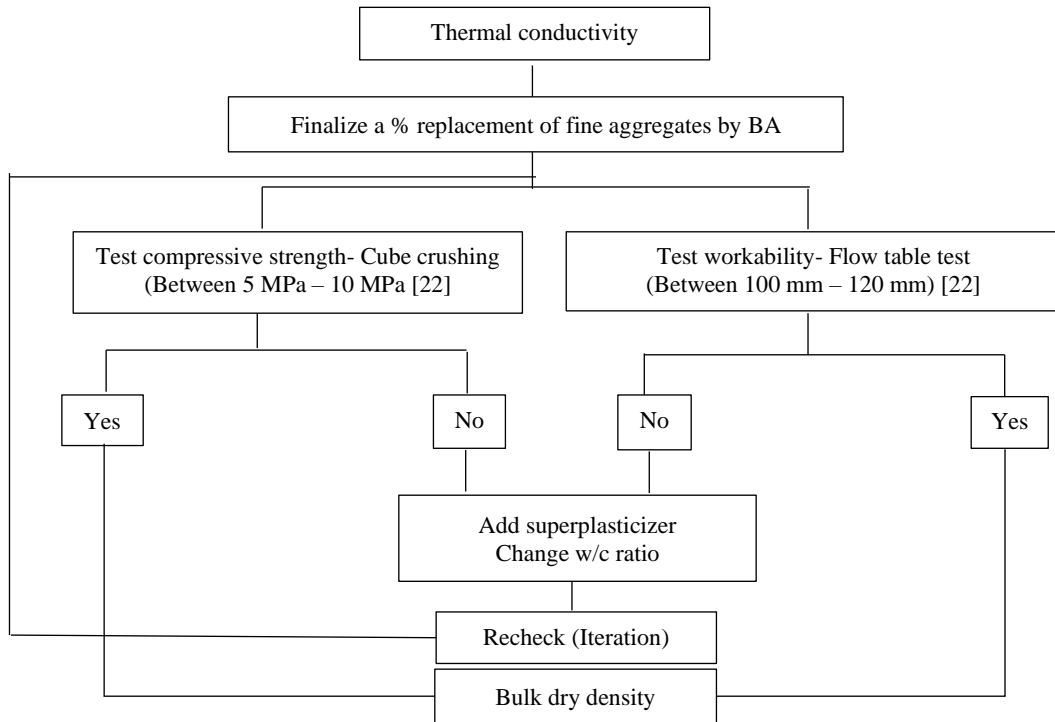


Figure 4-2 - Iterative process

4.2 Experimental program

4.2.1 Materials

Ordinary Portland Cement (OPC) of with a 28-day compressive strength of more than 42.5MPa [67] (Figure 4-3-a)) was used as the basic cementitious material for all the mixtures in accordance with BRE mix design method. River sand passing through 2.36 mm sieve (Figure 4-3-b))and BA obtained from Norochcholai coal power plant of Sri Lanka passing through 2.36 mm sieve were used (Figure 4-3-c)).



Figure 4-3 - Materials – a) Cement b) Sand c) Bottom ash

4.2.2 Sample Preparation

Samples were cast by replacing sand with BA from 10% to 100 % as given in Table 4-1. The samples were cast using 1:3 Cement: Sand ratio, the typical wall plaster mix design with w/c ratio of 0.6.

Table 4-1 - Mix proportions

Sample	% of Bottom Ash to Wt.	Cement (g)	Fine aggregate (g)	Bottom Ash (g)
BA0	0	50	150	0
BA10	10	50	135	15
BA20	20	50	120	30
BA30	30	50	105	45
BA40	40	50	90	60
BA50	50	50	75	75
BA60	60	50	60	90
BA70	70	50	45	105
BA80	80	50	30	120
BA90	90	50	15	135
BA100	100	50	0	150

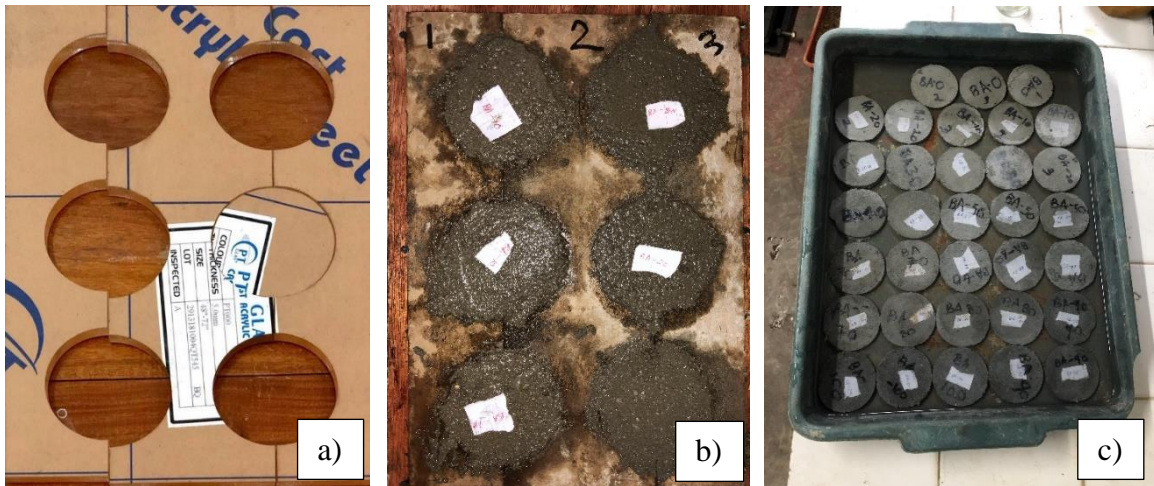


Figure 4-4 - Thermal conductivity samples - a) Molds b) Casting c) Curing

Samples with 60 mm diameter and 5 mm thickness were cast using a specially prepared molds as shown in Figure 4-4. They were kept for curing for 28 days and then tested for thermal conductivity using the Lee's disc apparatus (Figure 4-5) in accordance with ASTM D7340 – 07 [68].

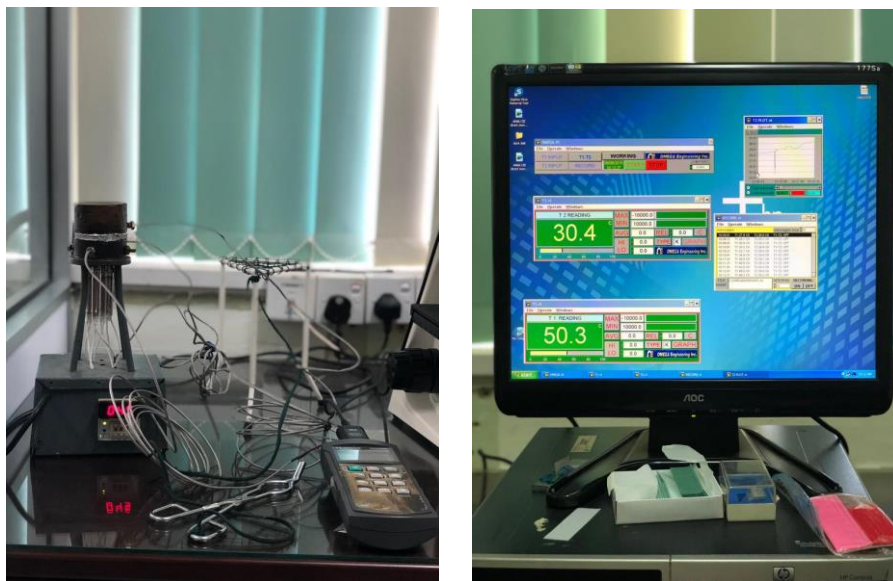


Figure 4-5 - Lee's disc apparatus

Several samples with adequate thermal conductivity were identified and mortar cubes with 70 mm dimensions were cast (Figure 4-6) for selected 3 mix proportions for compressive strength testing in accordance with ASTM C109 [69].



Figure 4-6 - a) Compressive strength test cubes b) Compressive strength testing

4.3 Results and Discussion

4.3.1 Thermal conductivity

It was decided to cast the control mortar samples for a Sand/Cement and water/cement ratios of 3 and 0.6, respectively to match the common industry practice. The thermal conductivity of the control sample (BA) was validated with results obtained from literature (Table 4-2).

Table 4-2 - Control sample thermal conductivity literature review

Reference	Thermal Conductivity (W/mK)	Method
Liu <i>et al.</i> [70]	2.71	Transient hot wire method
Demirbog[71]	1.17	Hot wire method
Olmeda <i>et al.</i> [72]	1.4	Mathis modified hot-wire technique
Mendes <i>et al.</i> [73]	1.26	Heat flow meter
Corinaldesi <i>et al.</i> [74]	0.739	Guarded hot plate method
Torkittikul <i>et al</i> [37]	1.66	Transient line heat source method
Current Study	1.44	Lee's disc method

The results obtained using Lee's disc method are given in Table 4-3. When calculating the thermal conductivity values from the Lee's Disk Method, it was assumed that the heat dissipated from the heat receiver of the Lee's disk apparatus was equal to the heat conducted through the sample and the heat loss due to environmental conditions is

negligible. The calculations for heat transfer analysis are discussed at length in Chapter 5. This variation was compared against the results of Torkittikul et al [37] in order to narrow the findings for further investigations .

Table 4-3 - Thermal Conductivity results

% of BA replacing sand to weight		Thermal Conductivity (W/m°C)	
Current Study	Torkittikul et al. [36]	Torkittikul et al. [36]	Current Study
0	0	1.7	1.44
10	7	1.65	1.36
20	14	1.6	1.15
30	22	1.4	1.24
40			0.99
50	40	1.1	0.82
60			0.8
70	61	0.9	-
80	73	0.8	0.5
100	100	0.5	

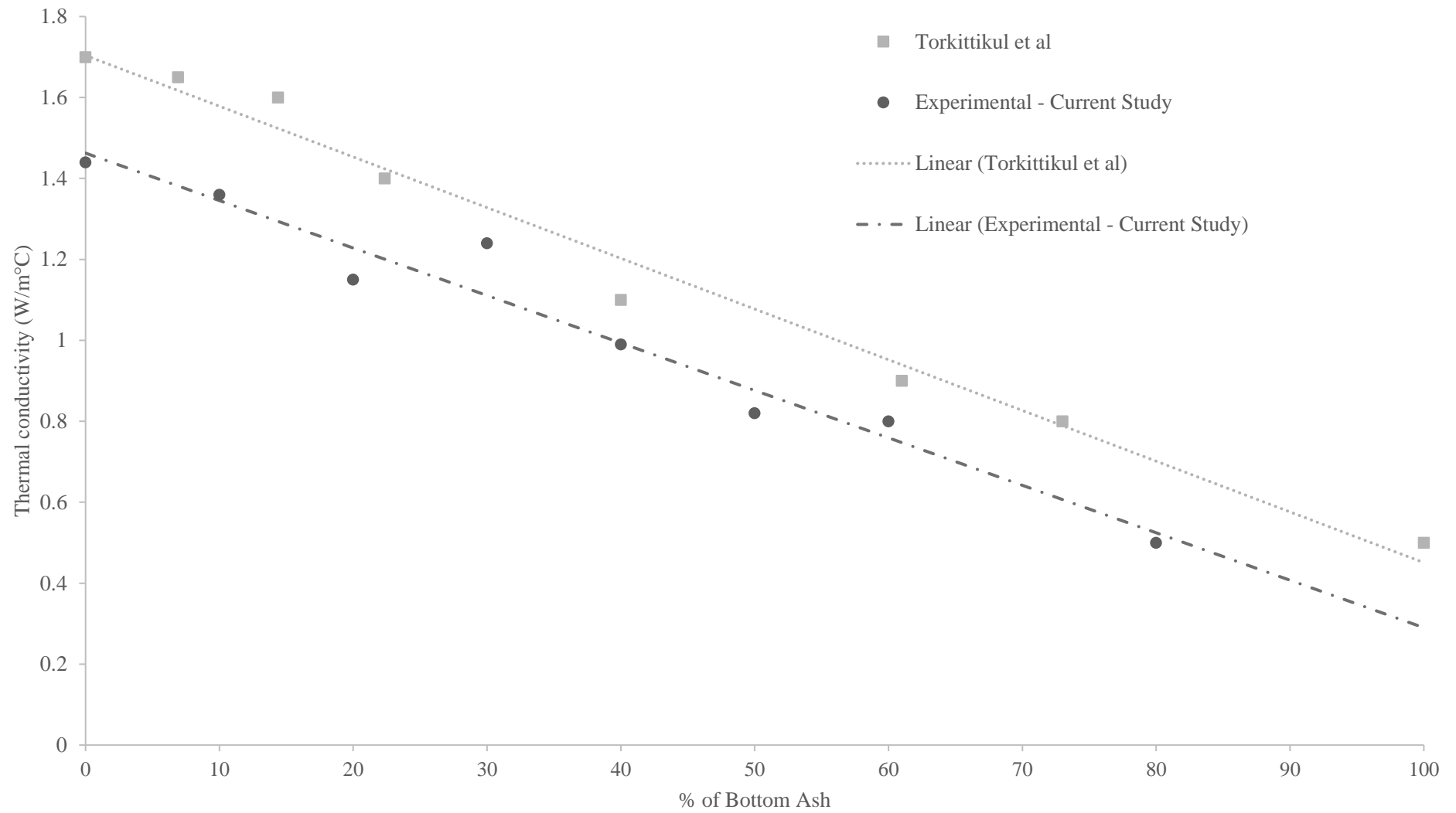


Figure 4-7 Thermal conductivity variation

The average thermal conductivity of the samples displayed a similar variation (Figure 4-7) with the results from studies of Torkittikul et al [37]. This implies that the introduction of BA a porous material to conventional mortar has the capacity of reducing the thermal conductivity of mortar by 86% at most. However, this also implies that the compressive strength of the mix should also reduce with the increase of percentage of BA. Therefore it was decided to choose a percentage replacement which would have moderate effects on both thermal conductivity and compressive strength. Thereby, 50%-70% of BA replacing fine aggregates of the mix design was selected and tested for compressive strength.

4.3.2 Compressive Strength

Three mix proportions were isolated from the above samples, namely 50%, 60%, 70% and then tested for their compressive strength at 7 days (Table 4-4 and Figure 4-8). The average compressive strength of the samples decrease with the increase of the % of BA in the samples. The increase of porosity of the samples with the increase in % of BA could be the main reason for this behavior as suggested in literature.

Table 4-4 Compressive strength results

Sample	Avg. Compressive Strength (N/mm ²)
BA0	20.63
BA50	4.41
BA60	3.62
BA70	4.11

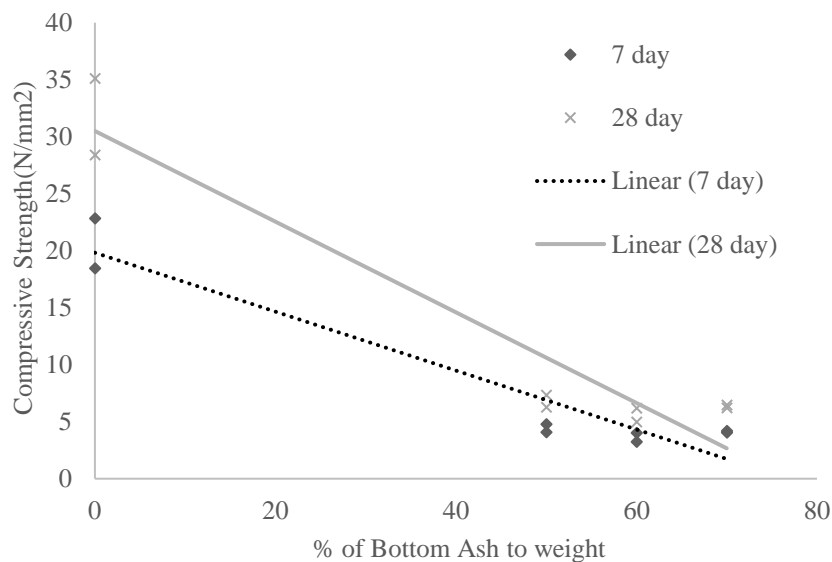


Figure 4-8 - Variation of compressive strength

The results from the compressive strength testing suggested that there is a drastically drop in the strength when BA was introduced. However, as mentioned in the literature review, this behavior can be expected when a porous material is introduced to the mix. The guidelines for N type mortars in ASTM C1329 / C1329M [66] suggests that the 28 days strength of the mortar should be around 5 MPa – 10 MPa. Therefore mitigation methods were required to improve the plaster.

When the workability and consistency of the mortars were observed, it was understood that the w/c ratio of 0.6 is not adequate for the water demand of the mix. BA was oven dried before using in order to make sure that no amount of water is supplied to the mix by BA. Therefore it was understood that, the w/c ratio should be increased in steps and a correct ratio should be identified which could increase the workability and strength of the plaster.

➤ Changing water/cement ratio

The w/c ratio was increased from 0.6 to 1.4 in step wise and the compressive strength and workability of the mixes were recorded.

Consistency of the plaster was the next issue to be addressed. Increasing the water cement ration could further add up to decrease in compressive strength. Or else considering the current consistency of the mix, it is susceptible for bleeding. Solution for both these issues could be resolved by introducing a superplasticizer to the mix.

➤ Adding superplasticizer

Generally, in civil engineering, strength enhancing and workability increasing admixtures are a common solution when in need. Therefore, it was decided to use a strength enhancing admixture as the second option of increasing the strength of the mixture. Two different percentages of superplasticizer was added to the plaster and compressive strength and workability was noted.

4.4 Experimental program

4.4.1 Materials

In all mixtures, Ordinary Portland Cement (OPC) with 28-day compressive strength of more than 42.5MPa [67] was used. The fine aggregates were river sand passing through 236 mm sieve and BA was extracted from Norochcholai power plant in Sri Lanka which is also passing through 2.36 mm sieve and oven dried. The superplasticizer used was Millennium Hypercrete [75] developed by Millennium Concrete Technologies (Figure 4-9).



Figure 4-9 - Materials measured for BA60

4.5 Sample preparation

The mix proportions that were used are given in Table 4-5. The mixing was carried out using a mechanical mixture. The superplasticizer was added to one third ($1/3$) of the amount of water measured and added at the beginning. Then the measured water was added considering the workability. 70 mm cubes were prepared and tested at 7 days and 28 days for compressive strength according to ASTM C109 [69].

Table 4-5 - Modified mix proportions

Sample	Cement (Kg)	Fine aggregate (Kg)	BA (Kg)	W/C ratio	Superplasticizer (ml/Kg of cement)
BA50	1	1.5	1.5	0.8	0
BA50	1	1.5	1.5	1	0
BA50	1	1.5	1.5	1	10
BA50	1	1.5	1.5	1	12
BA60	1	1.2	1.8	1	0
BA60	1	1.2	1.8	1.2	10
BA60	1	1.2	1.8	1.2	12

4.6 Results and Discussion

Firstly, the w/c ratio of BA60 sample mix was changed from 0.6 to 1.4 and approximate w/c proportion was selected (Table 4-6, Figure 4-10).

Table 4-6 - Results for compressive strength and workability of BA60 with different w/c ratios

w/c ratio	7 day Strength (N/mm ²)	Average Flow(mm)
0.6	4.0	
0.6	3.2	-
0.8	6.42	
0.8	6.38	-
1	8.43	
1	9.60	88.5
1.2	10.00	
1.2	10.50	150
1.4	6.68	
1.4	5.65	180
1.6	4.70	
1.6	3.83	220

The results gives a bell curve where the compressive strength increases until w/c reaches 1.2 and then decreases. Similar variation is shown in workability. This concludes that 1.2 can be the optimum w/c ratio for BA60. In case of mixes with less BA %, a lesser w/c could be used. For example, for BA50 w/c ratio can be 1.

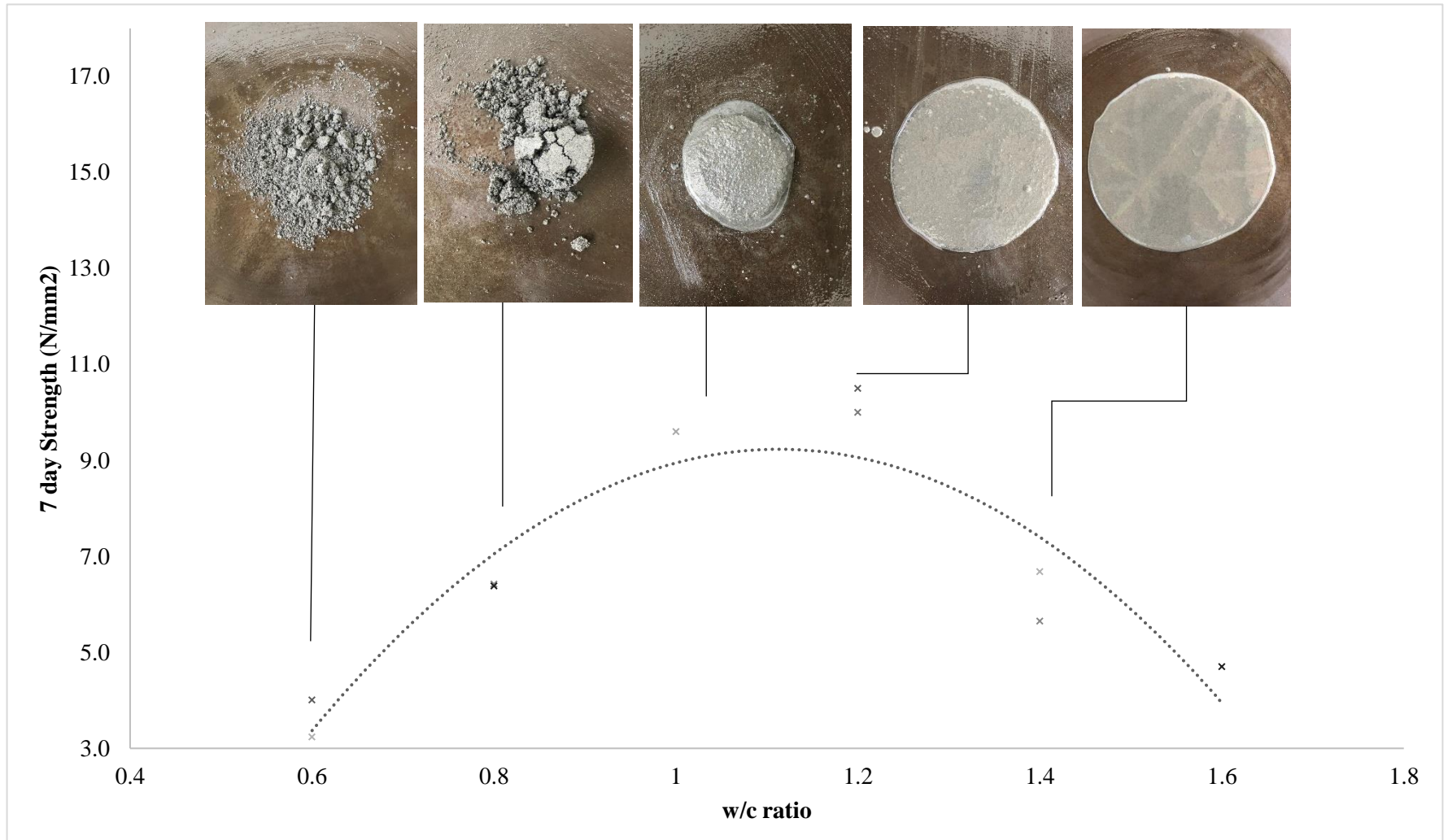


Figure 4-10 - Compressive strength and workability variation

The average results for the samples when, a) w/c ratio was changed and b) superplasticizer was added for BA50 and BA60 are given in Table 4-7.

Table 4-7- Average test results

Sample	w/c Ratio	Superplasticizer ml/Kg of Cement	Average Strength (N/mm ²)	Average Density (Kg/m ³)	Average Flow (mm)
BA50	1	0	13.07	1842	123
BA50	1	10	9.96	1763	147.5
BA50	1	12	11.32	1856	142.5
BA60	1	0	9.83	1713	97.5
BA60	1.2	10	5.08	1712	175
BA60	1.2	12	8.95	1725	150

The manufacture guidelines of the superplasticizer suggests that for 100 kg of cement, 1 l - 1.2 l of admixture can be used.

$$100 \text{ kg} \rightarrow 1.2 \text{ l} (= 1200 \text{ ml}) \text{ or } 1 \text{ l} (= 1000 \text{ ml})$$

$$1 \text{ kg} \rightarrow 12 \text{ ml} \text{ or } 10 \text{ ml}$$

Figure 4-11 shows flow table results for two trial mixes performed with and without admixtures. As it can be observed the mixture without admixture has low consistency and bleeding occurs when the test is performed. This advocates the need for admixtures in the plaster. Thereby, the optimum w/c ratios that were found during the previous test series was further modified for two different proportions of admixture (12 ml and 10 ml per 1 kg of cement) (Table 4-7).

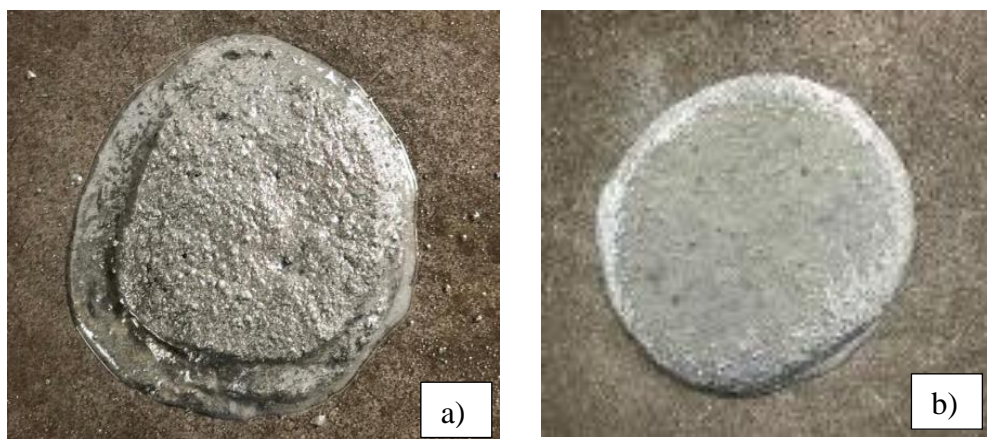


Figure 4-11 – a) Plaster without admixture b) Plaster with admixture

The variation of compressive strength of mixes for these proportions are given in Figure 4-12. As it can be observed, BA60 shows more improvement in results than that of BA50. Furthermore, when a higher percentage of admixture is used compressive strength increases over 10 MPa, which exceeds the standard requirements. Therefore using 10 ml of admixture could be recommended. In other words, spending more money on admixture to gain more strength than the requirement is futile.

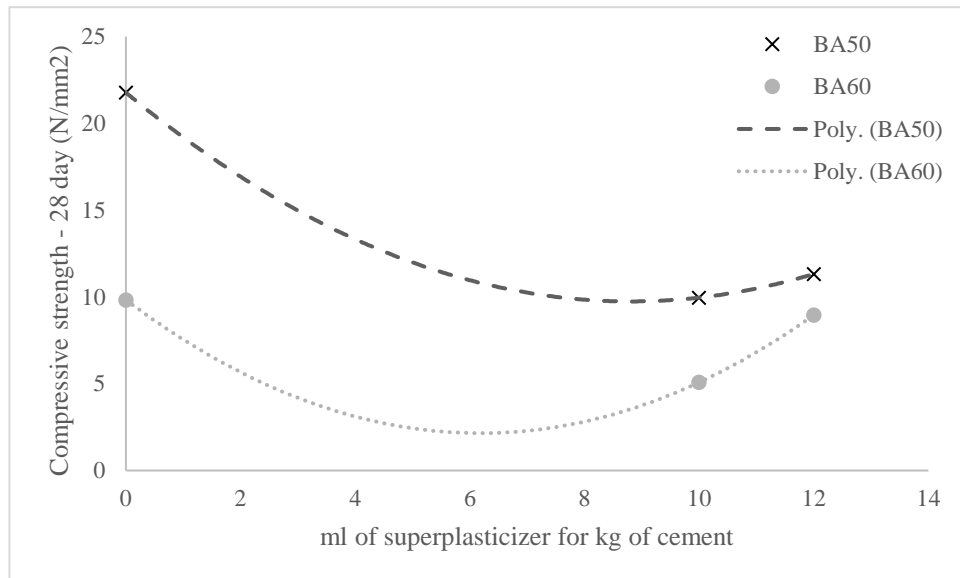


Figure 4-12 - Variation of compressive strength with amount of Superplasticizer

Figure 4-13 shows the variation of flow with the amount of admixtures. It can be observed that the flow has been improved with the introduction of superplasticizer along with consistency.

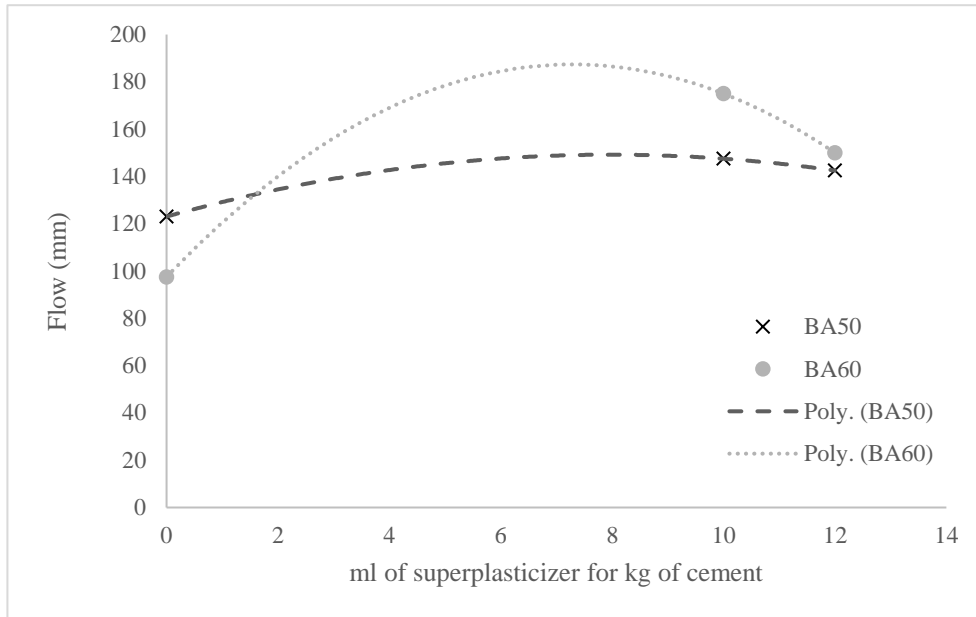


Figure 4-13 - Variation of flow with amount of Superplasticizer

Furthermore, Figure 4-14 shows the variation of dry bulk density of the plaster with the amount of admixtures used. Although BA50 has shown some inconsistencies BA60 has been able to maintain the density within the initially improved range in all cases.

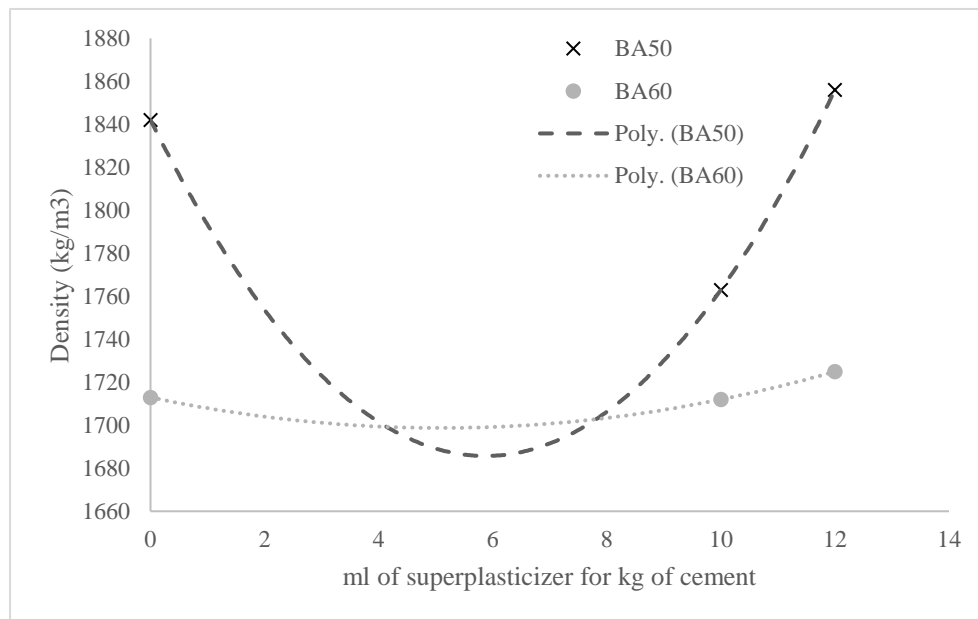


Figure 4-12 - Variation of density with amount of Superplasticizer

By the end of phase two of the research, an insulation plaster using BA as a replacement of sand was developed. With the results from changing the w/c ratio and

adding superplasticizer, it was decided that BA60 with 10ml admixture and 1.2 w/c ratio is the optimum mix proportion as an insulation plaster. It has the ability to reduce thermal conductivity by approximately 50%. The compressive strength and workability results were in agreement with ASTM guideline for N-type mortars.

4.7 Summary

The objective of phase two of this research was to develop an insulation plaster by replacing sand by BA in conventional plasters. The mechanical properties of the developed plaster was analyzed and compared against ASTM standards for N-type mortar. The thermal conductivity of samples were measured and an appropriate percentage of replacement of BA was selected. It was verified that the thermal conductivity of mortar mixed with BA will decrease with the % of replacement. The compressive strength results concluded that the increase of porosity of the mix have an adverse effect on strength. Then a plaster was developed using that percentage. The issues of the mix were identified as lack of workability and compressive strength. They were accountable for the high water demand of dry BA. The mix was improved by changing w/c ratio and adding superplasticizer in iterative steps. At the end of this phase BA60 with 10 ml admixture per kg of cement and 1.2 w/c ratio was concluded as the best case scenario.

5 HEAT TRANSFER ANALYSIS

5.1 Introduction

In case of an insulation material, the main concern lies on the amount of heat that would transfer through the material. That is, the amount of heat that can be resisted by the material. Therefore, the first part of the research was focused on the heat transfer or the thermal conductivity of BA mixed mortar. Figure 5-1 shows a schematic diagram of the experimental procedure.

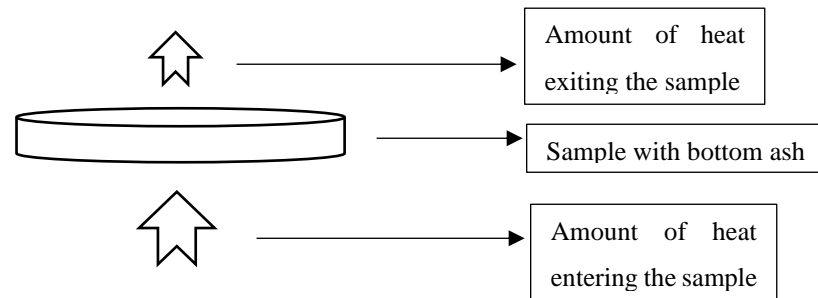


Figure 5-1 - Schematic Diagram for heat transfer

5.2 Procedure

The Lee's disc method was used to determine the heat transfer. The apparatus for Lee's disc is given in Figure 5-2. The sample that was used for this apparatus was in the form of a disc and it had relatively small thickness compared to its diameter as mentioned in chapter 3 (5 mm thickness, 60 mm diameter). The area of the disc ($\pi D^2/4$) being high compared to area exposed during the experiment ($\pi D\chi$) made the heat loss from the edge negligible.

As shown in the schematic diagram (Figure 5-1), heat flows through the sample bottom to top. In this case, the increment of heat in the top plate is monitored in order to understand how much heat is transferred through the sample.

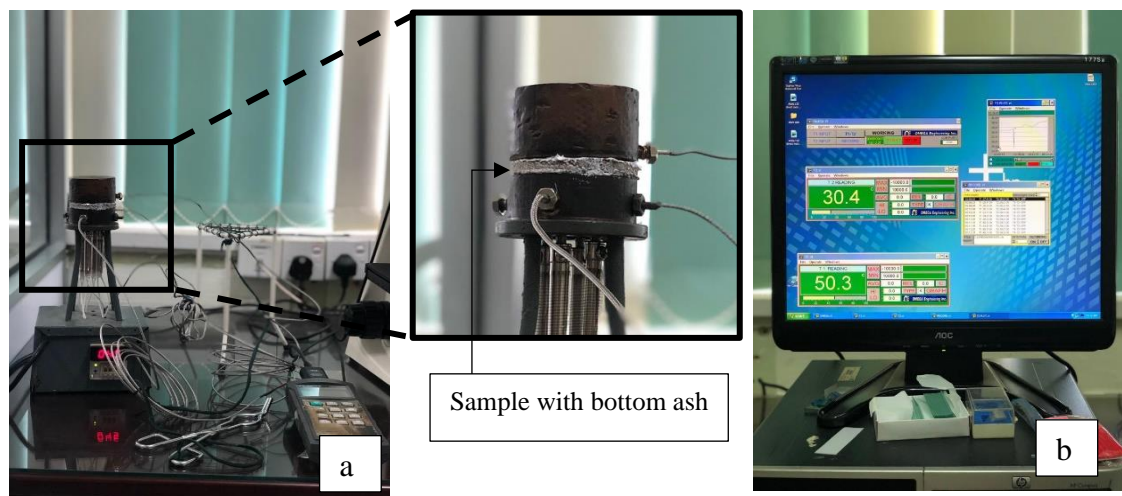


Figure 5-2 - Lee's Disc apparatus a) test setup b) Computer program

Once the sample was placed on the Lee's disc and the heat is provided, after a certain amount of time, the sample gets to an equilibrium state where it does not absorb any more heat. When this happened, the top plate of the apparatus is transferred to a cooling stand. Both the heating curve and cooling curve of the top plate is recorded. However, only the cooling curve is used for the calculation of thermal conductivity of the sample. The equation for the amount of heat transfer "Q" across the sample is as follows.

$$Q = KA \frac{(T_2 - T_1)}{x} \text{ ----- Equation 1}$$

Where K – thermal conductivity

Q – Thermal energy transfer through sample

(T₂ – T₁) – Temperature difference

A – Area of the cross section

x - Thickness

Figure 5-3 shows the cooling curve of BA0 sample i.e. the sample with conventional cement mortar. In order to find "Q" specific heat formula ($Q = m c \theta$) should be used. For that the thermal gradient of the turning point of the cooling curve must be identified.

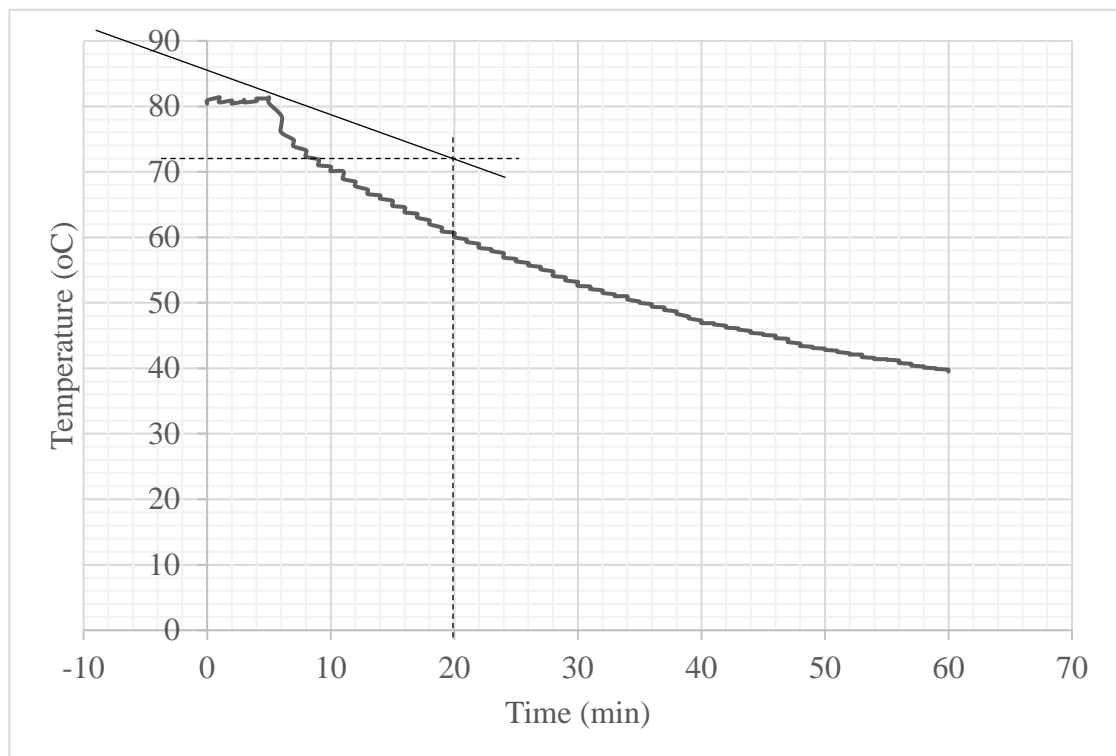


Figure 5-3 - Cooling curve for BA0

5.3 Calculation

Consider the equation,

$$Q = m c \theta$$

Here,

m is the weight of the copper top plate. This was measured as 880 g.

c is the specific heat capacity of copper. This is 385 J/kg. °C

θ is the temperature gradient at the turning point of the cooling curve.

From graph (Figure 5-3), this is,

$$\theta = \frac{85-72}{20 \times 60} \text{ } ^\circ\text{C/s}$$

$$\theta = 0.0108 \text{ } ^\circ\text{C/s}$$

Therefore,

$$Q = 880 \text{ g} \times 0.385 \text{ J/g. } ^\circ\text{C} \times 0.0108 \text{ } ^\circ\text{C/s}$$

$$Q = 3.659 \text{ J/s} = 3.659 \text{ W}$$

Now,

From equation 1,

$$Q = KA \frac{(T_2 - T_1)}{x}$$

Here,

$$(T_2 - T_1) = (125 - 80) = 45 \text{ } ^\circ\text{C}$$

$$x = 5 \text{ cm} = 0.05 \text{ m}$$

$$A = \pi \left(\frac{60}{2 \times 1000} \right)^2 = 0.0028274 \text{ m}^2$$

Therefore,

$$k = \frac{3.659 \text{ W} \times 0.05 \text{ m}}{0.0028274 \text{ m}^2 \times 45^\circ\text{C}}$$

$$k = 1.44 \text{ W/m } ^\circ\text{C}$$

Similarly, for all samples, k (thermal conductivity) was calculated.

Table 5-1 - Lee's disc method results

Sample	% of Bottom Ash to Wt.	Avg. Thermal Conductivity (W/m°C)
BA0	0	1.44
BA10	10	1.36
BA20	20	1.15
BA30	30	1.24
BA40	40	0.99
BA50	50	0.82
BA60	60	0.8
BA70	70	0.6
BA80	80	0.5

The cooling curves for all samples are given in Annex 1.

5.4 Summary

The heat transfer through the samples was calculated using the cooling curve of the top plate of the Lee's disc apparatus. The results tend to be more approximate than distinct. However, as for comparison of results in order to understand the percentage reduction of thermal conductivity of the mix proportions the experiment was successful.

6 MODIFICATION OF DEVELOPED PLASTER – PHASE 3

6.1 Introduction

At the end of phase 2 of the research, BA60 with 10 ml of superplasticizer per kg of cement was finalized as the best case mix proportion. Introducing BA reduced thermal conductivity by approximately 50% while reducing the compressive strength as well. Therefore, as the 3rd phase of the research program, attempts were made to modify the developed mortar. Figure 6-1 gives an overview of the test series carried out in this phase.

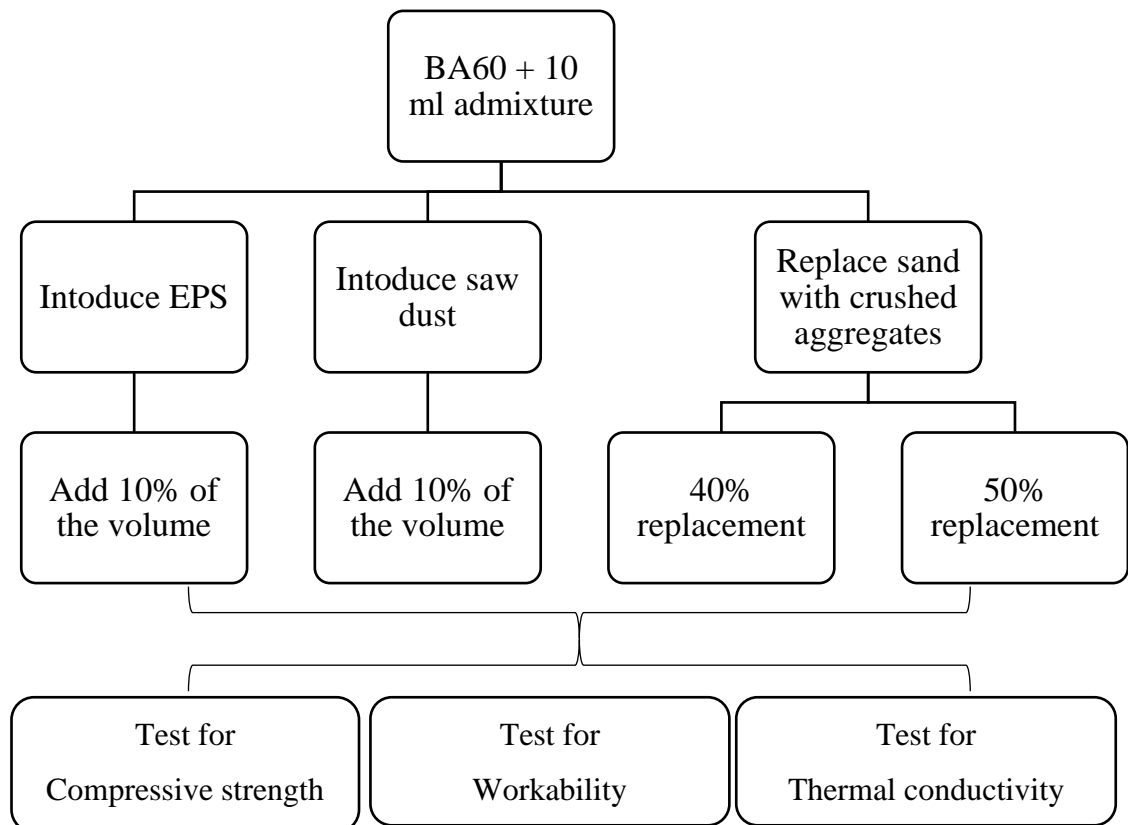


Figure 6-1- Overview of phase 3

In the literature, several other materials are often incorporated as insulation materials. EPS (Polystyrene) is commonly used in light weight concrete works and for general insulation purposes. However, EPS can be less sustainable and less environmental friendly. On the other hand, a material like saw dust which is a common waste material in a country like Sri Lanka can have thermal insulation properties. However, introducing both these materials to the BA mix could affect adversely to an already

weak material in strength. Therefore, attempts were made to improve the strength of the BA mix by replacing the fine aggregates by Aggregate chips.

6.2 Experimental program

6.2.1 Materials

The base materials for BA60 was as same as in chapter 4. Ordinary Portland Cement (OPC) of with a 28-day compressive strength of more than 42.5MPa [67], River sand passing through 2.36 mm sieve, BA passing through 2.36 mm sieve and Millennium Hypercrete [75] as the superplasticizer was used. Polystyrene (EPS) was blendered using a mechanical blender, and saw dust was added to the mix per volume and the mix proportions are given in Table 6-1.

Table 6-1 - Mix proportions

Sample	Water/Cement ratio	Superplasticizer (ml/Kg of cement)	Additional insulation materials		
			Material	Quantity % of volume	Quantity m ³
BA60	1.2	10	Polystyrene	10	0.002058
BA60	1.2	10	Saw dust	10	0.002058



Figure 6-2 – a) Polystyrene (EPS) b) Saw dust

A second batch was produced by replacing all the river sand (fine aggregates) of BA60 with Aggregate chips passing through 800 μm sieve (Figure 6-3). That is 40% of the weight is aggregate chips. Another batch was made for BA50, where all the sand in that mix was replaced by aggregate chips (50% Aggregate chips). The mix proportions are given in Table 6-2.

Table 6-2 - Mix proportions for Aggregate chips

Sample	Water/Cement ratio	Superplasticizer (ml/Kg of cement)	Additional insulation materials		
			Material	Quantity % per weight	Quantity Kg/kg of cement
BA60	1.2	10	Aggregate chips	40	1.2
BA60	1.2	10	Aggregate chips	50	1.5



Figure 6-3 - Aggregate chips passing through $\mu 00$ mm sieve

6.2.2 Sample preparation

The typical procedure of the iteration process followed in chapter 4 was to mix and test batch by batch while replacing or adding new materials. Since this was a modification for BA60, and both polystyrene and saw dust are light in weight, as the first batch they were added as 10% of the volume of mortar. Cement, Sand, BA and polystyrene (or saw dust) were added to the mechanical mixture and mixed. Then, one third (1/3) of the water measured was mixed with superplasticizer and added to the

mixture. Size 70 mm cubes were prepared and tested for compressive strength as per ASTM C109 [69] (Figure 6-4 a))

As the second batch two sets of 70 mm cubes were prepared for mixes with Aggregate chips. One set for 40% and one for set 50% replacement. All cubes were tested according to ASTM C109 [69] (Figure 6-4-b))

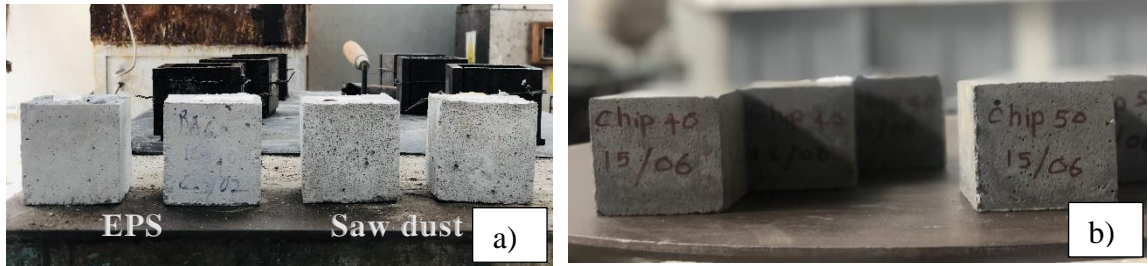


Figure 6-4 Compressive strength cubes a) EPS and saw dust b) Aggregate chips 40% and 50%

6.2.3 Results and Discussion

Consider the results in Table 6-3.

Table 6-3 - Results for mechanical and physical properties of modified mixes

Sample	Average strength – 7 day (N/mm ²)	Average flow (mm)	Average thermal conductivity (W/m ^{°C})
BA60	5.08	175	0.75
BA60 + EPS	4.03	135	0.55
BA60 + Sawdust	1.91	137	0.50
BA60 + Aggregate chips (40%)	6.13	200	0.82
BA60+Aggregate chips (50%)	8.84	180	0.86

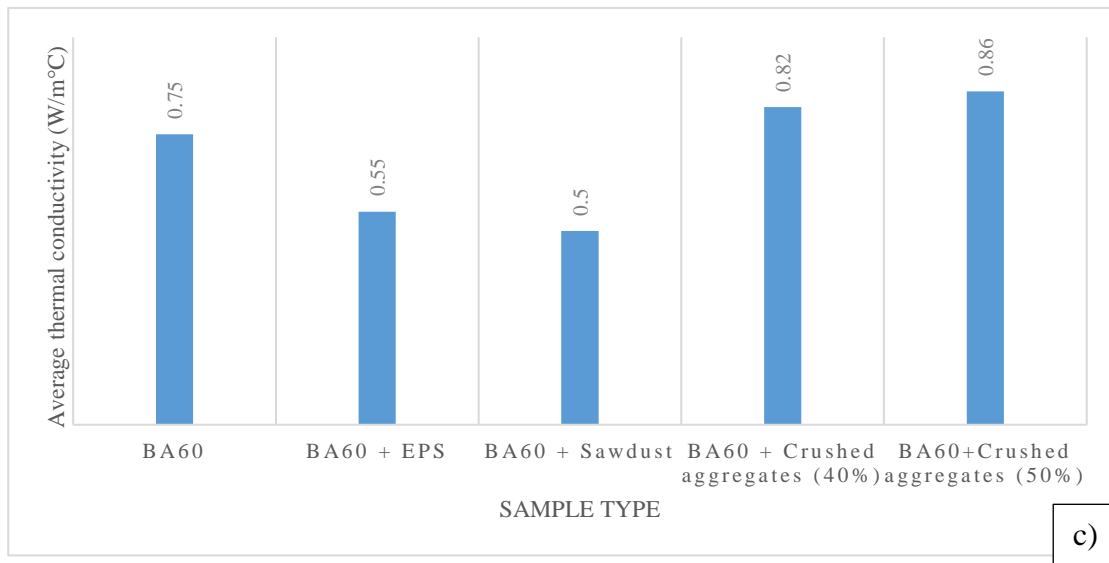
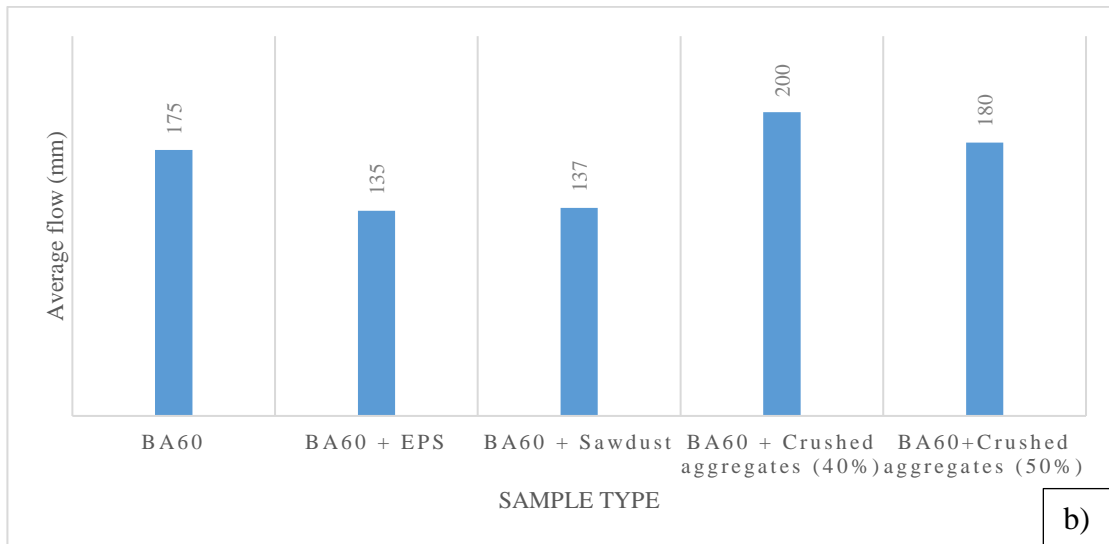
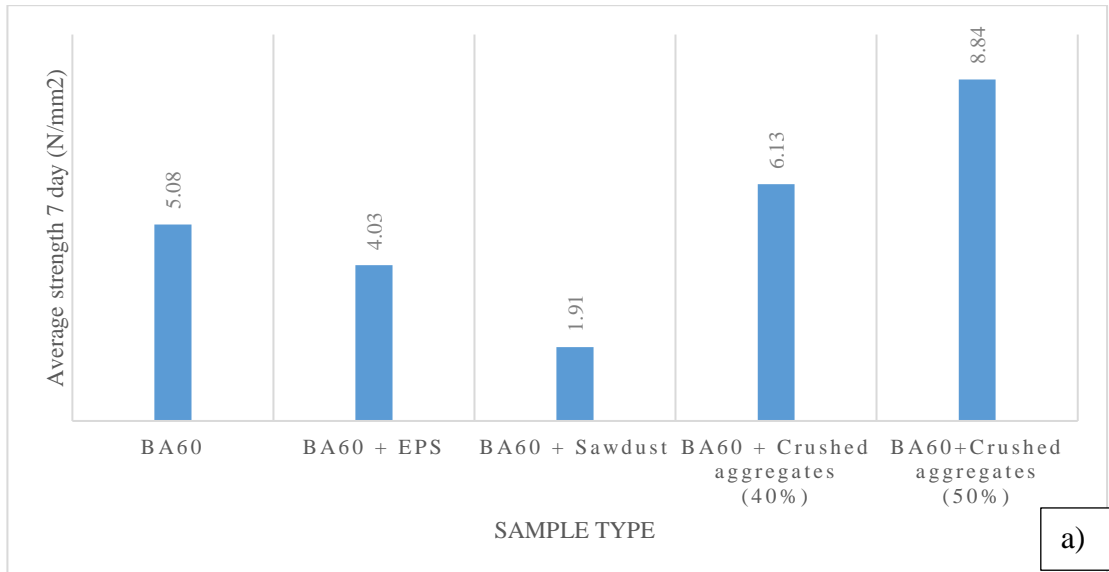


Figure 6-5 -Variation of a) Compressive Strength b) Flow c) Thermal Conductivity

As Table 6-3 (Figure 6-5-c)) suggests, the thermal resistivity of the plaster with EPS and saw dust increases when introduced to BA60. However, compressive strength decreases drastically as well (Figure 6-4-a)). On the other hand, when Aggregate chips are introduced, strength would increase but the plaster becomes more thermal conductive when compared to BA60.

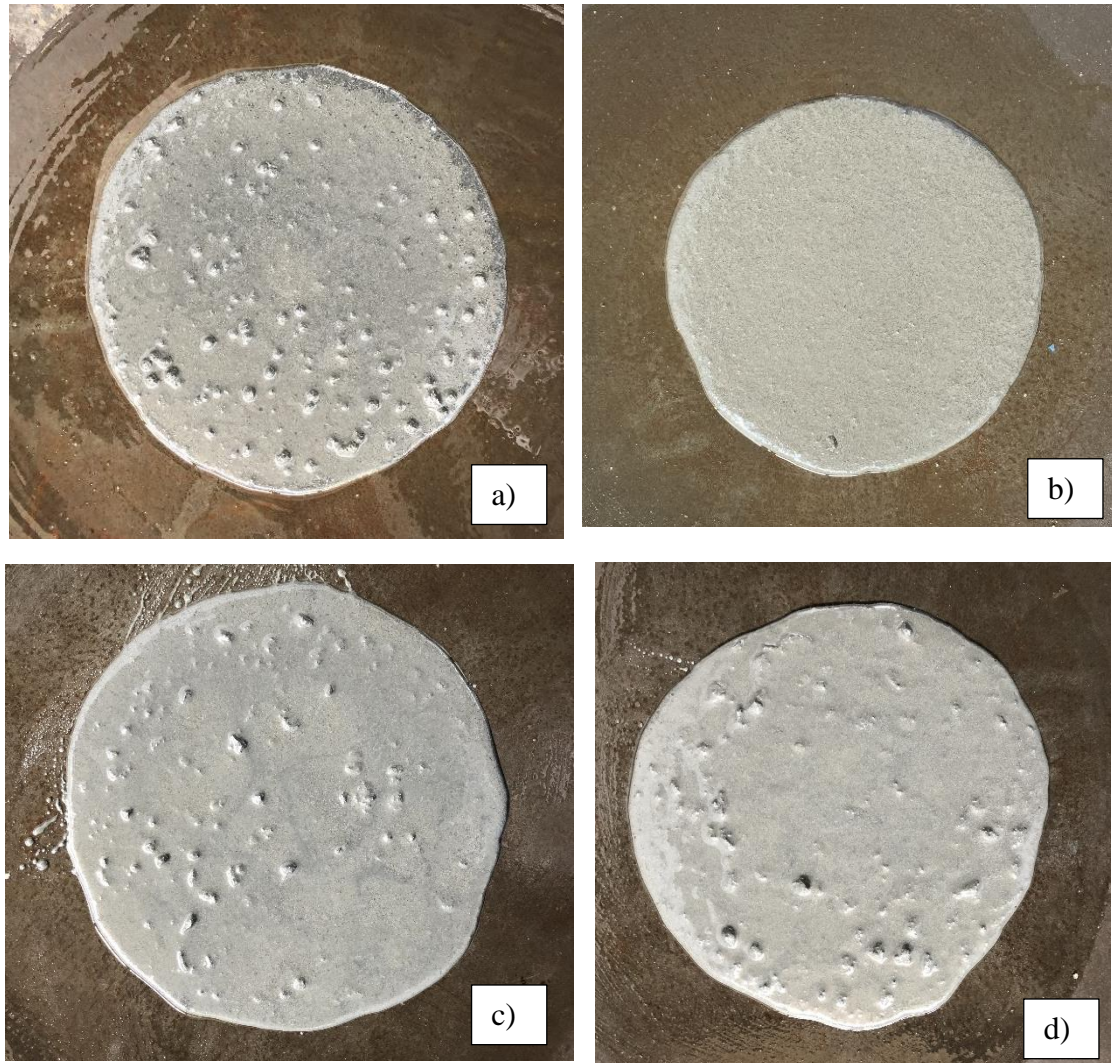


Figure 6-6 Flow table test a) EPS b) Saw dust c) Aggregate chips 40% d) Aggregate chips 50%

When flow of the plasters were observed (Figure 6-5 b), Figure 6-6), the plasters with EPS and Aggregate chips showed more inconsistency than that of saw dust. The main reason for this can be the larger particle size of both EPS and Aggregate chips. The finer particles of saw dust blends well with the plaster.

However, in both cases, EPS and saw dust, the adverse effect they had on compressive strength resulted in discontinuing the series at this batch. Introducing BA to the plaster already have severe adverse effect on the compressive strength of the plaster. Introducing a small percentage like 10% of EPS and saw dust has made the compressive strength go lower than the minimum permissible value (5 MPa). Introducing more can only make it worse. That will not be able to recover since already the amount of admixture that can be introduced the plaster is borderline.

On the other hand, although Aggregate chips are good in increasing compressive strength, it does not act as an insulation material. Thereby, the compressive strength is increased at the cost of thermal resistivity. This contradicts with the primary objective of the research. Therefore, research should be expanded such that either two or more these can produce a better insulation system than BA60.

6.3 Summary

The objective of phase three of developing a thermal insulation mortar was to expand the properties of BA60 using other possible insulation materials in order to achieve better insulation properties. Although thermal conductivity decreases when then new materials like EPS and saw dust are introduced, it was observed that the decrease in compressive strength is inevitable. On the other hand, introducing a material like Aggregate chips can increase the compressive strength. However, that will not help in the subject of thermal resistivity. There might be a better insulation system than BA60 if all these issues could be addressed which could be expanded to another research sequence.

7 APPLICATION OF DEVELOPED PLASTER ON CFRP/CONCRETE COMPOSITES – PHASE 4

7.1 Introduction

The phase 4 of the research program is mainly focused on CFRP/Concrete composites. The developed plaster BA60 has shown good progress when it comes to being as an insulation plaster. However, the question remains on how it would bond with FRP composites and if it is capable of getting the temperature of the epoxy layer below T_g . The insulation plaster has the ability to reduce thermal conductivity by approximately 50%. This suggest that if this were to be applied on CFRP/Concrete composites, it might be possible to go up to temperatures twice or thrice the possible T_g for the adhesive depending on the thickness of the later. On the other hand, if the insulation layer starts losing the bond strength with the CFRP layer at higher elevations before CFRP - concrete bond fails, then the purpose of the insulation layer will be lost. Figure 7-1 show the overview of the test series followed in this phase.

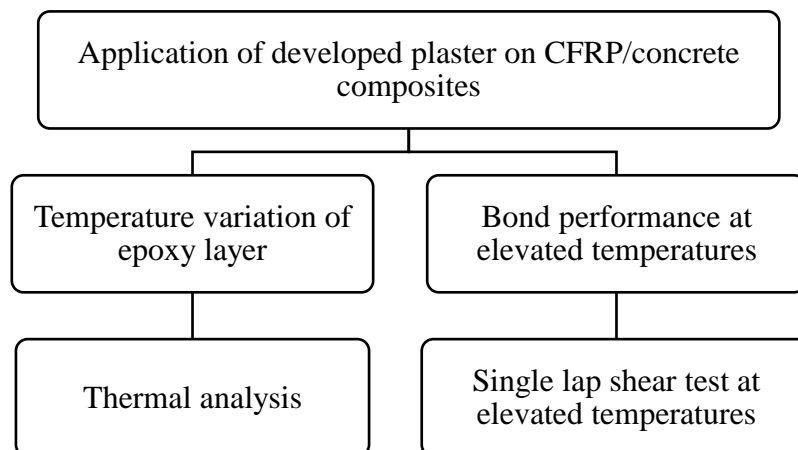


Figure 7-1 - Overview of phase 4

As the first part of the research, samples were tested inside a furnace which goes up to 550 °C, and the temperature variation of the epoxy layer was observed. Then, single lap shear tests were conducted by elevating the temperature of the samples for three different temperatures and the maximum pullout load was observed.

7.2 Experimental program

7.2.1 Materials

The materials for BA60 was as same as above. Ordinary Portland Cement (OPC) of with a 28-day compressive strength of more than 42.5MPa [67], river sand and BA passing through 2.36 mm sieve were used (Figure 7-2). For the concrete blocks, additionally 20-40 mm coarse aggregates were used (Figure 7-3-a)). The details of CFRP and epoxy adhesive used are given in Table 7-1 (Figure 7-3-b), c), d)).

Table 7-1 Material properties of FRP and adhesive

Material Property	Adhesive [76]	CFRP fabrics [77]
Density (kg/m ³)	1300	240
Average Elastic Modulus (GPa)	10	176
Average Tensile strength (N/mm ²)	23	1575

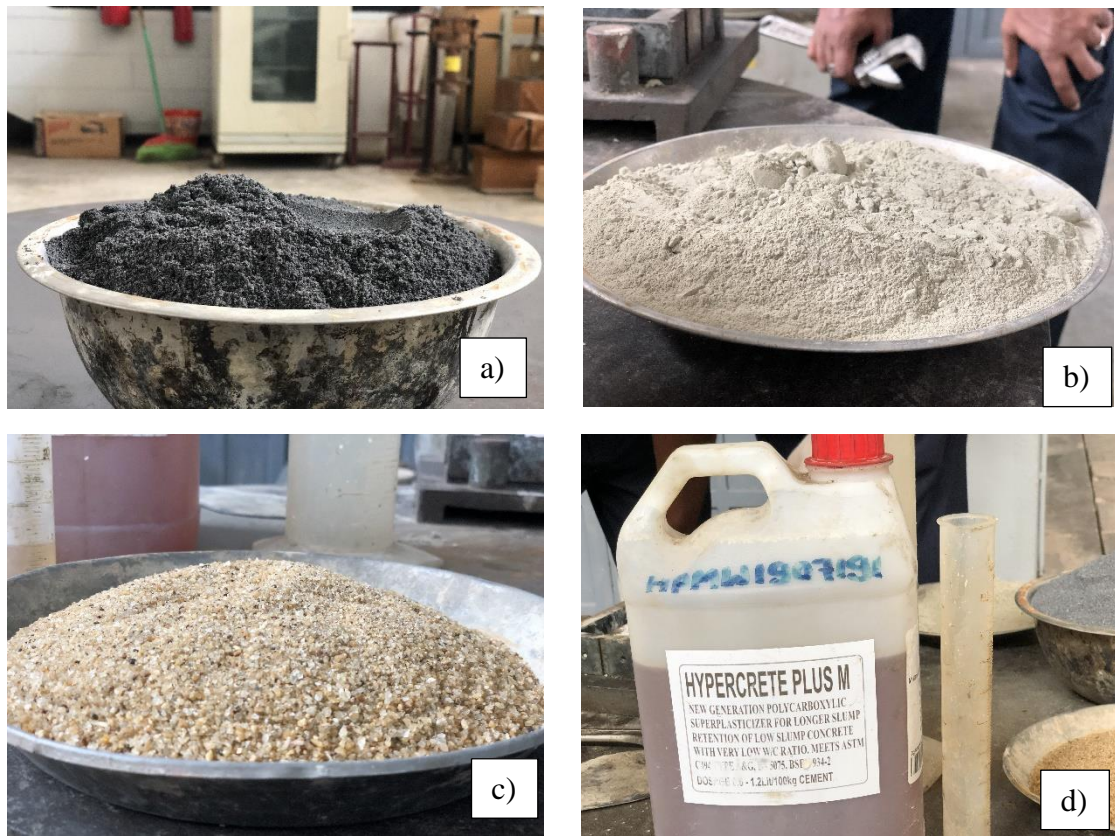


Figure 7-2 - Ingredients of BA60 a) bottom ash b) cement c) river sand d) admixture



Figure 7-3 - a) Coarse aggregates b) CFRP fabric c) Adhesive - base d) Adhesive - Hardener

7.2.2 Sample preparation

by taking Muffle furnace dimensions in to account, 100 mm (width) X 100 mm (height) X 200 mm (length) concrete blocks of grade 25 concrete was prepared (Figure 7-4-a)). The top surfaces were sand blasted as per the guidelines for application of CFRP by the manufacturer [20]. Then CFRP fabric was applied with thermo-couples installed at the epoxy layer (Figure 7-4-b)).

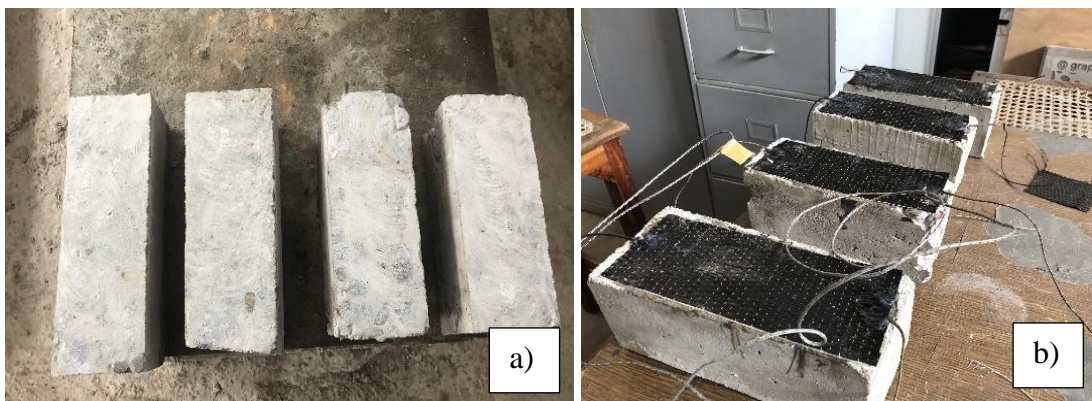


Figure 7-4 - a) Sand blasted blocks b) Application of CFRP and thermo-couples

Figure 7-5 shows a schematic diagram for the arrangement of thermo-couples.

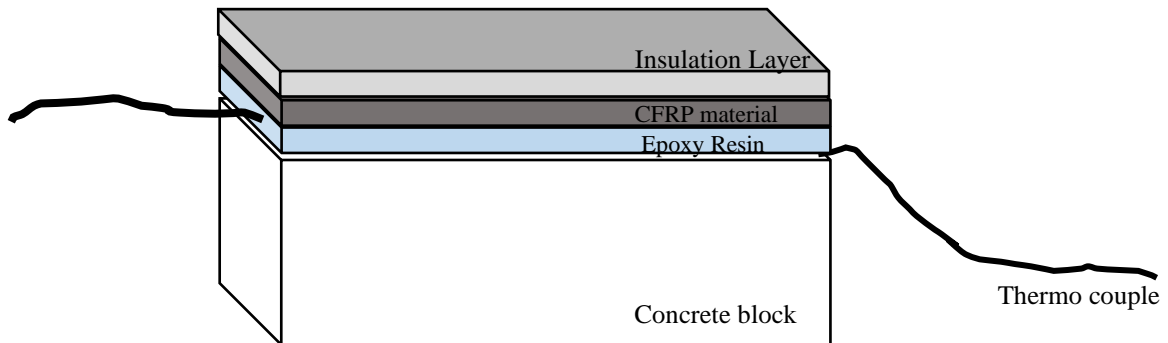


Figure 7-5 - Schematic diagram for arrangement of thermo couples

The CFRP applied samples were cured for a week and then the developed insulation layer (BA60) was applied with a thickness of 20 mm (Figure 7-6-a)) for two samples and two samples were applied with conventional mortar (BA0) for comparison. The insulation layer was again cured for a week and then the samples were tested at a muffle furnace which could go up to 550 °C (Figure 7-6-b)).



Figure 7-6 - a) Application of insulation layer b) Testing in Furnace

7.3 Results and Discussion

The furnace had a potential of 550°C. Two thermo-couples were installed at the epoxy layer between concrete and CFRP layer as per the schematic diagram (Figure 7-4) and the temperature of the epoxy layer was observed. The average temperature variation of the two thermo couples of the two samples for each case (i.e. 4 thermo couples) are given in Figure 7-7.

Both sample types were having insulation layers either conventional mortar or BA60. Therefore, the temperature of the epoxy layer does not reach 500 °C. It can be observed that the maximum temperature of the epoxy layer with conventional mortar (BA0) is around 330 °C, while the maximum temperature of the epoxy layer with BA60 is around 180 °C (Table 7-2). The detailed temperature values are provided in [Annex 2](#).

Table 7-2 - Thermal analysis test results - Summary

Sample	Maximum temperature (°C)	Average temperature (°C)	Average Time taken (s)	Decrement of temperature (%)	Time lag (%)
BA0 - 1	336				
BA0 - 2	330.2	333.1	1630		
BA60 - 1	185.44				
BA60 - 2	178.69	182.065	1140	45	30

This implies that, an insulation of 20 mm could reduce the heat transfer to the epoxy layer of a CFRP/Concrete composite by approximately 50%. Furthermore, the temperature increment will not progress as quickly as that of conventional plaster. In both cases the temperature will not start increasing immediately with the oven temperature. The BA60 plaster samples have started increasing the temperature even later than the conventional plasters which is a good quality for an insulation material.

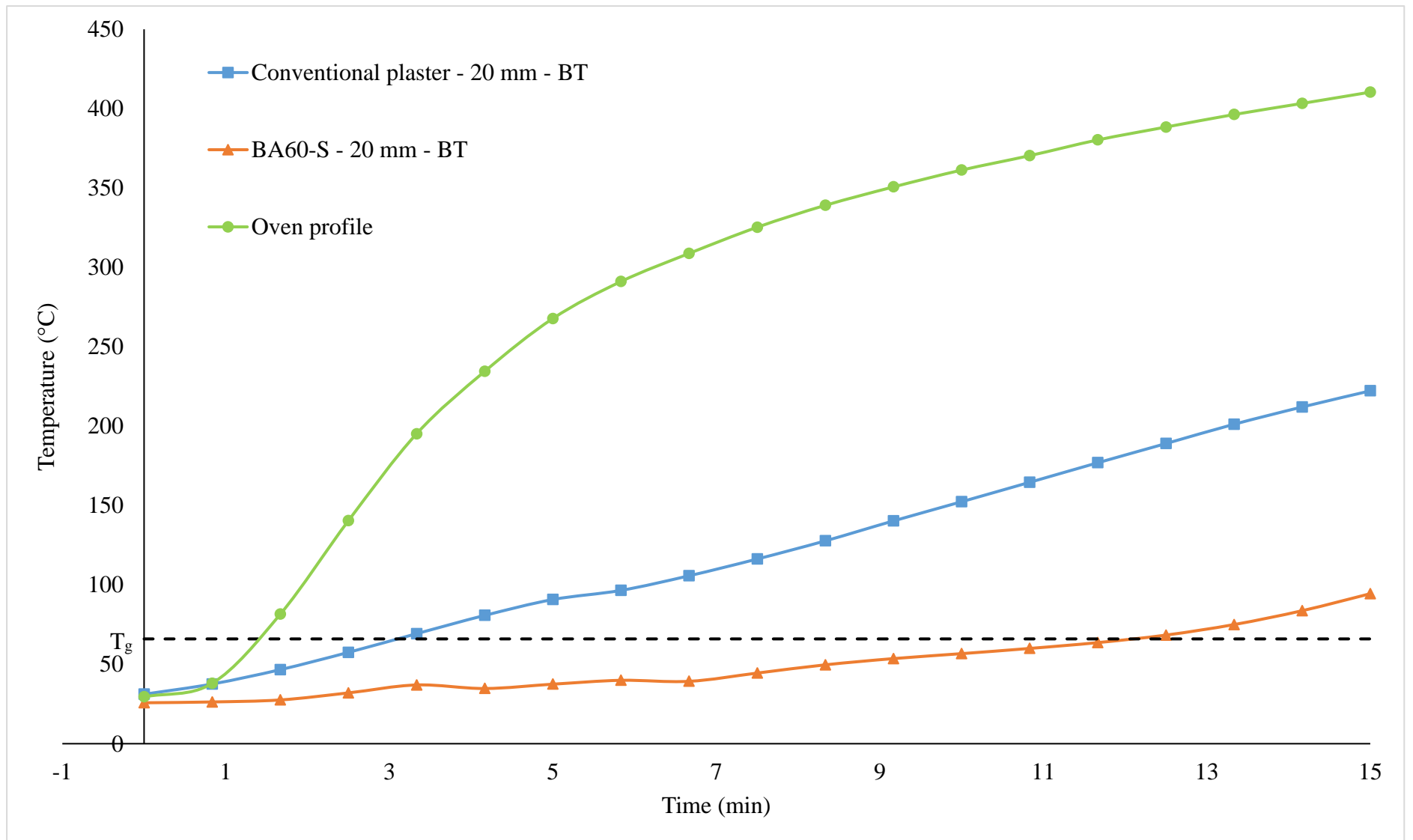


Figure 7-7 - Temperature variation

However, the next concern when it comes to applying the developed plaster to CFRP/Concrete composites is the bond performance of the plaster at elevated temperatures. If the plaster de-bonds before the CFRP, then the application of the insulation plaster will be rendered useless. Therefore it was decided to evaluate the bond performance of the insulation layer by conducting single lap shear tests for four different temperatures.

7.4 Experimental program

7.4.1 Sample preparation

100 mm X 100 mm X 200 mm concrete blocks were prepared and sand blasted for application of CFRP (Figure 7-8-a)). 75 mm wide CFRP strips were applied for half the length of the block (i.e. 100 mm) and thermo couples were installed at the epoxy layer between CFRP and concrete (Figure 7-8-b)).

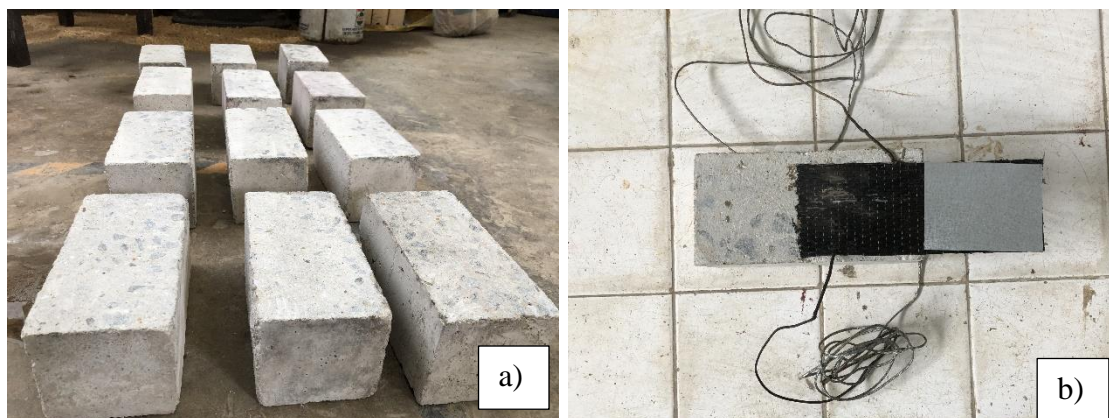


Figure 7-8- a) Sand blasted blocks b) Application of CFRP and thermo couples

Another 100 mm length part of the CFRP was left beyond the length of the concrete block for the grip of the universal testing machine. The grip was strengthened with steel plates to ensure the proper pullout grip. Figure 7-9 shows a schematic diagram for the sample setup for shear lap testing.

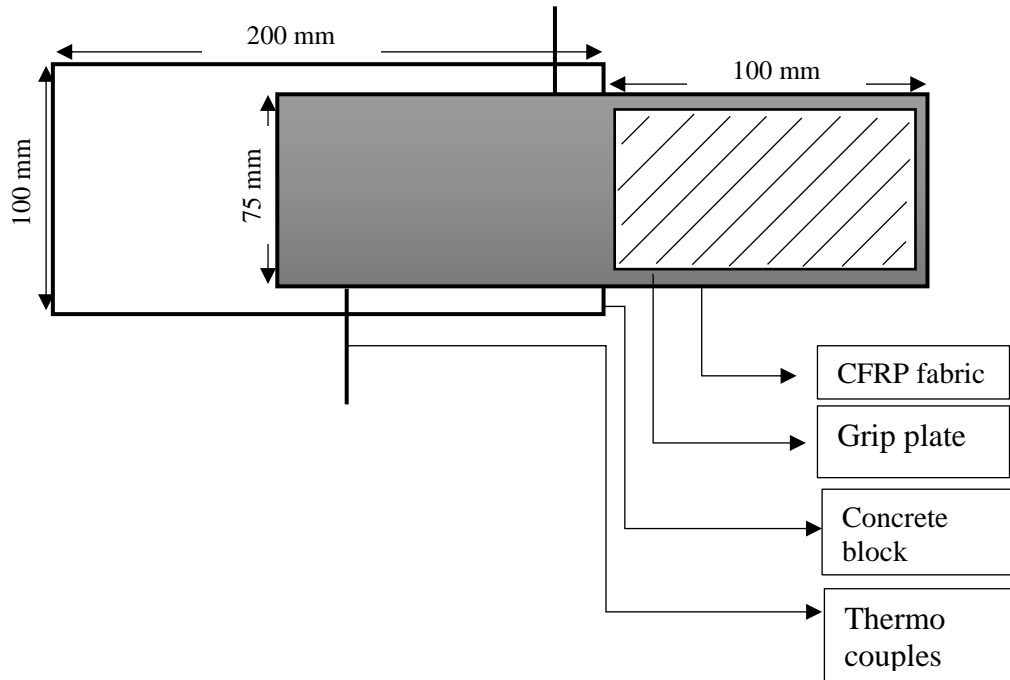


Figure 7-9 - Schematic diagram

Only 10 mm of insulation layer was applied (Figure 7-10-a)) considering the fact that temperature should be increased by only using halogen lamps. The samples temperatures were elevated using halogen lamps as shown in Figure 7-10-b).



Figure 7-10 - a) Application of insulation layer b) Halogen lamps for elevating temperature

The temperature was elevated 10 °C, 20 °C, 30 °C above the ambient temperature (30 °C) i.e. until 40 °C, 50 °C, and 60 °C. However, increasing temperature of epoxy layer with insulation applied was not easy. Therefore it was decided not to increase temperature beyond T_g of epoxy adhesive. The single lap shear test was carried out using the Universal Testing Machine (UTM) (Figure 7-11-a)). The grip plate was fixed to the top end of the machine and pulled as shown in Figure 7-11-b).

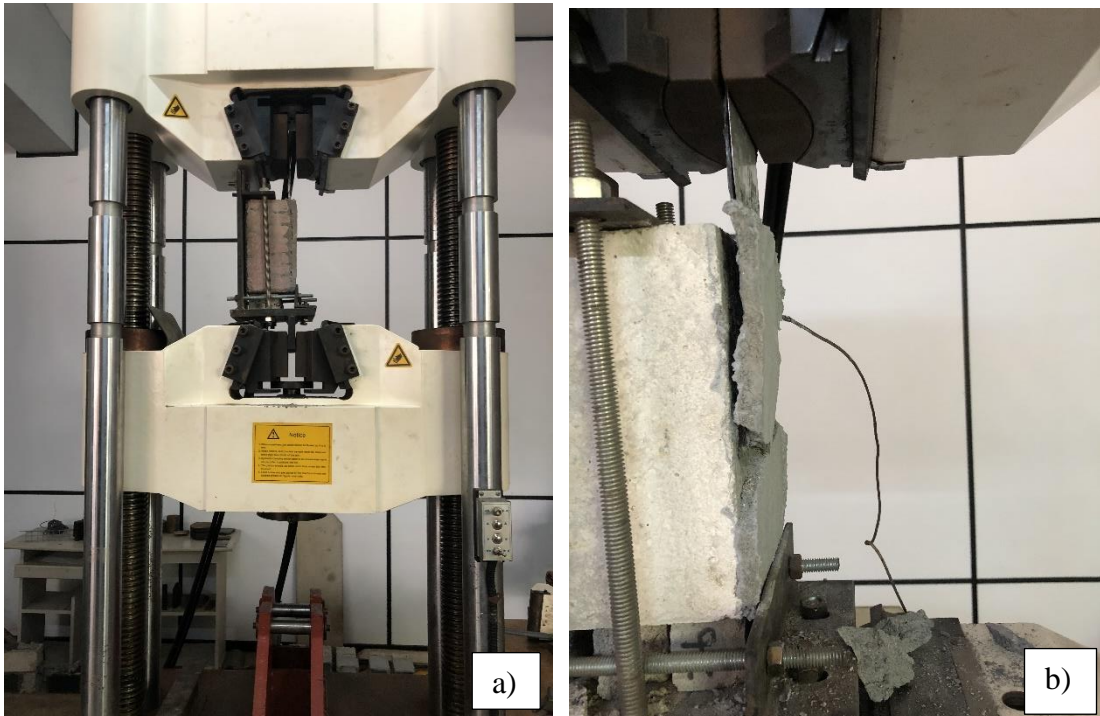


Figure 7-11 - a) Universal testing machine (UTM) b) Pullout failure

7.5 Results and Discussion

Table 7-3 shows the results for single lap shear test carried out.

Table 7-3 - Results for single lap shear test

Sample	Ambient temperature (°C)	Sample temperature (°C)	Elevated temperature (°C)	Maximum pullout strength (kN)	Average pullout strength (kN)
T-0	30	30	0	11.85	
T-0	30	30	0	9.50	
T-0	30	30	0	9.35	10.23
T-10	30	40	10	9.60	
T-10	30	40	10	12.90	
T-10	30	40	10	9.84	10.78
T-20	30	50	20	11.00	
T-20	30	50	20	9.42	
T-20	30	50	20	9.77	10.06
T-30	30	60	30	9.75	
T-30	30	60	30	9.61	
T-30	30	60	30	11.75	10.37

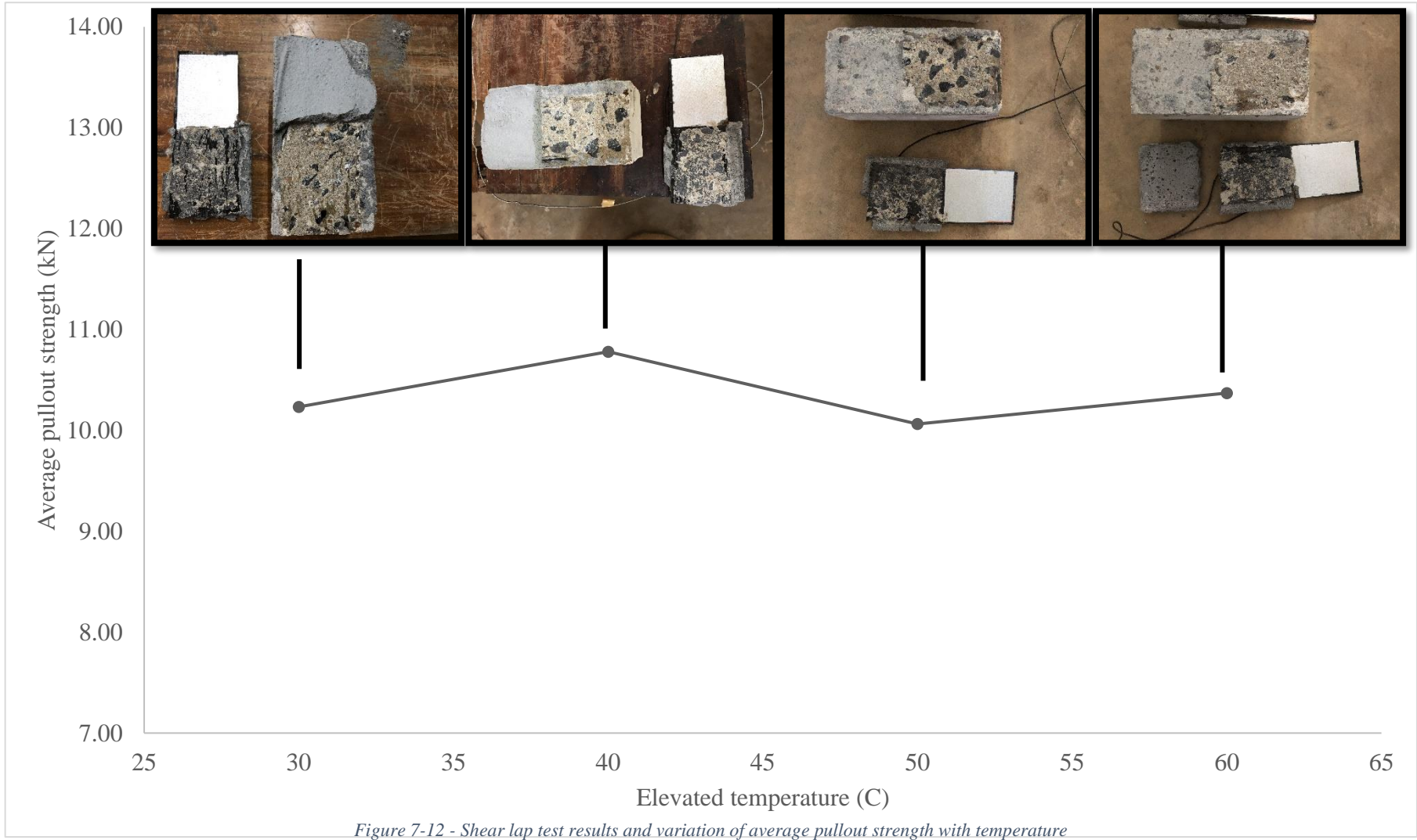


Figure 7-12 - Shear lap test results and variation of average pullout strength with temperature

It can be observed that the pullout strength does not vary much with the temperature variation of the temperature of the epoxy layer. And in all cases the failure occurred at the concrete – epoxy surface and in no case the insulation de-bonded from the CFRP fabric. This suggests that the developed insulation material is good in bond performance with the CFRP fabric than the bond between CFRP fabrics and concrete. Furthermore, the cementitious insulation layer increases the bond performance of the complete element than without any insulation at all.

7.6 Summary

The objective of this chapter was to investigate the applicability of the developed mortar for CFRP-Concrete composites. It was concluded that by applying the insulation material, the temperature of the epoxy layer can be reduced by at least 50% compared to conventional mortar when 20 mm layer was applied. This suggests that this percentage could be increased if the thickness of the sample could be increased. Moreover, the developed insulation plaster shows good bond performance with the CFRP fabric. The bond performance does not vary much when the temperature was increased. Therefore it can be summarized that the developed insulation material can be successfully applied to CFRP/Concrete composites.

8 COST ANALYSIS

A basic cost analysis was carried out in order to compare the developed BA plaster with conventional 1:3 cement sand plaster. Table 8-1 gives a detail calculation of the cost comparison between the two plasters.

Table 8-1 - Cost analysis

					Conventional mortar		BA 60 - admixture 10	
Purchasing material	Unit		Price (LKR)	Unit Price (LKR)	Amount (kg)	Cost (LKR.)	Amount (kg)	Cost (LKR)
Cement	Kg	50	960	19	1	19.2	1	19.2
Sand	Kg	1500	11500	8	3	23	1.2	9.2
Bottom ash	Kg	900	150	0	0	0	1.8	0.3
Admixture	ml	2000	2000	1	0	0	10	10
Transport								
Cement	Kg	50	85	2	1	1.7	1	1.7
Sand	Kg	1500	850	1	3	1.7	1.2	0.68
Bottom ash	Kg	900	15000	17	0	0	1.8	30
Storage	Assume none							
Total Cost (LKR)						45.6		71.08
Material cost (LKR)						42.2		38.7

The costs given in Table 8-1 represents the costs for 4 kg of material for conventional mortar and BA60. The market prices for cement, sand and superplasticizer was considered.

Since BA is a waste material it could be obtained for a price of 150 LKR per ton. The 150 LKR they charge is charged as a handling cost rather than a material cost. Transport costs were estimated considering the normal rates in Uber and Pickme local ride-hailing partners. The transportation cost was estimated such that the cost for the materials to be transported to University of Moratuwa, Sri Lanka from respective

places. That is Cement from Plant in Ratmalana, Sand from Mt. Lavinia and Bottom ash from Norochcholai power plant.

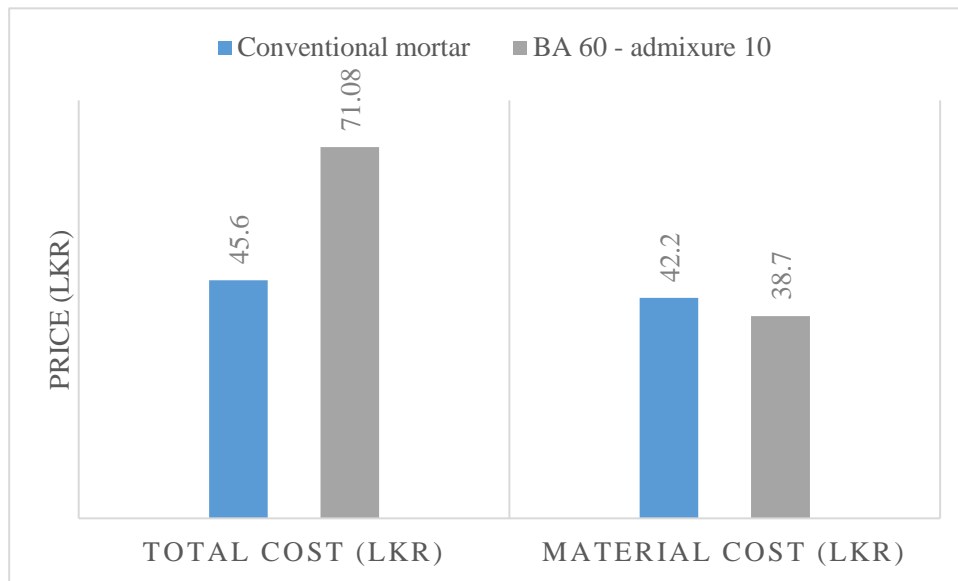


Figure 8-1 - Cost comparison

As it can be observed from Figure 8-1, this suggests that the total cost for BA60 would be higher than conventional mortar. However, the transportation costs can be unreliable or variable due to circumstantial reasons. Therefore, attention was focused to material cost itself.

Material costs suggest that the new material BA60 can be more cost effective than the conventional material. The material cost is reduced by about 8% when BA is incorporated. Furthermore, coming back to the original objective of the research, it could be cheaper than most of the imported existing insulation materials for CFRP/Concrete composites.

9 CONCLUSIONS AND RECOMMENDATIONS

The objective of the research was to develop an insulation material using the locally available materials. BA, which is a waste material from the coal power plants was used as replacement for sand in order to develop an insulation material.

9.1 Conclusions

The following conclusions can be made from the detailed test program carried out to develop a feasible insulation system for CFRP/Concrete composites.

- The thermal conductivity of the plaster decreases when sand is replaced with BA and hence introducing BA as an insulation material is viable. Test results from Lee's Disc method concluded that the decrease of thermal conductivity is in good agreement with the values from the literature.
- Introducing a porous material to the conventional plaster would decrease the thermal conductivity but it would also adversely affect the compressive strength.
- The conventional w/c ratio cannot be applied to BA mixed plaster due to their high water demand and hence the water content was increased until it reached the required workability. For 60% replacement of BA of sand w/c was identified as 1.2. It can be concluded that the water demand will increase with the porosity of the materials used in the mix.
- Adding a superplasticizer can increase the consistency and the workability of the mortar and maintain the strength at ASTM requirements.
- BA60 with 1.2 w/c ratio and 10 ml/kg of cement can be finalized as an optimum mix for thermal insulation (Datasheet: [Annex 3](#))
- Further modifying with polystyrene and saw dust would decrease the thermal conductivity of the samples but it would also affect adversely on the compressive strength. Incorporating Aggregate chips would increase the strength but it will decrease the thermal performance.
- When the insulation layer was applied on CFRP composites 45% reduction of heat transfer to the epoxy layer was observed. Also heat transferred 30% slower than conventional plaster.

- Bond performance of the developed insulation plaster with CFRP has less impact from the elevation of temperatures until 60°C.
- When the material costs are compared, BA60 is more economical than conventional mortar.

9.2 Recommendations

Although BA would be a solution for the said problem statement, the coal power generation is a non-renewable power source. Which implies that, there is a probability that coal power generation might be suspended within the next 10 to 20 years. Thereby, using BA would not be a permanent solution for the issue at hand although it is easily accessible and readily available today. However, when developing countries like Sri Lanka are considered, they are no closer to using cleaner energy than we were 20 years before. Therefore, in Sri Lankan context, the country might require a method to utilize BA for more than 30 years ahead. Therefore, it can be recommended that, this research should be continued and expanded for more sustainable solutions.

Moreover, when it comes to application on FRP composites, it can be recommended to use BA60 plaster developed as a low cost and sustainable insulation material. This would decrease the waste production through coal power plants as well as save the large land areas that are currently holding landfills of BA. However, further tests should be carried out to test for appropriate thickness to ensure required fire rating for buildings in case of fire. Furthermore, this could be applied to other forms of FRP materials and more application methods than EBR technique.

Furthermore, it is not recommended to use more than one porous material in mortar mixtures considering the adverse effect it has on strength of the plaster. However, the percentage of BA can be increased if the purpose of the plaster does not involve heavy weathering conditions which require strength.

REFERENCES

- [1] K. A. D. Y. T. Kahandawa Arachchi, J. C. P. H. Gamage, and E. R. K. Chandrathilaka, "Bond Performance of Carbon Fiber Reinforced Polymer (CFRP) Strengthened Reinforced Concrete Curved Beams," in *International Conference on Civil Engineering and Applications*, 2019.
- [2] M. Perner, S. Algermissen, R. Keimer, and H. P. Monner, "Robotics and Computer-Integrated Manufacturing Avoiding defects in manufacturing processes : A review for automated CFRP production," *Robot. Comput. Integr. Manuf.*, vol. 38, pp. 82–92, 2016.
- [3] S. Hegde, B. S. Shenoy, and K. N. Chethan, "Materials Today : Proceedings Review on carbon fiber reinforced polymer (CFRP) and their mechanical performance," *Mater. Today Proc.*, no. xxxx, pp. 1–5, 2019.
- [4] J. Yanagimoto and K. Ikeuchi, "CIRP Annals - Manufacturing Technology Sheet forming process of carbon fiber reinforced plastics for lightweight parts," *CIRP Ann. - Manuf. Technol.*, vol. 61, no. 1, pp. 247–250, 2012.
- [5] S. Visal and S. U. Deokar, "A Review Paper on Properties of Carbon Fiber Reinforced Polymers," *Int. J. Innov. Res. Sci. Technol.*, vol. 2, no. 12, pp. 238–243, 2016.
- [6] J. C. P. H. Gamage and M. B. Wong, "Bond characteristics of CFRP plated concrete members under elevated temperatures," *Compos. Struct.*, vol. 75, pp. 199–205, 2006.
- [7] S. Aaruga, "Finite Element Modelling on Flexural Performance of CFRP Strengthened Reinforced Concrete Curved Beams," *2019 Moratuwa Eng. Res. Conf.*, pp. 662–667, 2019.
- [8] K. A. D. Y. T. K. Arachchi, J. C. P. H. Gamage, and E. R. K. Chandrathilake, "Bond Performance of Carbon Fiber Reinforced Polymer (CFRP) Strengthened Reinforced Concrete Curved Beams," in *International Conference on Civil Engineering and Applications*, 2019.
- [9] Center of Composite Materials, "Annual Report," Newark, 1994.
- [10] K. Dong, K. Hu, and W. Gao, "Fire Behavior of Full-Scale CFRP-Strengthened RC Beams Protected with Different Insulation Systems," *J. Asian Archit. Build.*

- Eng.*, vol. 15, no. 3, pp. 581–588, 2016.
- [11] J. P. Firmo, J. R. Correia, and L. A. Bisby, “Fire behaviour of FRP-strengthened reinforced concrete structural elements: A state-of-the-art review,” *Compos. Part B Eng.*, vol. 80, pp. 198–216, 2015.
- [12] J. C. P. H. Gamage and M. B. Wong, “Durability of CFRP-Strengthened Concrete Members Under Extreme Temperature and Humidity Durability of CFRP-strengthened concrete members under extreme temperature and humidity *,” *Aust. J. Struct. Eng.*, vol. 9, no. 2, pp. 111–118, 2015.
- [13] J. C. P. H. Gamage, M. B. Wong, and R. Al-Mahadi, “Performance of CFRP strengthened concrete members under elevated temperatures,” *Proceeding Int. Symposium Bond Behav. FRP Struct. (BBFS 2005)*, no. Bbfs, pp. 113–118, 2005.
- [14] D. Cree, E. U. Chowdhury, M. F. Green, L. A. Bisby, and N. Bénichou, “Performance in fire of FRP-strengthened and insulated reinforced concrete columns,” *Fire Saf. J.*, vol. 54, pp. 86–95, 2012.
- [15] W. Jung, J. Park, J. Kang, and M. Keum, “Flexural Behavior of Concrete Beam Strengthened by Near-Surface Mounted CFRP Reinforcement Using Equivalent Section Model,” *Adv. Mater. Sci. Eng.*, vol. 2017, pp. 1–16, 2017.
- [16] A. U. R. Khan and S. Fareed, “Behaviour of Reinforced Concrete Beams Strengthened by CFRP Wraps with and without end anchorages,” *Procedia Eng.*, vol. 77, pp. 123–130, 2014.
- [17] V. K. R. Kodur and D. Baingo, “Fire Resistance of FRP Reinforced Concrete Slabs,” *Natl. Res. Counc. Canada*, no. 758, 1998.
- [18] L. A. Foster, S.K. and Bisby, “High temperature residual properties of externally-bonded FRP systems,” *Proc. 7th Int. Symp. fiber Reinf. Polym. Reinf. Reinf. Concr. Struct.*, vol. ACI-SP230, no. 7, p. SP-230-70, 2005.
- [19] E. R. . Chandrathilaka and G. J.C.P.H., “Fire Performance of CFRP Strengthened Steel I Beams Cured at Elevated Temperature,” *Springer, Singapore*, vol. 44, 2019.
- [20] E. R. K. Chandrathilaka, J. C. P. H. Gamage, and S. Fawzia, “Mechanical characterization of CFRP / steel bond cured and tested at elevated temperature,” *Compos. Struct.*, vol. 207, no. July 2018, pp. 471–477, 2019.
- [21] K. A. D. Y. T. Kahandawa Arachchi, J. C. P. H. Gamage, and G. I. P. De Silva,

- “Thermal Insulation Systems for CFRP/Concrete Composites: A Review,” in *International Conference on Structural Engineering and Construction Management*, 2019.
- [22] T. B. Carlos and J. P. C. Rodrigues, “Experimental bond behaviour of a CFRP strengthening system for concrete elements at elevated temperatures,” *Constr. Build. Mater.*, vol. 193, pp. 395–404, 2018.
- [23] J. P. Firmo, J. R. Correia, and P. França, “Fire behaviour of reinforced concrete beams strengthened with CFRP laminates: Protection systems with insulation of the anchorage zones,” *Compos. Part B Eng.*, vol. 43, no. 3, pp. 1545–1556, Apr. 2012.
- [24] AS 1530.4, *Methods for fire tests on building materials, components and structures - Fire-resistance test of elements of construction*. 2005.
- [25] R. Ranasinghe, D. Jinadasa, H. Srilal, and J. Gamage, “Bond performance of CFRP strengthened concrete subjected to fire,” in *Civil Engineering Research for Industry*, 2011, pp. 37–42.
- [26] J. C. P. H. Gamage, R. Al-Mahaidi, and M. B. Wong, “Effect of insulation on the bond behaviour of CFRP-Plated concrete elements,” in *Proceeding of the International Symposium on Bond Behaviour of FRP in Structures (BBFS 2005)*, 2005, pp. 119–123.
- [27] Z. S. Wu, K. Iwashita, S. Yagashiro, T. Ishikawa, and Y. Hamaguchi, “Temperature effect on bonding and debonding behavior between FRP sheets and concrete,” in *FRP composites in civil engineering - CICE 2004*, 2004, pp. 905–912.
- [28] J. C. P. H. Gamage, R. Al-Mahaidi, and M. B. Wong, “Effect of insulation on the bond behaviour of CFRP-Plated concrete elements,” in *Proceedings of the International Symposium on Bond Behaviour of FRP in Structures*, 2005, pp. 119–123.
- [29] K. H. Kim, S. E. Jeon, J. K. Kim, and S. Yang, “An experimental study on thermal conductivity of concrete,” *Cem. Concr. Res.*, vol. 33, no. 3, pp. 363–371, 2003.
- [30] C. Udawattha and R. Halwatura, “Thermal performance and structural cooling analysis of brick, cement block, and mud concrete block,” *Adv. Build. Energy*

- Res.*, vol. 12, no. 2, pp. 150–163, 2018.
- [31] F. Batool, M. M. Rafi, and V. Bindiganavile, “Microstructure and thermal conductivity of cement-based foam:A review,” *J. Build. Eng.*, vol. 20, no. February 2017, pp. 696–704, 2018.
- [32] B. Bhattacharjee and S. Krishnamoorthy, “Permeable Porosity and Thermal Conductivity of Construction Materials,” *J. Mater. Civ. Eng.*, vol. 16, no. 4, pp. 322–330, Aug. 2004.
- [33] V. Bindiganavile, F. Batool, and N. Suresh, “Effect of fly ash on thermal properties of cement based foams evaluated by transient plane heat source,” *Indian Concr. J.*, vol. 86, 2012.
- [34] I. Asadi, P. Shafigh, Z. F. Bin Abu Hassan, and N. B. Mahyuddin, “Thermal conductivity of concrete – A review,” *J. Build. Eng.*, vol. 20, no. July, pp. 81–93, 2018.
- [35] A. Ghosh, A. Ghosh, and S. Neogi, “Reuse of fly ash and bottom ash in mortars with improved thermal conductivity performance for buildings,” *Heliyon*, vol. 4, no. 11, p. e00934, 2018.
- [36] D. P. Bentz, M. A. Peltz, A. Durán-Herrera, P. Valdez, and C. A. Juárez, “Thermal properties of high-volume fly ash mortars and concretes,” *J. Build. Phys.*, vol. 34, no. 3, pp. 263–275, 2011.
- [37] P. Torkittikul, T. Nochaiya, W. Wongkeo, and A. Chaipanich, “Utilization of coal bottom ash to improve thermal insulation of construction material,” *J. Mater. Cycles Waste Manag.*, vol. 19, no. 1, pp. 305–317, 2017.
- [38] A. K. Mandal and O. P. Sinha, “Production of thermal insulation blocks from bottom ash of fluidized bed combustion system,” *Waste Manag. Res.*, vol. 35, no. 8, pp. 810–819, 2017.
- [39] R. Dylewski and J. Adamczyk, “The comparison of thermal insulation types of plaster with cement plaster,” *J. Clean. Prod.*, vol. 83, pp. 256–262, 2014.
- [40] K. Ganesan, K. Rajagopal, and K. Thangavel, “Rice husk ash blended cement : Assessment of optimal level of replacement for strength and permeability properties of concrete,” *Constr. Build. Mater.*, vol. 22, pp. 1675–1683, 2008.
- [41] G. A. Habeeb and H. Bin Mahmud, “Study on Properties of Rice Husk Ash and Its Use as Cement Replacement Material 3 . Experimental Work 2 . Scope of

- Work,” *Mater. Res.*, vol. 13, no. 2, pp. 185–190, 2010.
- [42] K. Selvaranjan, J. C. P. H. Gamage, and G. I. P. De Silva, “Thermal performance of rice husk ash mixed mortar in concrete and masonry buildings,” *Bud. i Archit.*, vol. 19, no. 4, pp. 43–52, 2020.
- [43] P. Ramadoss and T. Sundararajan, “Utilization of Lignite-Based Bottom Ash as Partial Replacement of Fine Aggregate in Masonry Mortar,” *Arab. J. Sci. Eng.*, vol. 39, no. 2, pp. 737–745, 2014.
- [44] P. Aggarwal, Y. Aggarwal, and S. M. Gupta, “Effect of bottom ash as replacement of fine aggregates in concrete,” *ASIAN J. Civ. Eng. (BUILDING HOUSING)*, vol. 8, no. 1, pp. 49–62, 2007.
- [45] A. K. Mandal and O. P. Sinha, “Review on Current Research Status on Bottom Ash: An Indian Prospective,” *J. Inst. Eng. Ser. A*, vol. 95, no. 4, pp. 277–297, 2014.
- [46] W. Wongkeo, P. Thongsanitgarn, K. Pimraksa, and A. Chaipanich, “Compressive strength, flexural strength and thermal conductivity of autoclaved concrete block made using bottom ash as cement replacement materials,” *Mater. Des.*, vol. 35, pp. 434–439, 2012.
- [47] G. Vasudevan, “Performance on Coal Bottom Ash in Hot Mix Asphalt,” *Int. J. Res. Eng. Technol.*, vol. 02, no. 08, pp. 24–33, 2015.
- [48] *RMRC User Guidelines*. 2007.
- [49] M. Cheriaf, J. Cavalcante Rocha, and J. Pera, “Pozzolanic properties of pulverized coal combustion bottom ash,” *Cem. Concr. Res.*, vol. 29, pp. 1387–1391, 1999.
- [50] S. U. Hendawitharana and S. M. A. Nanayakkara, “Use of bottom ash from coal fired thermal power plants in production of cellular lightweight concrete,” *MERCon 2018 - 4th Int. Multidiscip. Moratuwa Eng. Res. Conf.*, pp. 209–214, 2018.
- [51] ASTM International, “ASTM C618-19, Standard Specification for Coal Fly Ash and Raw or Calcined Natural Pozzolan for Use in Concrete,” West Conshohocken, PA, 2019.
- [52] P. Onprom, K. Chaimoon, and R. Cheerarot, “Influence of Bottom Ash Replacements as Fine Aggregate on the Property of Cellular Concrete with

- Various Foam Contents,” *Adv. Mater. Sci. Eng.*, vol. 2015, pp. 1–11, 2015.
- [53] K. Dharani, “Experimental Study on Properties of Concrete Using Bottom Ash With Addition of Polypropylene Fibre,” *Novat. Publ. Int. J. Res. Publ. Eng. Technol.*, vol. 3, no. 8, pp. 2454–7875, 2017.
- [54] M.-J. Yang, H.-Y. Wang, and H.-Y. Wang, “Effects on Strengths of Cement Mortar When Using Incinerator Bottom Ash as Fine Aggregate,” *World J. Eng. Technol.*, vol. 02, no. 03, pp. 42–47, 2014.
- [55] J. G. Jang, H. J. Kim, H. K. Kim, and H. K. Lee, “Resistance of coal bottom ash mortar against the coupled deterioration of carbonation and chloride penetration,” *Mater. Des.*, vol. 93, pp. 160–167, 2016.
- [56] P. Tang, M. V. . Florea, P. Spiesz, and H. J. . Brouwers, “The application of treated bottom ash in mortar as cement replacement,” *EurAsia Waste Manag. Symp. April 2014, YTU 2010 Congr. Center, Istanbul/Turkiye*, no. 2014, pp. 1077–1082, 2014.
- [57] R. M. I. E. Piyaathne and K. M. L. A. Udamulla, “Use of Bottom Ash in Replacement of River Sand in Making Cement Mortar,” in *International Symposium on Advances in Civil and Environmental Engineering Practices for Sustainable Development*, 2013, pp. 191–197.
- [58] A. Cheng, “Effect of incinerator bottom ash properties on mechanical and pore size of blended cement mortars,” *Mater. Des.*, vol. 36, pp. 859–864, 2012.
- [59] ASTM International, “ASTM E119-19, Standard Test Methods for Fire Tests of Building Construction and Materials,” West Conshohocken, PA, 2019.
- [60] B. Williams, V. Kodu, M. F. Green, and L. Bisby, “Fire Endurance of Fiber-Reinforced Polymer Strengthened Concrete T-Beams,” *ACI Struct. J.*, vol. 105, no. 1, 2008.
- [61] H. Blontrock, L. Taerwe, and P. Vandeveld, “Fire tests on concrete beams strengthened with fibre composite laminates,” in *Proceedings of the International PhD Symposium in Civil Engineering, Vienna (Austria)*, 2000, pp. 151–161.
- [62] International Organization for Standardization, “ISO 834-2:2019. Fire-resistance tests — Elements of building construction,” 2019.
- [63] A. G. Mal’Chik, S. V. Litovkin, and P. V. Rodionov, “Investigations of

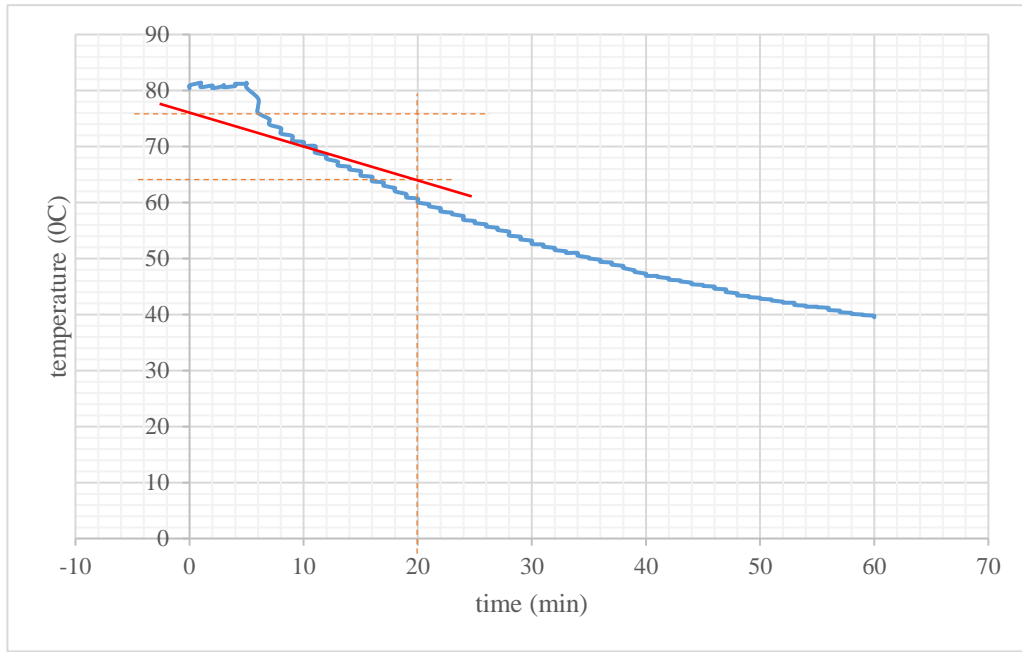
- physicochemical properties of bottom-ash materials for use them as secondary raw materials,” *IOP Conf. Ser. Mater. Sci. Eng.*, vol. 91, no. 1, 2015.
- [64] M. Mcquarrle, “Thermal Conductivity: VII, Analysis of Variation of Conductivity with Temperature for Al₂O₃, BeO, and MgO,” *J. Am. Ceram. Soc.*, vol. 37, no. 02, 1954.
- [65] British Standards, “BS1377:Part 2:1990, Methods of test for Soils for civil engineering,” 1990.
- [66] ASTM International, “ASTM C1329 / C1329M-16a, Standard Specification for Mortar Cement,” West Conshohocken, PA, 2016.
- [67] ASTM International, *ASTM C150 / C150M-19a, Standard Specification for Portland Cement*. West Conshohocken, 2019.
- [68] ASTM International, “ASTM D7340-07, Standard Practice for Thermal Conductivity of Leather,” West Conshohocken, PA, 2018.
- [69] ASTM International, “ASTM C109 / C109M-20a, Standard Test Method for Compressive Strength of Hydraulic Cement Mortars,” West Conshohocken, PA, 2020.
- [70] K. Liu, Z. Wang, C. Jin, F. Wang, and X. Lu, “An experimental study on thermal conductivity of iron ore sand cement mortar,” *Constr. Build. Mater.*, vol. 101, pp. 932–941, 2015.
- [71] R. Demirbog, “Influence of mineral admixtures on thermal conductivity and compressive strength of mortar,” *Energy Build.*, vol. 35, pp. 189–192, 2003.
- [72] J. Olmeda, M. I. S. De Rojas, M. Frías, S. Donatello, and C. R. Cheeseman, “Effect of petroleum (pet) coke addition on the density and thermal conductivity of cement pastes and mortars,” *Fuel*, vol. 107, no. 2013, pp. 138–146, 2015.
- [73] J. C. Mendes *et al.*, “On the relationship between morphology and thermal conductivity of cement-based composites,” *Cem. Concr. Compos.*, vol. 104, no. October 2018, p. 103365, 2019.
- [74] V. Corinaldesi, A. Mazzoli, and G. Moriconi, “Mechanical behaviour and thermal conductivity of mortars containing waste rubber particles,” *Mater. Des.*, vol. 32, no. 3, pp. 1646–1650, 2011.
- [75] Millennium Concrete Technologies (Pvt) Ltd., “Product datasheet,” 2017.

- [76] “Technical datasheet, X-Wrap Plate Adhesive, High performance epoxy adhesive for carbon fiber strengthening systems,” 2018. [Online]. Available: <http://www.x-calibur.us>. [Accessed: 05-Dec-2019].
- [77] “Technical datasheet, X-Wrap C300, High strength carbon fiber fabric for structural strengthening.” [Online]. Available: <http://www.x-calibur.us>. [Accessed: 05-Dec-2019].

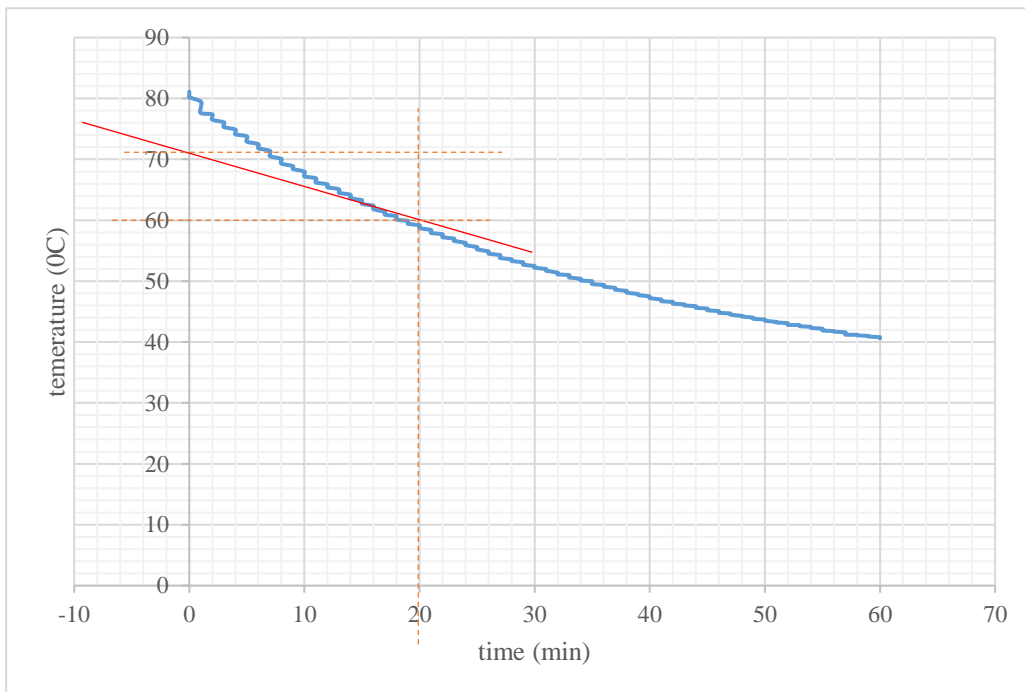
ANNEXES

Annex 1 – Thermal conductivity testing cooling curves

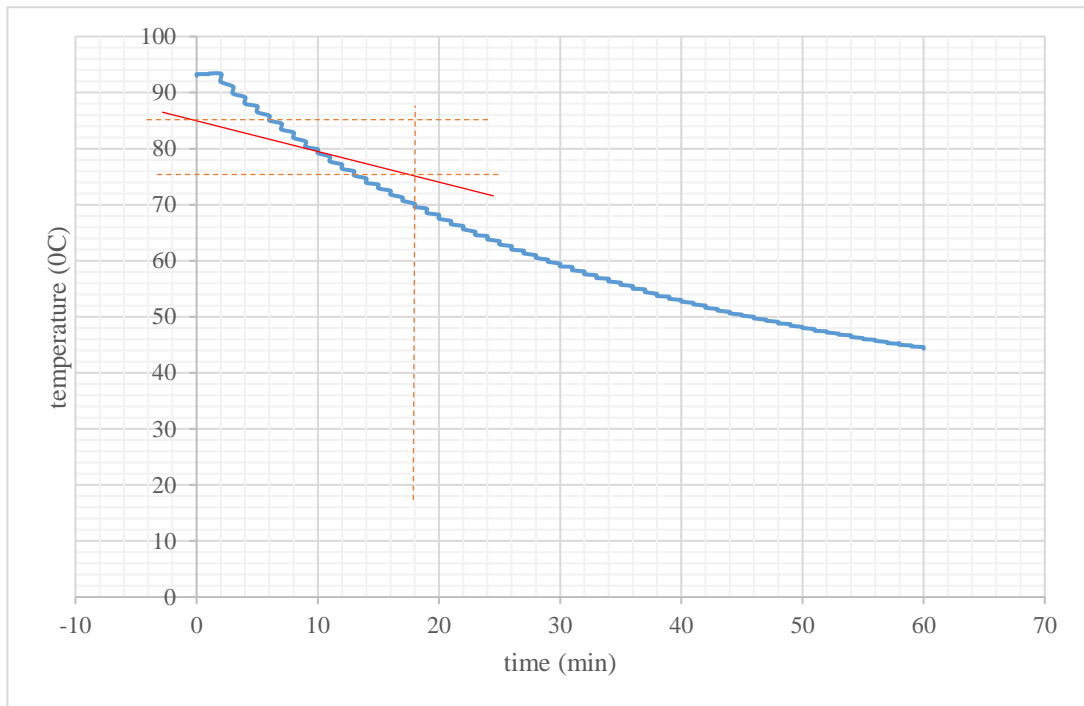
BA0 – Control sample



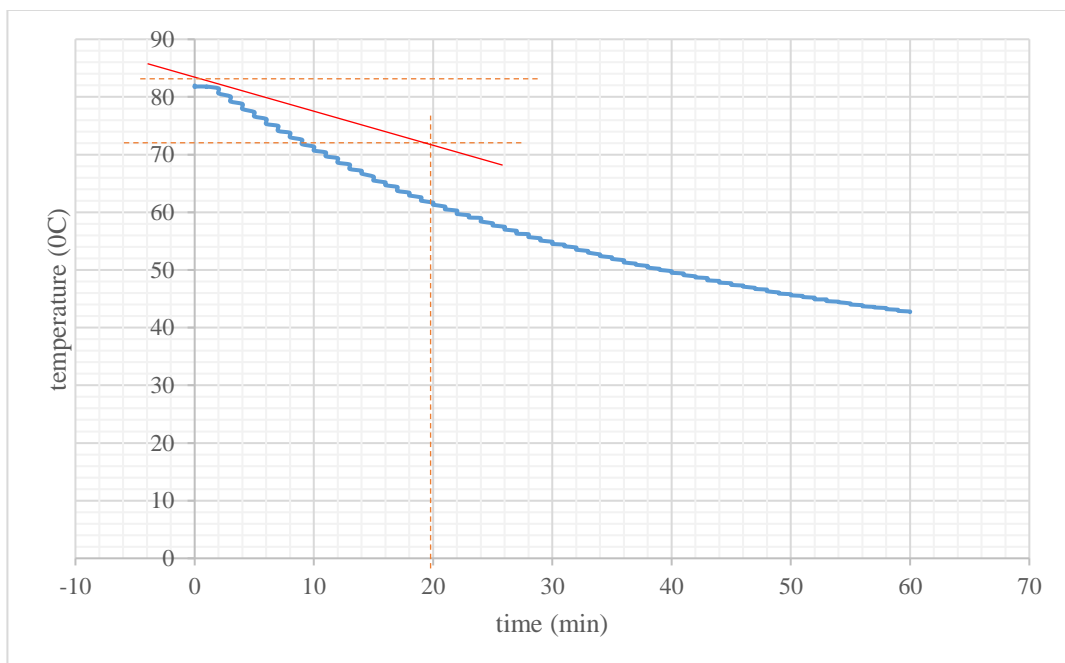
BA10



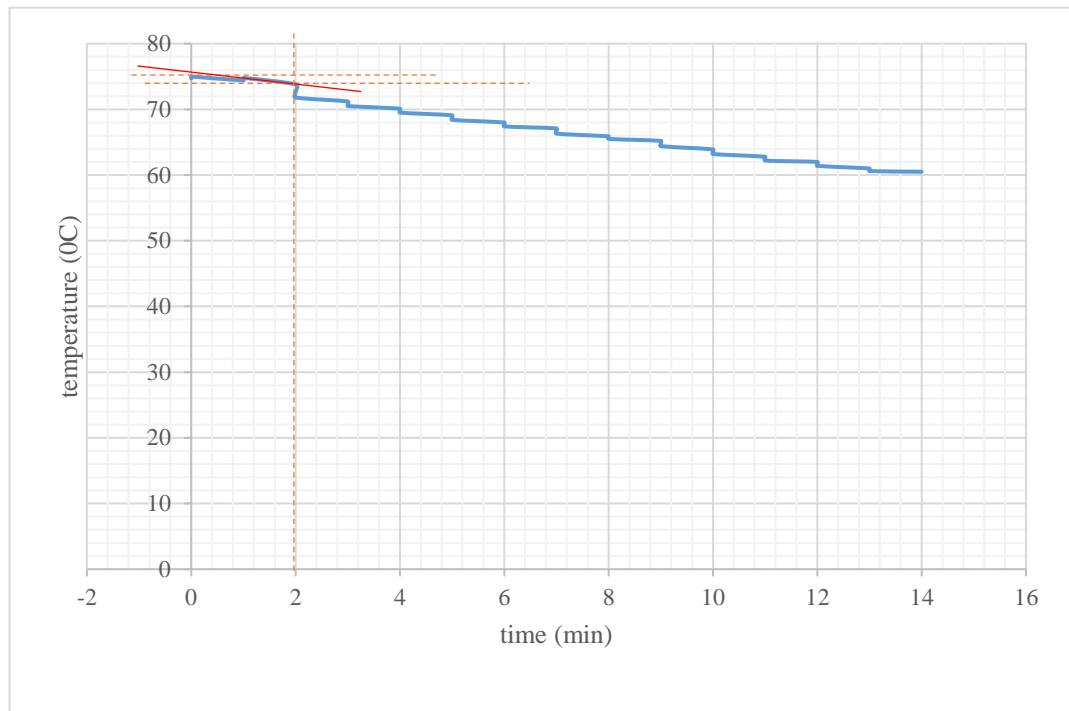
BA20



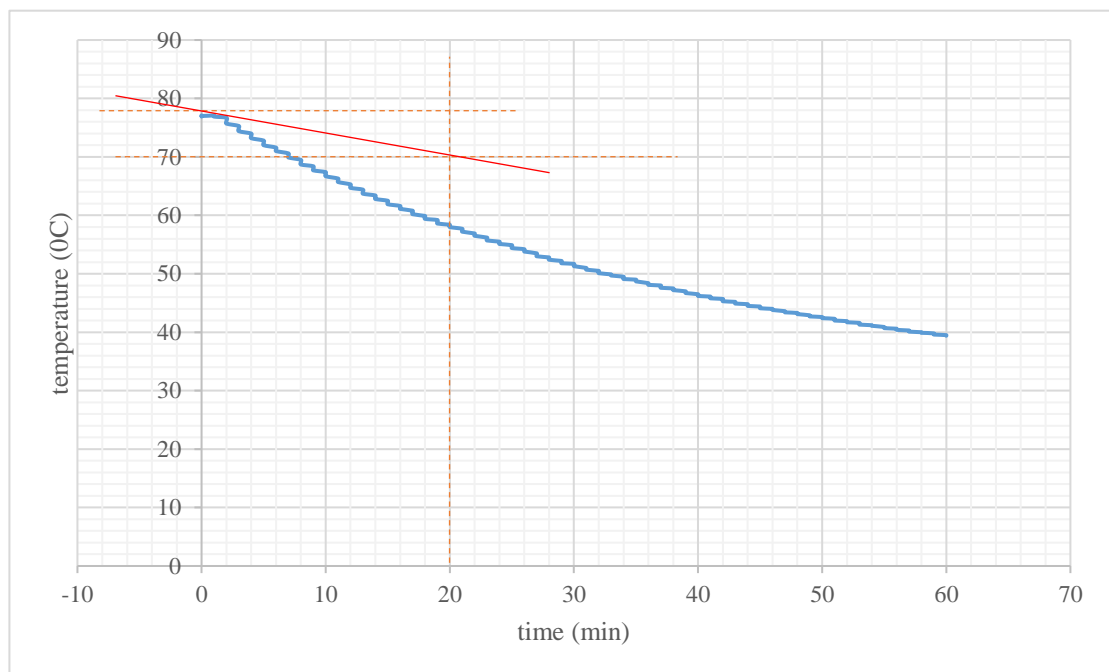
BA30



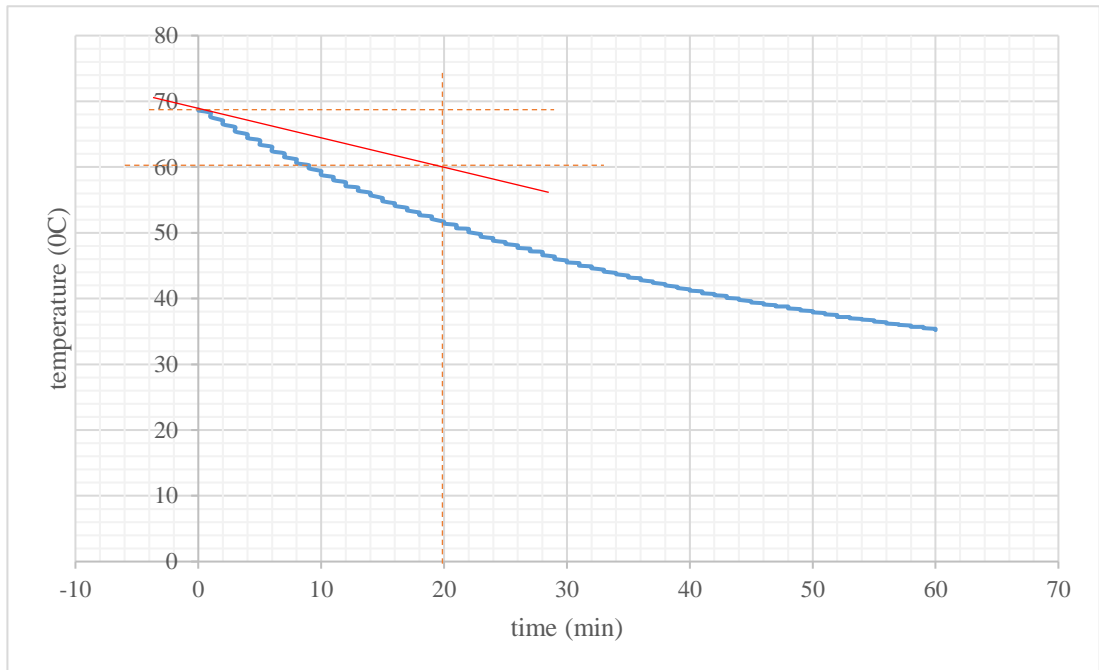
BA40



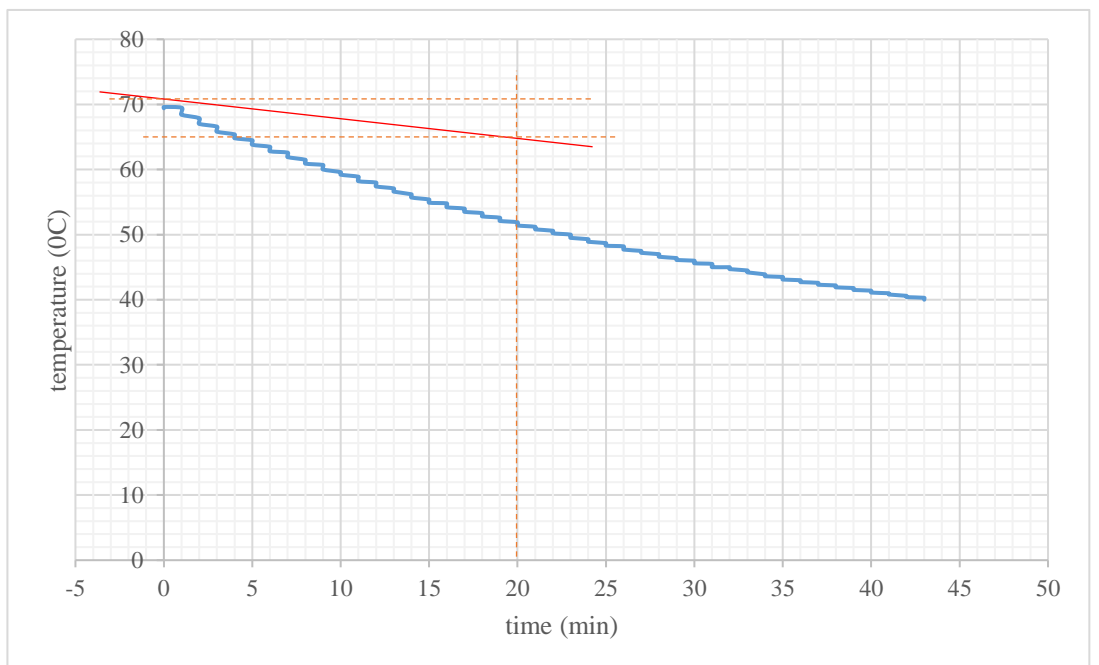
BA50



BA60



BA80



Annex 2 – Furnace test results

BA60			BA0		
Time (s)	Temp 1 (°C)	Temp 2 (°C)	Time (s)	Temp 1 (°C)	Temp 2 (°C)
0	25.78	26.45	0	31.14	26.99
10	25.9	26.71	10	32.24	28.51
20	26.25	26.89	20	33.39	29.95
30	26.5	26.91	30	34.68	31.24
40	26.87	27.01	40	36.09	32.51
50	27.29	27.25	50	37.6	33.82
60	27.79	27.29	60	39.21	35.24
70	28.43	27.35	70	40.96	36.87
80	29.1	27.91	80	42.72	38.58
90	29.8	28.34	90	44.64	40.36
100	30.56	28.56	100	46.64	42.24
110	31.41	28.61	110	48.72	44.24
120	32.31	29.78	120	50.8	46.32
130	33.31	29.89	130	53.04	48.4
140	34.39	32.41	140	55.2	50.4
150	35	33	150	57.52	52.56
160	36.56	33.85	160	59.84	54.56
170	37.92	34.21	170	62.16	56.64
180	39.24	36.47	180	64.56	58.56
190	40.6	35.93	190	66.88	60.56
200	42	38.45	200	69.28	62.72
210	43.52	38.99	210	71.6	64.96
220	45.04	40.12	220	74	67.12
230	46.56	41.56	230	76.32	69.04
240	48.16	42	240	78.64	71.84
250	49.76	42.5	250	80.8	74.48
260	51.44	43.27	260	83.04	77.12
270	53.12	46.83	270	85.2	80.08
280	54.88	47.32	280	87.28	83.04
290	56.72	49.8	290	89.2	85.76
300	58.48	51.28	300	90.8	87.76
310	60.4	53.69	310	92.16	89.84
320	62.24	55	320	93.2	92.08
330	64.16	57.69	330	94.4	93.76
340	66.08	60.89	340	95.44	95.52

350	67.92	64.28	350	96.56	97.28
360	69.84	66.78	360	98.08	98.72
370	71.76	68.99	370	99.92	100.32
380	73.68	70.11	380	101.92	102.16
390	75.52	70.56	390	103.84	103.52
400	77.28	71.64	400	105.76	104.64
410	78.96	73.69	410	107.68	105.52
420	80.48	76.89	420	109.76	106.56
430	81.92	77.01	430	112	107.76
440	83.28	80.59	440	114.16	107.81
450	84.48	81.56	450	116.32	107.94
460	85.6	83.12	460	118.56	108.17
470	86.72	84.56	470	120.8	108.32
480	87.76	86.49	480	122.88	108.56
490	88.72	87.63	490	124.96	108.64
500	89.68	90.56	500	127.76	111.28
510	90.48	91.48	510	130.32	113.12
520	91.44	91.53	520	132.96	114.72
530	92.16	92.83	530	135.36	118.48
540	92.88	93	540	138	121.44
550	93.6	94.58	550	140.32	123.04
560	94.32	95.73	560	142.88	126.32
570	94.88	96.81	570	145.28	128.64
580	95.52	98.67	580	147.52	132.08
590	96.08	99.11	590	150	135.76
600	96.72	100.59	600	152.4	140.08
610	97.36	99.84	610	154.96	144.72
620	98	102.56	620	157.44	147.28
630	98.64	103.44	630	159.84	154.64
640	99.28	105.96	640	161.76	158.8
650	100	108.9	650	164.64	163.2
660	100.64	110.17	660	166.96	167.36
670	101.36	111.87	670	169.68	173.28
680	102.08	110.72	680	172.08	178.96
690	102.88	110.99	690	174.56	181.6
700	103.68	111.74	700	176.96	185.76
710	104.48	107.92	710	179.36	188.4
720	105.44	107.64	720	181.84	189.28
730	106.32	107.36	730	184	189.2
740	107.36	105.36	740	186.72	191.52

750	108.4	106.48	750	189.04	193.2
760	109.52	105.68	760	191.52	193.12
770	110.88	104.86	770	194	195.76
780	112.16	106.93	780	196.4	198.24
790	113.52	105.55	790	198.8	200.8
800	115.04	105.02	800	201.2	202.8
810	116.64	104.28	810	203.44	205.28
820	118.24	104.04	820	205.68	207.92
830	119.92	107.32	830	207.92	208.48
840	120.72	110.36	840	210.08	209.92
850	123.76	114.76	850	212.08	210.72
860	125.6	118.4	860	214.08	212.32
870	127.68	126.5	870	216.24	213.92
880	130	128.88	880	218.32	215.92
890	132.4	133.6	890	220.32	215.52
900	134.48	138.8	900	222.24	216.88
910	137.28	141.84	910	224.08	216.48
920	140	145.12	920	226.08	218.96
930	142.64	145.96	930	227.44	218.48
940	145.2	147.32	940	229.84	219.44
950	147.6	150.76	950	231.68	220.4
960	150.16	151	960	233.6	220.48
970	152.56	153.96	970	235.36	221.28
980	154.96	153.16	980	237.2	223.28
990	157.6	156.2	990	239.04	223.2
1000	160	160.8	1000	240.8	224.16
1010	162.4	159.63	1010	242.64	225.84
1020	164.4	160.46	1020	244.4	224.96
1030	165.76	158.46	1030	246	224
1040	167.76	158.32	1040	247.6	226
1050	169.76	160.99	1050	249.2	228
1060	171.6	163.89	1060	250.56	227.84
1070	173.36	162.88	1070	252.16	228.24
1080	175.2	162.16	1080	253.52	228.24
1090	177.12	163.79	1090	254.88	230.4
1100	178.8	165.82	1100	256.24	232.64
1110	180.56	170.92	1110	257.44	234.24
1120	182.4	174.98	1120	258.8	235.84
1130	184	177.23	1130	259.84	236.64
1140	185.44	178.69	1140	260.48	236.32

			1150	262.48	239.28
			1160	263.76	241.6
			1170	264.8	243.2
			1180	266.24	245.04
			1190	267.44	246.72
			1200	268.8	248.32
			1210	270.08	249.28
			1220	271.28	251.12
			1230	272.64	252.88
			1240	274.16	255.44
			1250	275.52	257.6
			1260	277.28	259.68
			1270	278.88	261.76
			1280	280.4	263.28
			1290	282.16	265.04
			1300	284.88	269.76
			1310	287.68	272.56
			1320	290.48	277.28
			1330	292.48	280.08
			1340	294.32	282.64
			1350	296.24	285.6
			1360	298	288
			1370	299.6	290.48
			1380	301.52	292.08
			1390	303.28	294.4
			1400	304.96	296.08
			1410	306.56	296.72
			1420	308.24	299.2
			1430	309.92	300.4
			1440	311.6	302.96
			1450	313.28	304.96
			1460	315.12	306.32
			1470	316.56	308.64
			1480	318.24	310.4
			1490	319.84	311.76
			1500	321.36	313.12
			1510	322.96	314.48
			1520	324.48	316
			1530	325.84	317.6
			1540	327.44	318.96

			1550	328.3	321.04
			1560	329.6	322.72
			1570	330.9	323.92
			1580	332.2	325.36
			1590	333.4	326.72
			1600	333.4	326.08
			1610	334.7	328.3
			1620	335.4	329.6
			1630	336	330.2

Annex 3 – Datasheet

Datasheet for Bottom ash mixed thermal insulation plaster



ECO –MIX

Thermal Insulation Plaster



Description



ECO MIX is a thermal insulation plaster specifically designed for external application of structural members. Ordinary Portland Cement blended with bottom ash and fine aggregates to manufacture ECO MIX. When hardened the mortar will be dark grey in color.

The ECO MIX is an N type insulation plaster as per ASTM C270 standards.

Properties

Properties	Unit	Mix					
		A	B	C	D	E	F
28 day Strength	N/m ²	10 to 15	8 to 12	10 to 15	8 to 12	5 to 10	5 to 10
Thermal Conductivity	W/m °C	0.65 - 0.7	0.6 - 0.7	0.6 - 0.7	0.55 - 0.65	0.6 - 0.75	0.7 - 0.75
Density	kg/m ³	approx. 1500	approx. 1800	approx. 1800	approx. 1650	approx. 1700	approx. 1700
Flow	mm	120	150	140	100	175	150

Limitations

For best results, use the mortar within 30 minutes of mixing with water. Protect newly placed mortar from the weather until fully hardened. Mortar strengths are improved by keeping the mortar damp during hardening.

Application temperature: +5°C to +35°C.

Instructions for Use

For best results, mix thoroughly using a mechanical mixer, empty the bag of ECO MIX into the mixer and blend until uniform. Slowly add clean water mixing continuously to make the mix workable.

Alternatively, empty the bag of ECO MIX onto a clean, flat moisture resistant surface, such as a mortar tray. Slowly add clean water mixing continuously to make the mix workable.

Too much water will weaken the mix.



Annex 4 - Publications

International Conferences

1. **K.A.D.Y.T. Kahandawa Arachchi**, J.C.P.H. Gamage and G.I.P. De Silva, “Thermal insulation systems for CFRP/Concrete Composites: A Review”, in *International Conference on Structural and Construction Management*, 2019 - Published
2. **K.A.D.Y.T. Kahandawa Arachchi**, J.C.P.H. Gamage and E.R.K. Chandrathilake, “Bond Performance of Carbon Fiber Reinforced Polymer (CFRP) strengthened Reinforced Curved Beams”, in *International Conference on Civil Engineering and Applications*, 2019 – Published
3. **K.A.D.Y.T. Kahandawa Arachchi**, J.C.P.H. Gamage and G.I.P. De Silva, “Modification of a Bottom Ash Based Insulation Material using Saw Dust, EPS and Aggregate Chips”, in *International Conference on Structural and Construction Management*, 2020 - Submitted

International Journals

1. Selvaratnam, **K.A.D.Y.T. Kahandawa Arachchi**, S. Kajian and J.C.P.H. Gamage, “Behavior of Carbon Fiber Reinforced Polymer strengthened out-of-plane Curved Reinforced Concrete beams” – In Preparation
2. **Kahandawa Arachchi K.A.D.Y.T.**, Selvaratnam A., Gamage J.C.P.H. and De Silva G.I.P, “Development of an Innovative Insulated Plaster using Bottom Ash to Enhance Thermal Comfort in Buildings” – In Preparation
3. **K.A.D.Y.T. Kahandawa Arachchi**, A. Selvaratnam, J.C.P.H. Gamage, V. Attanayaka, “Development and Application of a Bottom Ash based Cementitious Insulation material on CFRP/Concrete Composites” – In preparation
4. Selvaratnam A., **Kahandawa Arachchi K.A.D.Y.T.**, Gamage J.C.P.H, “Experimental and Numerical analysis of an Innovative Wall Plaster Developed using Recycled EPS to Enhance the Thermal Comfort in Buildings” – In preparation